CELL AND MATERIAL INTERACTIONS IN BONE AND CARTILAGE TISSUE ENGINEERING

by

Allison Corinne Bean

B.S. in Bioengineering, Rice University, 2005

Submitted to the Graduate Faculty of

Swanson School of Engineering in partial fulfillment

of the requirements for the degree of

Doctor of Philosophy

University of Pittsburgh

2013

UNIVERSITY OF PITTSBURGH

SWANSON SCHOOL OF ENGINEERING

This dissertation was presented

by

Allison Corinne Bean

It was defended on

November 15, 2013

and approved by

Ipsita Banerjee, Ph.D., Assistant Professor, Department of Chemical and Petroleum Engineering

Kacey G. Marra, Ph.D., Associate Professor, Department of Plastic Surgery

Donna Beer-Stolz, Ph.D., Associate Professor, Department of Cell Biology

Yadong Wang, Ph.D., Associate Professor, Department of Bioengineering

Dissertation Director: Rocky S. Tuan, Ph.D., Professor, Department of Orthopaedic Surgery

CELL AND MATERIAL INTERACTIONS IN BONE AND CARTILAGE TISSUE ENGINEERING

Allison Corinne Bean, PhD

University of Pittsburgh, 2013

Due to their structural similarity to the native collagenous extracellular matrix (ECM), fibrous scaffolds are widely studied in cell-based cartilage and bone tissue engineering research. Recent studies report that cell behavior is affected by scaffold fiber diameter, although findings are inconsistent regarding whether fibers less than or greater than 1 μm are better substrates for chondrogenesis and osteogenesis. Differences in other experimental parameters between studies likely influence the outcomes, resulting in seemingly conflicting conclusions. Therefore, we explored the effects of scaffold fiber diameter on human mesenchymal stem cell (MSC) differentiation in conjunction with other culture parameters. Poly(ε-caprolactone) (PCL) electrospun microfibers (3-4 μm diameter) and nanofibers (300-400 nm diameter) were fabricated and utilized. First, we showed that microfibrous scaffolds are superior for inducing chondrogenesis at high initial seeding densities (2-4x10^6 cells/cm^3-scaffold), likely due to larger pore sizes within the scaffold promoting cell-cell contact as well as improved cellular infiltration. At lower seeding densities (1-5x10^5 cells/cm^3-scaffold) chondrogenesis is not strongly induced regardless of fiber diameter, suggesting high cell seeding densities are required to assess effects of biomaterials on chondrogenesis. Next, enhanced chondrogenesis on microfibers was found to

be independent of tissue origin of MSCs, with much more robust chondrogenesis seen on microfibers than nanofibers for both bone marrow-derived MSCs (BMSCs) and adipose-derived MSCs (ADSCs), although the latter is generally less chondrogenic on either fiber diameter. Interestingly, under osteogenic conditions, BMSCs were not as sensitive to fiber diameter, but ADSCs demonstrated increased osteogenic potential on microfibers. Therefore, not only the lineage of differentiation, but also cell source must be taken into account when determining the optimal scaffold fiber diameter for cell-based skeletal tissue engineering. Lastly, we assessed the potential of enhancing MSC osteogenesis via sequential co-seeding with endothelial cells (ECs). Seeding MSCs onto scaffolds three days prior to ECs resulted in enhanced osteogenic differentiation in comparison to MSC monoculture, seeding ECs first, or simultaneously seeding both cell types. Taken together, these studies demonstrate that detailed examination of the interactions between different culture parameters, including scaffold architecture, seeding density, cell source, and differentiation lineage is essential for developing effective skeletal tissue engineering strategies.

TABLE OF CONTENTS

LIST OF TABLES

LIST OF FIGURES

PREFACE

First, I'd like to thank my advisor, Dr. Rocky Tuan, who happily agreed to take me on as a graduate student within days of arriving in Pittsburgh. I am inspired by your incredible depth and breadth of knowledge—I don't think my brain has even 10% of the capacity to retain information that yours does. Thank you for always having confidence in me and always being there to help with any aspect of my research—from troubleshooting minor details of a protocol to discussing the overall implications of the results. If not for your encouragement and dedication to my success, I am certain I would be in a very different place right now.

I would also like to thank my thesis committee: Dr. Ipsita Banerjee, Dr. Kasey Marra, Dr. Donna Stolz, and Dr. Yadong Wang. Your feedback over the past year was invaluable and I greatly appreciate your honesty and encouragement despite my always seemingly insane proposed timeline. A huge thank you in particular to Dr. Stoltz for being willing to help me with imaging at absolutely any time, and for trusting me enough to let me use the restricted confocal microscope in the middle of the night. It's always nice to have someone who will get as excited about my (very beautiful) confocal images as I do.

I owe a great deal of thanks to everyone at the Center of Biologic Imaging. In particular, I would like to acknowledge Jonathan Franks for teaching me SEM and Morgan Jessup and Callen Wallace for always letting me invade their lab area to do staining and helping with troubleshooting and analyzing images. I know that having the opportunity to master these

imaging techniques during graduate school will continue to benefit my research throughout my career and give me an advantage over most other bioengineers. Thank you also to Dr. Sanjeev Shroff and the Cardiovascular Bioengineering Training Program (NIH T32 HL076124) for providing funding for a significant portion of my graduate studies.

A huge thank you as well to each member of the CCME. I am always astounded by everyone's intelligence, dedication to research, and willingness to help others. It was great to spend days (and nights and weekends) around such a great group of people who are always able to find ways to have a little bit of fun no matter how overwhelming the workload becomes. I truly hope that as each of us move forward in our careers that we will have opportunities to work together in the future.

There is nothing more important during graduate school than having friends who understand exactly what you are going through. Thanks to my fellow bioengineering graduate students Laurie Meszaros, Heidi Hofer, Brandon Mikulis, and Maria Jaramillo, as well as my MD/PhD classmates Yvonne Chao and Jean Lin for always being there to listen and remind me that I was never alone and that it would all work out in the end. Carey Morewedge and Mina Cikara: not only do you inspire me with your academic prowess, but also your dedication to each other despite the distance that kept you apart for so long. Your support and love throughout these years gave me essential confidence that I wouldn't have had without your friendship. To Mike Wolff and Joie Love, thank you for always being there when I needed a break from work and for providing an endless supply of fun, laughs, and love. Thanks also to Lauren Smith, JD Schroeder, and Cory Weibel for their friendship and willingness to put up with me under any circumstance.

Finally, I would like my family. Dad, thank you for supporting me throughout my entire life, always being excited to hear about my accomplishments, and never questioning my decision to pursue a joint degree program that would ensure that I would not have a real job until my mid-thirties. Mom, I miss you more than words can say, but you continue to influence my life on a daily basis. Thanks to you and your determination to prove that mental strength and intelligence are far more important to success than gender, I never once thought of engineering or science as a man's field. You will always be my main inspiration in life. Last, but not least, I would like to thank the love of my life. Andrew, your unwavering support throughout these years means more than I could ever tell you. You believed in me even when I didn't believe in myself and stuck by me no matter how tired and grumpy I became. Your willingness to drive to Pittsburgh to see me and not complain a single time even if I spent most of the weekend working was comforting beyond imagination. I could not have done this without you.

1.0 INTRODUCTION

1.1 BONE BIOLOGY AND DISEASE

1.1.1 Bone development

Bone formation occurs through two types of processes: intramembranous and endochondral ossification. Intramembranous ossification occurs directly by differentiation of mesenchymal osteoprogenitors into osteoblasts that form ossification centers. Intramembranous ossification is the process through which many craniofacial bones are formed. Endochondral ossification is the pathway that leads to formation of long bones as well as the vertebrae and occurs through a cartilage intermediate as described below.

Limb development is initiated as undifferentiated mesenchymal cells from the lateral plate mesoderm proliferate and migrate under a layer of specialized epithelial cells known as the apical ectodermal ridge (AER), bulging outwards to form the limb bud.[1] Eventually, the mesenchymal cells in the elongating limb bud slow their migration and proliferation and begin to aggregate. As the inter-cellular distance decreases, cell-cell contacts are formed via proteins including N-cadherin and neural cell adhesion molecule (N-CAM),[2,3] and cells begin to differentiate into pre-chondrocytes. A shift in extracellular matrix (ECM) production also

occurs, as collagen type I produced by the undifferentiated mesenchyme is degraded and replaced with collagen type II and aggrecan, producing a cartilaginous matrix and resulting in formation of a cartilage anlage.[4]

Chondrocytes in the cartilage anlagen continue to proliferate and deposit ECM, extending the length of the tissue. Eventually, cells in the center are triggered to exit the cell cycle and become hypertrophic, increasing in size and mineralizing the surrounding matrix. Hypertrophic chondrocytes also secrete signals inducing sprouting angiogenesis and blood vessel invasion from the surrounding perichondrial vessels. Osteoclasts arriving through the blood vessels then degrade the cartilage ECM, aiding further vessel invasion towards the center of the tissue. At the same time, hypertrophic chondrocytes undergo apoptosis and are replaced by bone-forming osteoblasts and bone marrow cells, resulting in formation of the primary ossification center. Osteoblasts from the perichondrium also deposit tissue on the outside edge of the cartilage, forming a compact bone collar around the cartilage and the primary ossification center. Postnatally, secondary ossification centers also form at the epiphyses of bones. The cartilage in between the primary and secondary ossification centers forms the ephiphyseal growth plate, which is eventually ossified during adolescence, often referred to as “closure of the growth plate”, as the primary and secondary centers meet.[5,6]

1.1.2 Bone structure and composition

The overall structure of mature bone consists of a dense cortical outer layer that surrounds the spongy trabecular bone that contains the bone marrow compartment. Fifty to 70% of bone is calcium phosphate mineral, mostly in the form of hydroxyapatite, which provides the strength of the tissue. Organic matrix makes up 20-40% of bone, while 5-10% is water and a small

percentage is lipids.[7] Collagen type I is by far the most abundant protein secreted by osteoblasts, comprising 90% of the protein components of the bone, and provides the elasticity needed to withstand repeated loading.[7] Osteocalcin and osteonectin are the other major components, comprising approximately 40-50% of the non-collagenous proteins. Biglycan and decorin, along with cell-binding proteins bone sialoprotein, osteopontin, fibronectin, vitronectin, and thrombospondin are also present in lower abundance.[8]

1.1.3 Bone remodeling

Bone is continuously remodeling throughout life in a tightly coupled process of resorption and deposition. As osteoclasts advance, digesting old tissue, osteoblasts follow behind, depositing new matrix.[8] During initial bone formation, as well as during fracture repair, osteoblasts lay down a relatively weak and disorganized bone matrix, termed “woven” bone. This is quickly resorbed by osteoclasts and replaced by a more organized, stronger lamellar bone with collagen arranged in concentric, orthogonally oriented layers around a blood vessel, in a structure called the osteon. As osteoblasts mature, they become surrounded by mineralized matrix, and undergo terminal differentiation to become osteocytes. Osteocytes communicate with the surrounding cells and bone surface using dendritic cell processes that travel through an extensive canalicular system.[9]

1.1.4 Bone defects and treatment

Most bone fractures in healthy patients heal without intervention beyond immobilization and stabilization. However, approximately 5-10% of fractures suffer from delayed or non-union, and

other problems including trauma, surgical tumor removal, genetic disease, and joint replacement revision surgery result in the need for more than 1.5 million bone graft procedures to be performed in the US each year.[10] Autologous bone grafts, typically obtained from the iliac crest, are the clinical gold standard and have relatively high success rates, but there is a limited amount of tissue that can be obtained, as well as potential donor site morbidity.[11,12] Allografts from deceased donors can be used to circumvent availability issues, but suffer from potential immune rejection, disease transmission, and reduced osteoinductive capabilities due to the need to pre-treat the tissue./sup> Osteoconductive synthetic grafts, fabricated from such materials as collagen, hydroxyapatite, and tricalcium phosphate, are currently used clinically, but due to non-ideal mechanical properties are typically utilized only as a supplement to autologous or allogeneic bone grafts rather than as a replacement by themselves.

1.2 CARTILAGE BIOLOGY AND DISEASE

1.2.1 Cartilage development

While most of the cartilage anlagen are completely replaced by bone, the cartilage tissue that is found at the surface of the articulating joints such as the knee and hip is permanent. The “stable” chondrocytes that make up the articular cartilage are derived from mesenchymal cells that arise near the interzone, the location where joint formation takes place. As joint development begins, the interzone divides into three layers: two chondrogenic layers and an intermediate layer. It is thought that the articular cartilage arises from the intermediate layer, while the deeper

chondrogenic layers become incorporated into the epiphysis as the ECM becomes reorganized and cavitation occurs to form the joint space, with articular cartilage lining the surface of the bone.[14–16]

1.2.2 Cartilage structure and composition

Mature articular cartilage is a hypocellular, avascular tissue with chondrocytes the only type of cells normally found within the tissue. Cartilage may contain up to 80% water by weight, while 60-70% of the dry weight of cartilage is collagen, mostly collagen type II, and 25-35% is proteoglycans, mostly aggrecan.[17] Articular cartilage is arranged into four zones: superficial, intermediate, deep, and calcified. In the superficial zone, chondrocytes have a flattened morphology and the collagen fibers are arranged parallel to the surface. Proteoglycan content in the superficial zone is also lower than in other regions. In the intermediate zone, chondrocytes become more spherical in shape, organizing themselves into vertical columns, and collagen fibers are arranged randomly. In the deep zone, collagen is oriented perpendicular to the surface of the joint, forming struts that cross the tidemark to integrate into the calcified cartilage zone. The calcified cartilage zone serves as the transition between the cartilage above and the subchondral bone below.[17]

1.2.3 Cartilage remodeling

Since cartilage is avascular, chondrocytes exist under chronically hypoxic conditions. Therefore, in the absence of significant physiological perturbations, the metabolic activity of chondrocytes is low. However, chondrocytes are sensitive to both cytokines as well as mechanical loading, and can modify the cartilage matrix in response, although its capacity for repair is limited.[17–19]

1.2.4 Osteoarthritis disease and treatment

Conservative estimates find that nearly 14% of the United States population over the age of 25 is affected by osteoarthritis (OA) with over $185 billion spent in the United States on healthcare related to the disease in 2007.[20] As the population continues to age, the prevalence of OA is predicted to increase.[21,22] OA is caused by degeneration of the articular cartilage over time and can be due to a previous acute injury (post-traumatic OA), chronic altered joint loading, or both, as well as other yet to be ascertained factors, including genetics and aging. Under these conditions, chemical or mechanical stimuli shift chondrocytes towards a more catabolic phenotype, increasing their secretion of matrix metalloproteases and pro-inflammatory cytokines, and the organization of the collagen network decreases.[2324] Glycosaminoglycans, a major component of the sulfated proteoglycans of cartilage, are also lost and tissue hydration decreases. The result is an overall deterioration of the cartilage, with loss of surface smoothness and increasing tissue loss, potentially reaching the level of the osteochondral layer. The result of this breakdown is pain and limited physical functioning, leading to a decreased quality of life.

Symptomatic management with non-steroidal anti-inflammatory drugs, cyclooxygenase-2 inhibitors, or intra-articular corticosteroid injections are the current standard of care, while joint replacement surgery, or arthroplasty, is the only currently available treatment for advanced stages of osteoarthritis. Nearly one million hip and knee replacements are performed in the US annually,[25] and while arthroplasty can alleviate symptoms, these implants typically only last 10-15 years, primarily due to the failure of the tissue-implant interface, and revision surgery is often required — 17.5% and 8.2% of hip and knee replacements, respectively, needed revision between 1990 and 2002. Additionally, patients undergoing joint replacement are still typically unable to match the functional abilities of their healthy counterparts following the procedure.[26]

1.3 TISSUE ENGINEERING

1.3.1 Definition

Improved methods for treating cartilage and bone defects are needed. Over the last two decades, tissue engineering has emerged as an attractive approach, as it eliminates the issue of donor tissue shortages as well as immune rejection. As defined by Langer and Vacanti, tissue engineering is "an interdisciplinary field of research that applies the principles of engineering and the life sciences towards the development of biological substitutes that restore, maintain, or improve tissue function."[27] More specifically, tissue engineering utilizes a combination of cells, scaffolds and bioactive factors in strategic combinations to direct the *in vitro* formation of new tissues or organs.

1.3.2 Cells in tissue engineering

In order to eliminate the need for immunosuppression, regenerative medicine and tissue engineering approaches have generally focused on using autologous donor-derived cells or cells that will not elicit an immune response. However, terminally differentiated cells are typically limited in their ability to proliferate and it is therefore difficult to obtain sufficient cell number for regeneration of tissues. In addition, cells from tissues to be treated or replaced are likely to have undesirable defects that require structural repair. Because of this limited potential using differentiated cells, the use of stem or progenitor cells has become ubiquitous in the fields tissue engineering and regenerative medicine. The characteristics that define stem cells—capacity for self-renewal, long-term proliferation and the ability to differentiate into several different cell types—make them the optimal cell source for the development of new tissues and organs.

Stem cells are typically classified into two main groups: embryonic and adult. Embryonic stem cells (ESCs) are derived from the inner cell mass of blastocysts in the developing embryo prior to implantation. These cells are pluripotent, i.e., ESCs have the ability to differentiate into cells comprising all three germ layers, and can be maintained in culture in an undifferentiated state for indefinite periods of time.[28] While these characteristics render ESCs an attractive cell source for regeneration of tissues and organs, they suffer from several limitations. First, ESCs present an ethical issue since embryos are destroyed in the process of obtaining the cells; second, since they are obtained from allogeneic sources, there is the possibility of an immune response, although research suggests that this response may be weaker than with traditional organ transplant; third, due to their undifferentiated state, there is a possibility that ESCs can become tumorigenic and malignant.[29]

Adult stem cells, on the other hand, are isolated from post-natal tissues. They can also differentiate down multiple lineages, but are more restricted in the types of cells that they can become and have more limited proliferation potential in comparison to ESCs. One advantage of adult stem cells compared to ESCs is that they can often be obtained from the patient themselves, thereby obviating the issue of immune rejection. However, if the tissue that cells are desired from is diseased, or has limited availability of stem cells (e.g., nervous tissue), it may not be possible to obtain autologous cells. One type of adult stem cells that have been found to be particularly well-suited for bone and cartilage tissue engineering are mesenchymal stem cells (MSCs). These cells have been isolated from many different adult tissues including but not limited to bone marrow, fat, synovium, cartilage, muscle, and dental pulp. MSCs have also been isolated from prenatal and perinatal tissues such as the umbilical cord, umbilical cord blood, and placenta[30] Bone marrow-derived MSCs (BMSCs) and adipose-derived MSCs (ADSCs) are the most commonly utilized MSCs. Both of these cell types have shown the ability to differentiate into cartilage, bone, and fat, making them particularly useful for regeneration of musculoskeletal and connective tissues. In addition to their multipotent differentiation ability, MSCs have been shown to be hypoimmunogenic as well as immunosuppressive, even after differentiation.[31–33]

While adult stem cells are multipotent, unlike ESCs they are somewhat lineage-restricted and typically only differentiate readily towards a few cell types and therefore are useful for a limited number of tissues. Recent advances, however, have led to the ability to reprogram somatic cells, including those that have undergone lineage specific differentiation, into an ESC-like state. Takahashi, et. al. showed that the retroviral mediated expression of four nuclear transcription factors—Oct4, Sox2, Klf4, and c-Myc—resulted in cells with expression patterns and differentiation capacity cells similar to ESCs. These induced pluripotent stem cells (iPS

cells) may allow scientists to overcome the ethical and immune rejection concerns of ESCs while retaining the increased proliferation and differentiation capacity that make the use of ESCs over typical adult stem cells desirable. Initial concerns that utilizing viruses or vectors that integrate into the genome may lead to the development of tumors are being addressed by using transient or removable vectors or by directly delivering proteins.[34–39] Despite autologous cells being used, recent studies show that iPS cells may generate an immune response upon implantation,[40] suggesting that while these cells may have promise, significantly more research must be conducted prior to clinical translation.

1.3.3 Biomaterials in tissue engineering

In tissue engineering, biomaterials serve as the scaffolding upon which cells build tissues. The definition of biomaterials has recently been re-visited and is now interpreted as encompassing natural or synthetic materials that interact with biological systems. The use of biomaterials in medicine has been studied for centuries, with dental implants made from wood and contact lenses comprised of glass being among the first common applications of biomaterials. Because early implants were designed to be permanent and little was known about the mechanisms behind the foreign body response, initial biocompatibility studies in the 1940's focused on determining which materials were the least chemically reactive. However, this changed with the development of applications where it was desirable for the biomaterial to interact directly with the host tissue as well as degrade over time. Therefore, the definition of biocompatibility has become focused on materials having an "appropriate host response" rather than limiting the response.[41] Today, in addition to being biocompatible, biomaterials in tissue engineering applications have become increasingly sophisticated and are designed to meet several criteria.[42]

First, they should provide appropriate mechanical strength to ensure that the tissue can withstand the normal forces it experiences and/or perform its physical functions *in vivo*. Second, they must provide a compatible surface for cell attachment and appropriate topographical information. Third, they should ideally be designed to degrade over a length of time that is appropriate for the specific application, such that the ultimate engineered tissue is able to approximate its original state.

Synthetic polymers have an advantage over natural polymers as biomaterials for tissue engineering since they may be produced using defined processes, and have highly tunable mechanical and chemical properties to enhance biocompatibility. However, nature's biomaterial—the extracellular matrix (ECM)—already possesses the optimal properties to support cellular attachment and tissue growth, often in a tissue-specific manner. This has led tissue engineers to study in depth the structure and composition of the native ECM as well as investigate the cell-material interactions with the goal of recreating this environment.

The native ECM is a complex and dynamic network of proteins that provide both structural and biochemical support to the cells it surrounds. Rather than just serving as a passive scaffold, the ECM also provides important mechanical, topographic, and biochemical cues that can influence cell attachment, survival, shape, proliferation, migration, and differentiation.[43] The most abundant protein in the ECM is collagen, which makes up approximately 30% of the total protein in the human body. Mature collagen is a triple-helix of three polypeptides that align and combine themselves to form collagen fibrils that are typically between 50 and 500 nm in diameter.[44,45] Other fibrous proteins such as fibronectin, laminin and elastin are also present in significant quantities and influence the structural and mechanical properties of the tissue. In addition to the fibrous proteins, the ECM also contains glycoproteins as well as bound or

entrapped growth factors that can significantly influence the properties of the tissue. Each component of the ECM influences cell behavior via specific interactions, often involving ligand-specific receptors on the cell membrane. Therefore, recapitulation of the structure of the native microenvironment using biomaterials with nanoscale features may provide the optimal biomimetic topographic structure for cells to form tissues with similar properties to the native tissue.

There are two levels of interactions that must be investigated in order to develop the optimal tissue engineered solution for clinical use: (1) the cell-material interactions *in vitro* after initial cell seeding, and (2) the interactions of the tissue-engineered constructs with the host tissues following implantation. While the ultimate goal of tissue engineering research is to develop a construct that can be implanted and function *in vivo*, it is imperative to first gain a thorough understanding of the cell-scaffold interactions in well-defined *in vitro* environments. Tissue engineering research currently focuses on applying knowledge of the biological characteristics of native cellular and tissue microenvironment to the development of biomaterial-based constructs that mimic these behaviors when combined with cells.

1.3.4 Three-dimensional scaffolds

Extensive studies have shown that there are clear differences in cell behavior and tissue formation on flat surfaces in comparison to 3D ECM scaffolds, and that these differences occur at the protein and sub-protein level. Furthermore, these differences are present even when the 2D scaffold has the same chemical and molecular composition.[46,47] These findings, in combination with the evidence that nanoscale topography affects cell behavior, have pushed scientists to utilize tissue-engineering approaches that mimic the 3D sub-micron structure of the native ECM.

The currently available techniques for scaffold fabrication do not approach the complexity of the native ECM structure, nor can the environment be as closely controlled as with the 2D nanotopography described above. However, this may not be necessary as scaffolds in tissue engineering studies are designed to act primarily as a temporary structure to support cells until they are able to synthesize their own functional ECM. Therefore the goal in successful application of 3D tissue engineered scaffolds is to identify and enhance key components that will provide the appropriate signals to cells in order to generate a functional tissue that can be translated into clinical use.

1.3.5 Electrospinning

Electrospinning has recently become among the most commonly used method for the fabriction of nanofibrous biomaterials. This method involves the application of a high electric field to a polymer solution delivered at a constant rate through a needle. At a high enough voltage, the charge on the polymer overcomes the surface tension of the solution and causes emission of a fine polymer jet. This jet undergoes a whipping process and the fibers are further elongated as the solvent evaporates and fibers are deposited on a grounded collector. Both natural and synthetic polymer scaffolds have been successfully created using the electrospinning method. The ability to generate three-dimensional scaffolds with tailored architecture, mechanical properties and degradation characteristics, has made electrospinning a popular method in tissue engineering applications. Altering parameters during the electrospinning process, such as polymer concentration, flow rate of the solution and voltage applied, can generate fibers ranging

from approximately 100 nanometers to several micrometers in diameter. Scaffolds with aligned fibers can be created by collecting fibers on a drum or mandrel rotating at high speeds, while randomly oriented fibers are generated on slow rotating or stationary collectors.

Various polymers have been used in electrospinning of nanofiber scaffolds. These include synthetic polymers such as poly (L-lactic acid) (PLLA), poly(ε-caprolactone) (PCL), and polyurethane,[48] as well as natural polymers such as collagen,[49–52] elastin, silk fibroin, dextran,[53] and chitosan.[54,55] Because the synthetic polymers typically used in electrospinning are hydrophobic and lack biologically active functional groups, they are often modified either physically or chemically following the electrospinning process to increase their hydrophilicity and ability to interact with cells and biomolecules.

Plasma etching, similar to that performed on tissue-culture polystyrene, can generate functional carboxyl or amine groups on the surface of the fibers, which has been shown to enhance cell attachment and proliferation either alone,[56,57] or via the coating of the functionalized fiber with a natural ECM protein such as collagen[58] or gelatin.[59] Wet chemical etching methods may provide more homogeneous functionalization in thicker scaffolds since plasma etching can only penetrate the outer surface of a thicker scaffold. This method typically involves NaOH hydrolysis or aminolysis of the polymer, breaking the ester bond at random points and creating a hydroxyl or amino group, respectively.[60] One study demonstrated that esophageal epithelial cells seeded on aminolyzed poly(L-lactide-co-caprolactone) coated with fibronectin exhibited higher collagen type IV synthesis than those seeded on the unmodified polymer, suggesting that this method may be useful in tissue engineering studies.[58,61]

Composite scaffolds formed from co-electrospinning of different polymers have been utilized to control the mechanical as well as structural properties of the scaffold. Perhaps the biggest challenge using the electrospinning method is that the pore size is typically much smaller than the diameter of a typical cell, a property that makes cell and nutrient infiltration into the middle of the scaffold difficult. Several methods have been used to overcome this problem, including spinning of mixed microfiber and nanofibers scaffolds,[62] as well as using water-soluble polymers (i.e. polyethylene oxide (PEO)) in combination with slower-degrading materials (i.e. PCL), that can be quickly dissolved after spinning, leaving the non-soluble, slower-degrading polymer behind with larger pore sizes.

In order to more closely tailor the properties of a scaffold—including biological, mechanical, and degradation characteristics—researchers have begun to combine two or more different components within a single scaffold. This can be done prior to electrospinning by mixing several polymers within a single solution, which results in a single fiber containing each component, or by electrospinning multiple solutions of polymers onto the same collector, thereby creating a scaffold with multiple fiber types.

While natural polymer scaffolds composed of ECM proteins such as collagen and elastin show increased cellular response, when used alone they lack sufficient mechanical properties to function in the *in vivo* setting. Combining ECM derived from urinary bladder matrix with poly(ester-urethane)urea, Stankus et. al. were able to develop electrospun scaffolds with improved mechanical and biological properties than possible using the individual polymers alone.[63] Similarly, Lee et. al. mixed collagen and elastin with several biodegradable synthetic polymers in order to develop scaffolds to utilize as vascular grafts.

Some polymers cannot be dissolved in the same solvent, therefore limiting the options for combining several different polymers within the same solution. Additionally, it may be desirable to utilize fibers of different dimensions or mechanical properties within the same scaffold. This has led to the development of multi-jet electrospinning in which different polymer solutions can either be electrospun at the same time to generate a homogeneous mixed scaffold or sequentially to generate a layered scaffold.[64] For example, Baker, et. al. co-electrospun three different solutions containing polymers with varying degradation rates and mechanical properties to develop a scaffold that allowed for both improved cellular infiltration by increasing pore size over time as well as more closely mimicked the properties of the native tissue.[65]

Electrospinning is a relatively simple, cost-effective technique that has shown significant potential in studies aimed at repair of many different types of tissues. When seeded with stem cells, nanofiber scaffolds have been shown to enhance differentiation towards many different cell types, including bone, cartilage, cardiac and skeletal muscle, blood vessels, and nerve.[66,67]

1.3.6 Bioactive factors in tissue engineering

While the scaffold structure plays an essential role in controlling cell behavior, chemical or biological modulators of cell activity and phenotype heavily influence tissue formation both *in vitro* and *in vivo.* In native tissues, growth factors provide specific signals to cells that direct cell activity including cell migration, proliferation, and differentiation. The effects of growth factors are quite complex and are dependent on the nature, active state, and concentration of the growth factor, phenotype of the target cell type(s), and functional characteristics of the specific cell receptor interacting with the growth factor.

In vitro tissue engineering studies often supply relevant growth factors in the culture medium to induce cellular differentiation. Transforming growth factor-beta (TGF-β) and bone morphogenetic proteins (BMPs) have been shown to have potential for inducing chondrogenesis in serum-free base medium also containing ascorbic acid and dexamethasone *in vitro*. On the other hand, MSC osteogenic medium typically contains fetal bovine serum (FBS) in addition to ascorbic acid, dexamethasone, and β-glycerophosphate. Vitamin D is also often added, in addition to β-glycerophosphate, to enhance matrix mineralization during osteogenesis.[69]

The concentrations and combinations of growth factors utilized can significantly affect cell growth and behavior, and synergistic effects of two or more growth factors may promote or inhibit differentiation of MSCs differently than when the growth factors are used independently. Additionally, culture conditions should be optimized for the specific type of cells, since cells from different tissue sources may respond differently to a specific growth factor cocktail. The importance and complexity of developing an optimal culture medium has led to a large number of research studies being performed that focus on examining the effects of different medium compositions on cell differentiation *in vitro*.

1.3.7 Bone tissue engineering

Electrospun scaffolds have been widely used in bone tissue engineering, demonstrating the ability to promote osteogenesis when seeded with either osteoblasts or stem cells. PCL nanofiber scaffolds with diameters of approximately 370 nm seeded with rat MSCs showed enhanced cell attachment and differentiation in comparison to flat substrates, with increased alkaline phosphatase activity, calcium deposition and expression of bone-specific matrix proteins, osteocalcin and osteopontin.[70] Addition of proteins such as collagen to polymer scaffolds has

also been examined as a method for generating scaffolds with favorable material properties due to the synthetic scaffold, while increasing the bioactivity due to the protein coating. In one study, using PCL nanofibers coated with a collagen sheath resulted in increased calcium deposition by adipose-derived stem cells on scaffolds after two weeks in osteogenic medium,[71] while another utilizing a chitosan/hydroxyapatite composite doped with collagen increased the osteogenic potential of fetal osteoblasts.[72] Scaffolds containing a mixture of microfibers and nanofibers have also been examined for bone tissue engineering applications. Early studies showed that PCL scaffolds with fibers ranging from 20 nm to 5 μm seeded with rat MSCs had increased mineralization *in vitro*[73] and *in vivo*.[74]

While the above studies demonstrate the potential for cells to undergo osteogenesis on electrospun fibers, this approach may have limited potential *in vivo*. Bone contains a robust vascular network, with cells requiring the presence of a capillary within the 200 μm oxygen diffusion radius in order to survive *in vivo*.[75] Previous work has shown that vascular invasion into porous scaffolds occurs very slowly, on the order of tenths of mm per day, [76] and smaller pores due to tissue deposition by other cells during *in vitro* culture may further slow the rate. Therefore, once implanted *in vivo*, the interior regions of a large tissue engineered bone construct without pre-vascularization would be unlikely to receive sufficient oxygen and nutrients, resulting in avascular necrosis and subsequent failure of the graft.

Several approaches have been utilized to ensure successful vascularization of engineered bone. The first is to implant a cell-free scaffold *in vivo* in proximity to vasculature in order to induce blood vessel invasion. [77] The vascularized implant can then be extracted, seeded with osteogenic cells, and cultured *in vitro* before implanting the construct into the bone defect where it can be immediately anastamosed with the host vasculature. Limitations of this strategy include

the need for multiple invasive procedures as well as an inability to prevent invasion of non-vascular cells during the initial *in vivo* culture period that may form unwanted tissue and inhibit later osteogenesis.

Development of scaffolds containing angiogenic factors can also enhance recruitment of endothelial cells (EC) and promote blood vessel invasion into the scaffold.[78] Due to advances in drug delivery techniques, the timing and rate of secretion of these growth factors from scaffolds can be relatively controlled. Alternatively, rather than adding growth factors directly, osteogenic cells could be genetically engineered to over-express specific angiogenic factors. This strategy eliminates need for an *in vivo* pre-vascularization step prior to seeding osteogenic cells. However, it is difficult to establish the optimal combination and release rate profile of growth factors that will promote a tightly controlled vascular invasion of the scaffold with formation of maturation, stable blood vessels within the scaffold, in addition to supporting bone formation by osteogenic cells.

The above strategies cover potential *in vivo* approaches that rely on host blood vessels to be drawn towards and into the scaffold and induced to undergo branching angiogenesis in a controlled manner. During bone development and healing, there is evidence that osteoblastic precursors migrate with blood vessels, both as pericytes in tight association with endothelial cells and alongside the invading vascular front. Addition of ECs has been shown to induce MSCs to secrete increased amounts of VEGF, which upregulates EC secretion of BMP-2, causing enhancement of the osteogenic differentiation of MSCs cultured alone.[79] This positive feedback loop suggests that ECs can directly promote osteogenic differentiation of MSCs in addition to initiating the establishment of a functional vascular network that will allow for successful survival and integration of the tissue. Futhermore, the perivascular location of MSCs *in vivo*

suggests that mutually enhancing interactions exist between MSCs and ECs. Therefore, another potential approach for bone tissue engineering is to induce blood vessel and bony tissue formation *in vitro* by co-culturing ECs or EC progenitors with osteogenic cells. The co-cultured construct can then be implanted into a bone defect, where the seeded ECs will elicit the initiation or maturation of a functional vascular bed that will anastamose with the host vasculature, thus providing the essential oxygen and nutrients to the interior tissue engineered bone construct, thereby preventing necrosis and promoting tissue integration.

1.3.8 Cartilage tissue engineering

The fibrous nature of the native collageneous matrix makes electrospinning an attractive method for fabrication of scaffolds for cartilage tissue engineering. Similar to findings in bone tissue engineering applications, studies have shown enhanced chondrogenesis of both MSCs and chondrocytes seeded onto electrospun PCL nanofibers fibers in comparison to flat surfaces.[80,81] Additionally, implantation of nanofibrous PCL scaffolds seeded with MSCs enhanced healing of a cartilage defect in a swine model.[82]

Electrospinning can also be utilized to fabricate scaffolds with multiple orientations such as those seen in collagen fibers in different zones of articular cartilage. For example, one experiment utilized aligned electrospun PCL fibers designed to mimic the aligned orientation of collagen fibers seen in the superficial zone of cartilage, and showed potential for MSC chondrogenesis *in vitro*.[83] In another study, a trilayer scaffold with an aligned superficial layer, and random middle and deep layers with increasing fiber diameters had improved mechanical properties compared to homogeneous scaffolds and supported MSC chondrogenesis.[84]

1.4 SUMMARY

Understanding the interactions between cells and biomaterial scaffolds is essential for guiding the development of functional tissue engineered constructs for bone and cartilage engineering. Many variables including, but not limited to, media composition, scaffold composition, scaffold architecture, biomechanical stimulation, cell source, and cell seeding density must be optimized in order to develop a successful tissue engineered construct. It has been previously demonstrated that the cellular response to a biomaterial is not only dependent on the chemistry of the scaffold, but also on the architecture. Because of the structural similarity to the native ECM, electrospun fibrous scaffolds composed of either natural or synthetic polymers have become popular as biomaterials for cartilage and bone tissue engineering. Recent research suggests that cell behavior on these scaffolds is dependent on the diameter of the fibers, but findings among different researchers often seem to be contradictory due to the presence of non-controlled experimental parameters between studies. Additionally, while cartilage is an avascular tissue, bone requires vasculature to survive in vivo, necessitating co-culture of multiple cell types. Understanding the mechanisms that guide cell-material and cell-cell interactions may lead to improve strategies for designing functional tissue engineered bone and cartilage constructs. To this end, we performed the following investigations:

Specific Aim #1: Determine the effects of fiber diameter and seeding density on chondrogenesis of MSCs on PCL scaffolds.

Specific Aim #2: Determine the effects of fiber diameter and MSC tissue source on chondrogenesis and osteogenesis of MSCs on PCL scaffolds.

Specific Aim #3: Determine the effects of sequential seeding on osteogenesis during co-culture of MSCs and endothelial cells on PCL fibrous scaffolds

Our overall hypothesis is that by varying multiple culture parameters simultaneously in a systematic manner, we will obtain a more thorough understanding of the optimal conditions for promoting chondrogenesis and osteogenesis of MSCs on electrospun scaffolds that mimic the structural aspects of the native ECM. The following chapters detail the results of our experiments of each of the above specific aims.

2.0 EFFECTS OF SEEDING DENSITY AND FIBER DIAMETER ON CHONDROGENIC DIFFERENTIATION OF MESENCHYMAL STEM CELLS

2.0 INTRODUCTION

Several studies have examined the effects of electrospun scaffold fiber diameter on different cell types and tissue applications including bone, nerve,[85–88] ligament,[48,89] skin,[90,91] blood vessels, and cartilage.[83,92–94] The results of these studies suggest that the optimal fiber diameter may be highly dependent on various experimental factors and it may be impossible to isolate a single ideal fiber diameter independent of other conditions. For example, one study concluded that differentiation of mesenchymal stem cells (MSCs) towards a cartilage phenotype was better on electrospun poly(ε-caprolactone) (PCL) fibers that were 500nm in diameter than on fibers 3μm in diameter,[83] while another group concluded that chondrogenesis was enhanced on poly(L-lactide) fibers with diameters of 5μm or 9μm in comparison to those between 300nm and 1400nm in diameter.[92] While these studies appear to have conflicting results regarding the optimal fiber diameter for chondrogenesis, differences in other experimental parameters including differences in scaffold material, fiber alignment, medium composition, and initial cell seeding density may have contributed to the differences in outcome.

In tissue engineering studies, wide ranges of initial seeding densities have been examined. Seeding densities as low as $1x10^4$ cells/cm^3-scaffold up to $4x10^6$ cells/cm^3-scaffold have been used to examine MSC differentiation into a cartilage phenotype on fibrous scaffolds[80,92]. Even higher seeding densities, up to $100x10^6$ cells/cm^3-scaffold have been used when chondrocytes rather than stem cells were seeded, due to their reduced proliferation potential[95]. Higher seeding densities typically facilitate a greater amount of GAG and collagen produced per construct. However, some studies have found that there is a saturation point where further increases in the number of cells seeded do not result in increased matrix deposition or mechanical properties[96,97], and in some cases may even lead to a decrease in matrix production on a per cell basis[98,99].

To begin to probe how induced chondrogenic differentiation of MSCs may be influenced by cell-cell and cell-biomaterial interactions, we have first examined the chondrogenic activity of human bone marrow-derived MSCs seeded onto electrospun PCL nanofiber and microfiber scaffolds. In addition, initial cell seeding density was also varied to determine if the number of cells on the scaffold influences the chondrogenic potential of the cells seeded onto scaffolds with fibers of different diameters.

2.1 METHODS

2.1.1 Scaffold Fabrication

Nanofiber and microfiber PCL scaffolds were created by electrospinning using a custom made apparatus. PCL (80kDa, Sigma-Aldrich, St. Louis, MO) was dissolved at 40°C overnight in a 1:1

mixture of *N*,*N*-dimethylformamide and tetrahydrofuran (Fisher Scientific, Pittsburgh, PA) at a concentration of 11.5% and 22% w/v for nanofibers and microfibers, respectively. 0.06% w/v sodium chloride was added to the 11.5% solution to increase conductivity and improve homogeneity of fiber diameter. The polymer solution was drawn into a 20 ml syringe connected to a stainless steel needle. A syringe pump (Harvard Apparatus, Holliston, MA) was used to deliver the solution at constant rate of 2.0 ml/hr. Microfibers were electrospun using a 12-inch, 18G blunt-ended needle charged to 8 kV with a high voltage power supply (Gamma High Voltage Research Inc., Ormond, FL) at a distance of 23 cm from the collector. For nanofiber scaffolds, a 4-inch, 22G blunt-ended needle was charged to 13.5 kV at a distance of 15 cm from the collector. The collector was a custom-made grounded aluminum mandrel rotating at 0.75 m/s. Additionally, aluminum shields were placed on either side of the mandrel and plate and charged to either 10 kV or 2 kV for nanofibers and microfibers, respectively, in order to guide the fibers onto the grounded surface. A summary of these conditions is presented in Table 1.

Table 1. Electrospinning parameters of scaffold fabrication

Fiber Type	Nanofibers	Microfibers
PCL concentration (w/v) (%)	11.5	22.0
Solution composition[a]	1:1 DMF:THF + 0.06% NaCl	1:1 DMF:THF
Needle size (gauge)	22	18
Needle to mandrel distance (cm)	15	23
Voltage (kV)	13.5	8.0

[a]DMF=Dimethylformamide (Fisher), THF=Tetrahydrofuran (Fisher)

2.1.2 Scaffold characterization

The structure of microfibers and nanofibers was examined using scanning electron microscopy (SEM) (JSM6335F; JEOL, Peabody, MA). Scaffolds were mounted onto aluminum studs, sputter-coated with 3.5 nm of palladium/gold alloy, and imaged under an accelerating voltage of 5 kV and a working distance of 8 mm. Image analysis for scaffold characterization was performed using a previously validated automated algorithm[100]. Briefly, the average pore size of the scaffolds was determined using SEM images by identifying and isolating the fibers on the surface of the image using a series of threshholding and filtering steps. The same software was also used to estimate fiber diameter by evaluating gradients in pixel intensities along points perpendicular to the fiber direction.

2.1.3 Cell culture and seeding

MSCs were isolated from bone marrow obtained from the femoral heads of patients undergoing total hip arthroplasty with approval from the Institutional Review Board (University of Washington, Seattle, WA and University of Pittsburgh, Pittsburgh, PA). Trabecular bone was isolated and the marrow was harvested using a bone curet and washed with DMEM containing 10% fetal bovine serum (FBS) (Gibco, Carlsbad, CA). The marrow solution was then passed through a 40 μm filter into a 50 mL conical tube and centrifuged for 5 min at 1,100 RPM. The pellet that formed was washed with phosphate buffered saline (PBS), and cells were plated onto tissue culture-treated flasks. Cells were maintained in growth medium consisting of DMEM supplemented with 10% FBS and 1% antibiotic-antimycotic (anti-anti) (Gibco) at 37°C and 5%

CO_2. Cells were passaged when they reached approximately 80% confluency using 0.5% trypsin/EDTA (Gibco), and all experiments were performed using passage 5 MSCs. Scaffolds were cut using a 1 cm diameter punch (McMaster-Carr, Elmhurst, IL) and then hydrated and sterilized in 70% ethanol for 2 hours. Scaffolds were then rinsed with PBS twice for 30 minutes each, and left overnight in growth medium. To seed MSCs onto scaffolds, cells were first trypsinized, resuspended and 50 μl of the solution was pipetted onto scaffolds to give initial cell seeding densities of 100,000 (100k), 500,000 (500k), 2,000,000 (2,000k) or 4,000,000 (4,000k) cells/cm^3 of scaffold. Cells were allowed to attach for 2 hours prior to adding 1 ml of growth medium to each well of a 24-well plate coated with Sigmacote (Sigma).

2.1.4 Chondrogenic differentiation

After 24 hours of culture, growth medium was replaced with 2 ml of chondrogenic medium (Appendix A) and constructs were maintained at 37°C and 5% CO_2. Medium was changed every 3 days for 3 to 6 weeks prior to harvesting.

2.1.5 RNA isolation and quantitative polymerase chain reaction (qPCR)

Constructs from each group were rinsed with PBS, minced and placed into tubes. Six scaffolds were pooled into each tube in order to obtain sufficient RNA from low seeding density scaffolds. 700 μl of TRIZOL (Invitrogen, Carlsbad, CA) was then added to each tube and the scaffolds were manually homogenized before storing at -80°C until the next step was performed. After addition of 140 μl of chloroform (Fisher Scientific), each solution was incubated at room temperature for 5 minutes prior to centrifuging at 12,000 rpm and 4°C for 15 min. One volume

of 70% ethanol was added to each sample followed by completing the RNA extraction using the RNeasy Micro Kit (Qiagen, Valencia, CA) following the manufacturer's protocol. The concentration and purity of RNA was determined using a Nanodrop 2000c (Thermoscientific NanoDrop Technologies, Wilmington, DE). 200 ng of RNA from each sample was reverse transcribed into cDNA using the SuperScript III First-Strand Synthesis Super Mix (Invitrogen) following the manufacturers protocol using Oligo$(dT)_{20}$ primers.

Gene-specific primers were designed using Primer-Blast software (NIH, Bethesda, MD)[101] and purchased from Integrated DNA Technologies (IDT, Coralville, IA). The primer concentrations and annealing temperatures were optimized for efficiency (95-105% efficiency) and specificity (melting curve analysis and product size by electrophoresis). Information for the genes analyzed (aggrecan, ACAN; collagen type II, COL2; collagen type I, COL1), including primer sequences, annealing temperatures, and concentrations, is provided in Appendix B.

cDNA (10 ng) was added to 10 μl SYBR® Green PCR mastermix (Applied Biosystems, Carlsbad, CA) and 150 nM primers to a final volume of 20 μl and qPCR was performed using the StepOnePlus Real-Time PCR system (Applied Biosystems). After initial denaturation at 95°C for 10 min, 40 cycles of 15 sec at 95°C and 1 min at the primer-specific annealing temperature were completed to amplify DNA. Quantification of the target gene expression, relative to the 100k nanofiber sample at each time point, was performed using the $\Delta\Delta C_T$ method with cyclophilin A used as an endogenous control.

2.1.6 Biochemical Assays

After washing with PBS, constructs were lyophilized and digested for 18 hours in 200 μl of a papain solution (125 μg/ml papain, 50 mmol sodium phosphate buffer, 2 mmol N-acetyl cysteine (Sigma), pH 6.5). Following digestion, samples were stored at -20°C. The DNA content in the scaffolds was quantified using the Quant-iT PicoGreen dsDNA Assay Kit (Invitrogen), following the manufacturers protocol. The fluorescence of the PicoGreen-DNA solution was measured using a Synergy HT plate reader (BioTek, Highland Park, VT) at an excitation/emission of 485/528 nm, and DNA content in the samples was estimated using the DNA standard provided in the kit. Quantification of sulfated GAGs in the scaffolds was performed using a commercial Blyscan Glycosaminoglycan Assay kit (Accurate Chemical & Scientific, Westbury, NY). The absorbance at 656nm was measured using a plate reader and a chondroitin-4-sulfate solution provided with the kit was used as a standard. The collagen content of the scaffolds was determined using a modified hydroxyproline assay[102] using bovine collagen type I as a standard. Briefly, each sample and standard were hydrolyzed with 125 μl of 4N sodium hydroxide (Fisher) at 121°C for 20 min. 125 μl of 4N hydrochloric acid (Fisher) added added and the solution was titrated to a neutral pH. 187.5 μl of chloramine-T solution (Sigma) (14.1 g/L chloramine-T, 50 g/L citric acid, 120 g/L sodium acetate trihydrate, 34 g sodium hydroxide, 0.21M acetic acid) was incubated with the sample at room temperature for 25 min followed by addition of 187.5 μl of 15 g/L p-dimethylaminobenzaldehyde in 2:1 isopropanol:perchloric acid and incubation in a 60°C water bath for 20 min. Finally, 200 μl of each sample in triplicate was added into a 96 well plate and absorbance was read at 550 nm.

2.1.7 Immunofluorescence & confocal laser scanning microscopy

Whole mounts were utilized for examination of matrix components. Briefly, constructs were fixed in 4% paraformaldehyde for 20 minutes, washed, and stored in PBS at 4°C until staining was performed.

Details about primary and secondary antibodies used can be found in Appendix C. Prior to antibody application, enzymatic antigen retrieval was performed, with constructs incubated in 0.1% pepsin in 0.01 HCl, pH 3.0 for 20 minutes at 37°C to unmask antigens. Following retrieval, non-specific antibody binding was blocked with 5% normal goat serum (Vector) for 1 hour, followed by incubation with primary antibodies for collagen types I and II overnight at 4°C. Following washing with 0.5% bovine serum albumin in PBS, scaffolds were then incubated for 1 hour with the appropriate AlexaFluor fluorescent secondary antibodies (Invitrogen). Nuclei were stained using 40,6-diamidino-2-phenylindole (DAPI; 1:10000; Invitrogen) for 2 minutes. Negative controls included omission of the primary antibody as well as species-specific isotype controls.

Scaffolds were imaged by confocal laser scanning microscopy (CLSM; Fluoview 1000; Olympus, Center Valley, PA) and image processing and analysis were performed using NIS Elements software (Nikon Instruments, Inc., Melville, NY). Scaffolds were cut in half and nuclei were examined in cross-section in order to visualize the cell distribution through the scaffold thickness. Stacks of 10 images were acquired with 5 μm between each image and flattened. A separate image was acquired by increasing the laser intensity until scaffold autofluorescence was

sufficient to visualize the edge of the scaffold. The distance between the edge of the scaffold and the deepest nucleus was measured to determine the overall depth of cell penetration from the scaffold surface.

En face imaging of scaffolds to detect collagen types I and II, and to quantify cell density was also performed using CLSM. Images for nuclear quantification were taken 20μm deep in 2 μm increments, while staining for collagen types I and II were visualized simultaneously to determine their respective distributions on the scaffold. Three images on different scaffolds were acquired and the number of cells was counted to determine the overall cell density as well as examine the collagen distribution.

2.1.8 Statistical Analysis

All data were expressed at mean ± standard deviation. Statistical analysis was performed using two-way analysis of variance with Tukey's *post-hoc* test for multiple comparisons. A threshold of $p<0.05$ was used to determine statistical significance.

2.2 RESULTS

2.2.1 Scaffold characterization

Electrospun nanofiber scaffolds had an average of diameter of 445±173 nm, an average pore size of 1.2 μm^2 and an overall porosity of 88%, while microfiber scaffolds had average diameter of 4.37±0.78 μm, an average pore size of 91 μm^2, and an overall porosity of 90% (Figure 1).

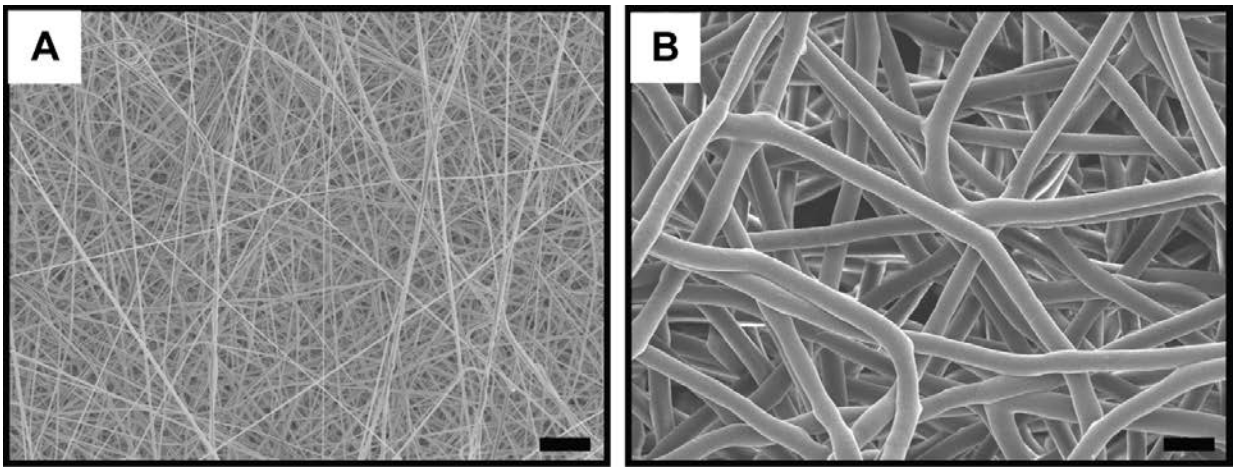

Figure 1. SEM of nanofibers and microfibers

(A) Nanofiber scaffolds have a diameter of 445±173 nm and an average pore size of 1.2 μm^2. (B) Microfiber scaffolds have a diameter of 4.37±0.78 μm and an average pore size of 91 μm^2 Images were taken at 1000x magnification. Scale bars =10μm.

2.2.2 Gene expression

At 3 and 6 weeks following induction of chondrogenic differentiation, ACAN expression was significantly higher overall when cells were seeded on microfibers in comparison to nanofibers (Figure 2a,b). Within each initial seeding density, post-hoc analysis showed significant differences at week 3 between microfibers and nanofibers in the two higher seeding density groups, and expression was significantly greater with an initial seeding density of at least 2,000k cells/cm^3 than in the lower seeding density groups, although no significant differences were found between 2,000k and 4,000k groups. At week 6 there were no significant differences between expression in 500k, 2,000k and 4,000k microfiber groups, and while 500k and 2,000k groups had higher ACAN expression on microfibers than nanofibers, while there was seemingly no difference in expression between nanofibers and microfibers at the 4,000k seeding density.

COL1 and COL2 gene expression at week 3 followed a similar trend, with higher seeding densities showing increased expression on microfibers in comparison to nanofibers. At week 6, however, COL1 expression was similar in microfibers and nanofibers in the 2,000k group and significantly decreased on microfibers in the 4,000k group, while COL2 expression remained high (Figure 2c-f). Finally, the COL2/COL1 ratio, where high values indicate a more hyaline cartilage phenotype, was significantly greater at both 3 and 6 weeks for the higher seeding densities on microfibers than nanofibers and in comparison to the lower seeding densities (Figure 2g,h).

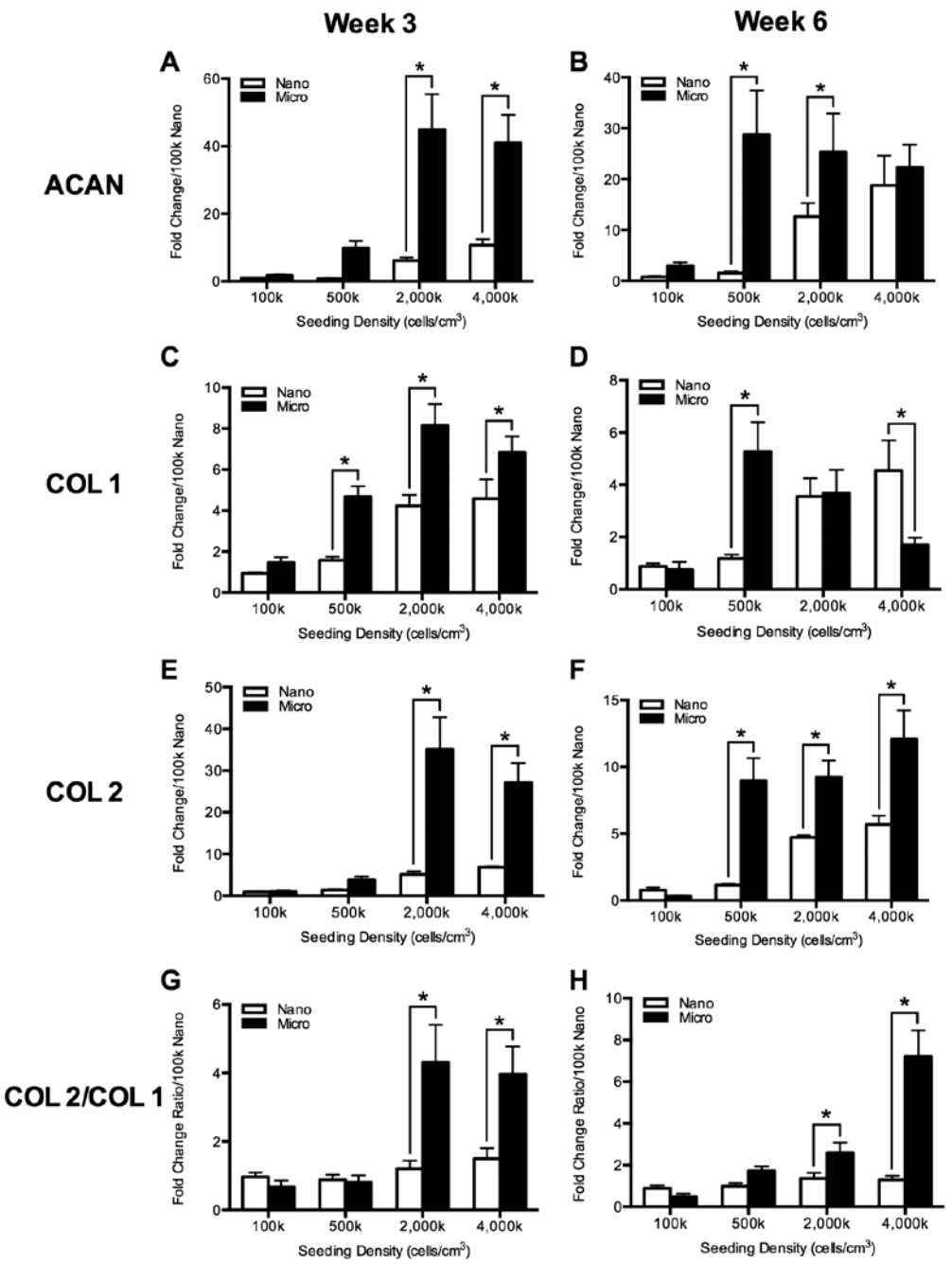

Figure 2. Gene expression on microfiber and nanofiber scaffolds at different seeding densities.

Quantification of relative mRNA expression for chondrogenic markers after 3 and 6 weeks of culture. Fold change differences in gene expression normalized to the 100k cells/cm^3-scaffold group at each time point. COL2/COL1 ratio represents the ratio of COL2 to COL1 expression. *$p<0.05$, n=3.

2.2.3 Biochemical characterization

There were no significant differences in DNA content seen between microfiber and nanofiber groups on Day 1 after seeding (Figure 3a). However, the DNA content in scaffolds at week 3 was significantly higher overall in microfibers than nanofibers, and significantly more DNA was found in microfiber than nanofiber constructs in the high initial seeding density group (Figure 3b). There was also no significant difference between the amount of DNA in the 2,000k and 4,000k groups seeding on scaffolds with the same fiber diameter. A similar trend was seen in week 6, with a significantly higher amount of DNA also found on microfibers in the 500k group (Figure 3c).

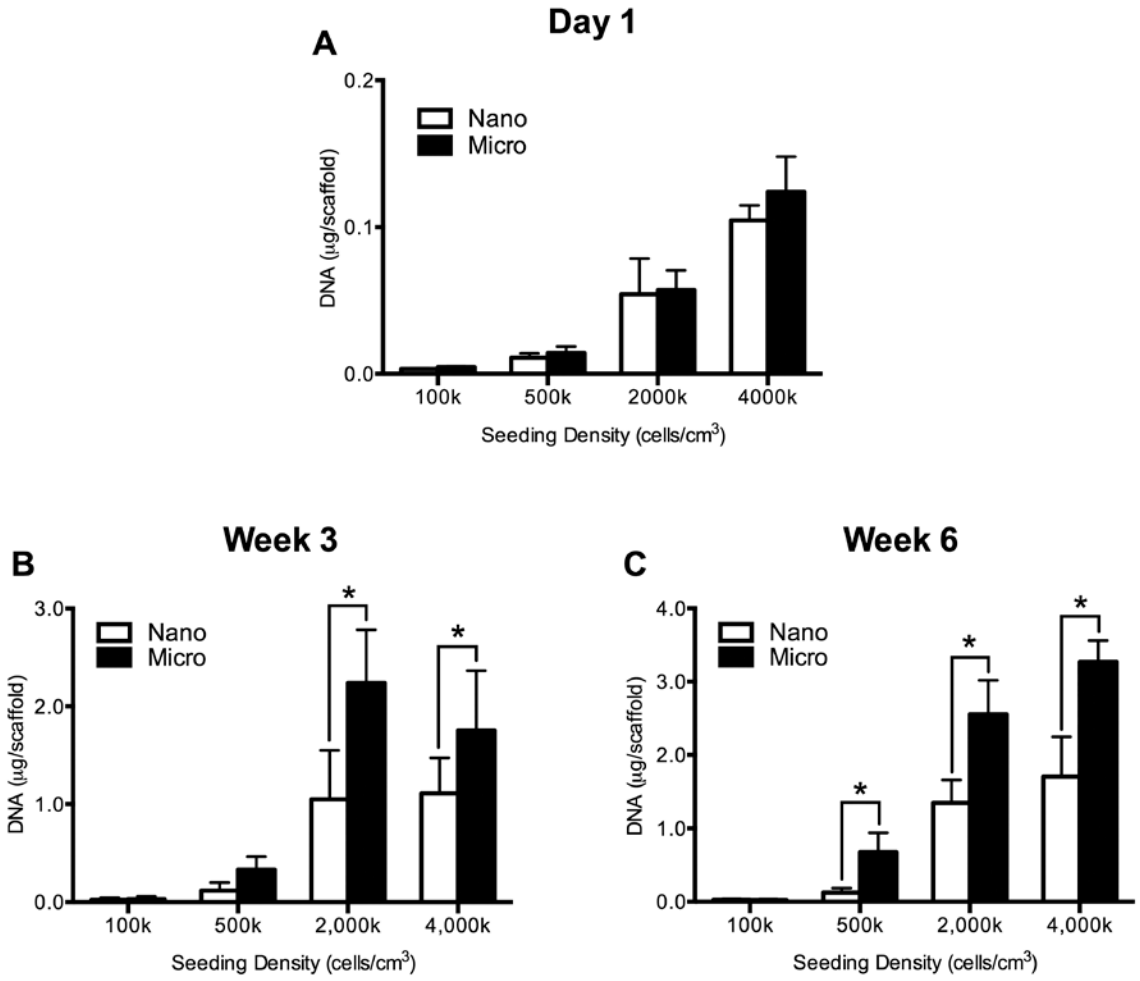

Figure 3. DNA content for microfiber and nanofiber scaffolds at different seeding densities.
(A) 1 day, (B) 3 weeks, and (C) 6 weeks after seeding. *$p<0.05$, n=6.

GAG production paralleled the DNA content at the week 3 time point, with significantly more GAG being produced by high seeding density microfiber groups (Figure 4a). However, there was no significant difference when the GAG was normalized to DNA content, suggesting that on a per cell basis, there were similar amounts of GAG production on the different scaffold times (Figure 4c). The GAG production at week 3 in the 100k or 500k groups was below the level of detection of the assay and thus was excluded in the analysis. At week 6, both the total GAG and the GAG/DNA values were significantly higher in the 2,000k and 4,000k groups (Figure 4b). The 500k group produced enough GAG to meet the assay's threshold of detection at the 6 week time point, and while the total GAG production was lower than the higher seeding density groups, the GAG/DNA in the 500k group was not significantly different at 6 weeks than the 2,000k group (Figure 4d).

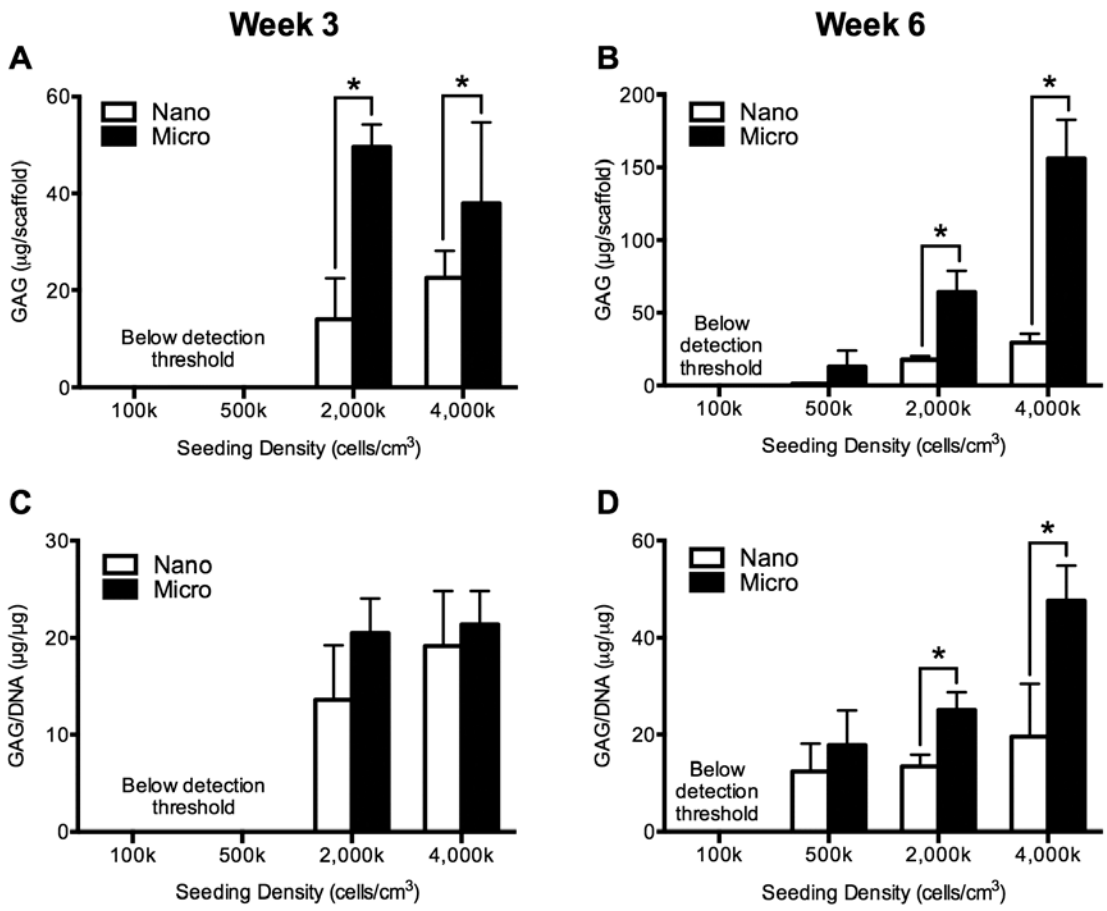

Figure 4. GAG deposition on microfiber and nanofiber scaffolds at different seeding densities

Total GAG/scaffold at (A) 3 weeks and (B) 6 weeks. GAG normalized to DNA at (C) 3 weeks and (D) 6 weeks. *$p<0.05$, n=6.

Trends in total collagen production and collagen/DNA were similar to those seen with GAG production, with the addition of the 500k group having significantly higher collagen deposition on microfibers than nanofibers at week 6 both in terms of total collagen and collagen/DNA. Furthermore, there were no significant differences seen in the amount of collagen/DNA in any of the detectable groups seeded on microfibers.

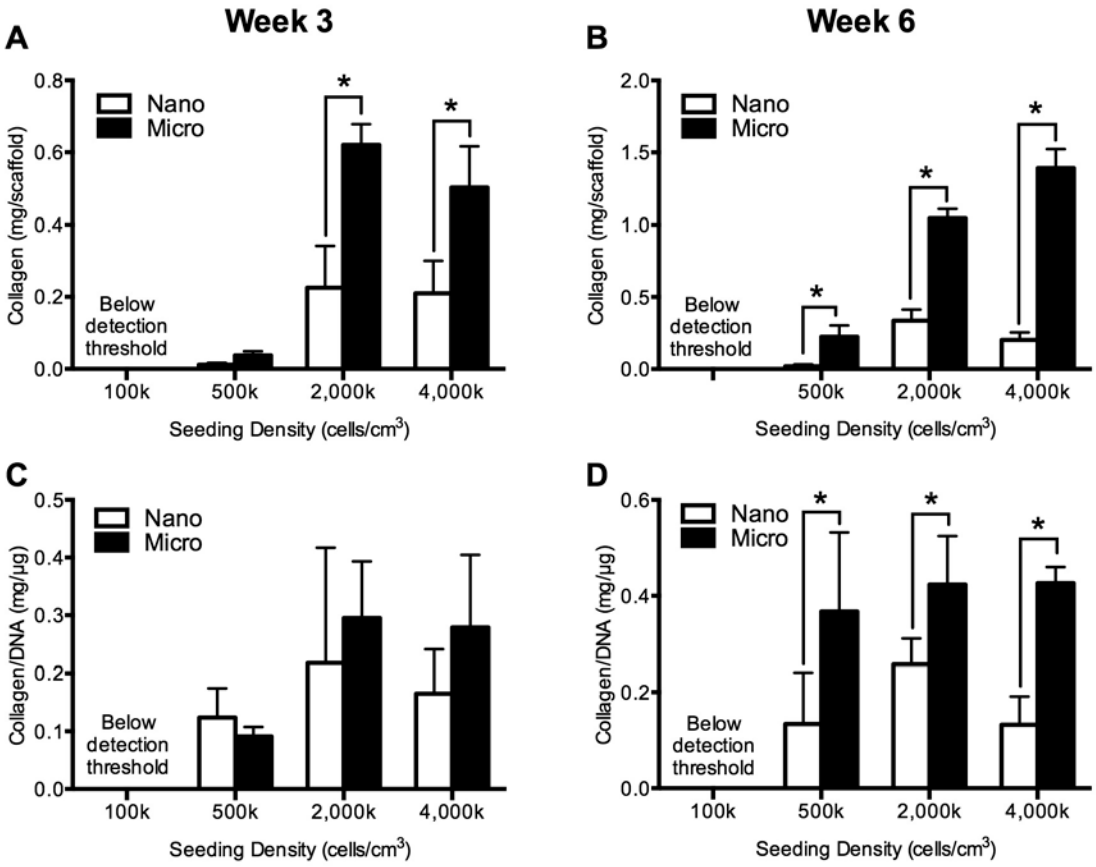

Figure 5. Collagen deposition on microfiber and nanofiber scaffolds at different seeding densities

Total GAG/scaffold at (A) 3 weeks and (B) 6 weeks. GAG normalized to DNA at (C) 3 weeks and (D) 6 weeks. *$p<0.05$, n=6.

2.2.4 Cell distribution and matrix deposition

Cross-sectional views of scaffolds stained nuclei are shown in Figure 6. While cells were found to be present throughout the entire depth of the microfiber scaffolds, on nanofiber scaffolds they were restricted to the scaffold surface. The depth of penetration of cells on nanofibers was approximately 25 μm for both 100k and 500k groups, while cells penetrated somewhat deeper with higher seeding densities, reaching depths of ~50 and 85 μm for the 200k and 400k groups, respectively.

Scaffolds seeded with 100k or 500k cells/cm^3-scaffold stained positively for collagen type I around sparse nuclei, but were negative for collagen type II (Figure 7). At high seeding densities, collagen type I aligned parallel to the surface of the scaffold was seen on all groups (Figure 8). Only nanofibers seeded at the highest density stained positively for collagen type II, while both the 2000k and 4000k microfiber groups appeared to have similar amounts and structure of collagen type II deposition. Images taken at the edge of 4,000k nanofiber and microfiber groups display some differences in the arrangement of collagen fibers. While collagen type II staining appears to be mainly on the surface of microfibers, with collagen type I below, the collagen type II staining appears to be mixed within the same layer as the collagen type I on nanofiber scaffolds (Figure 9).

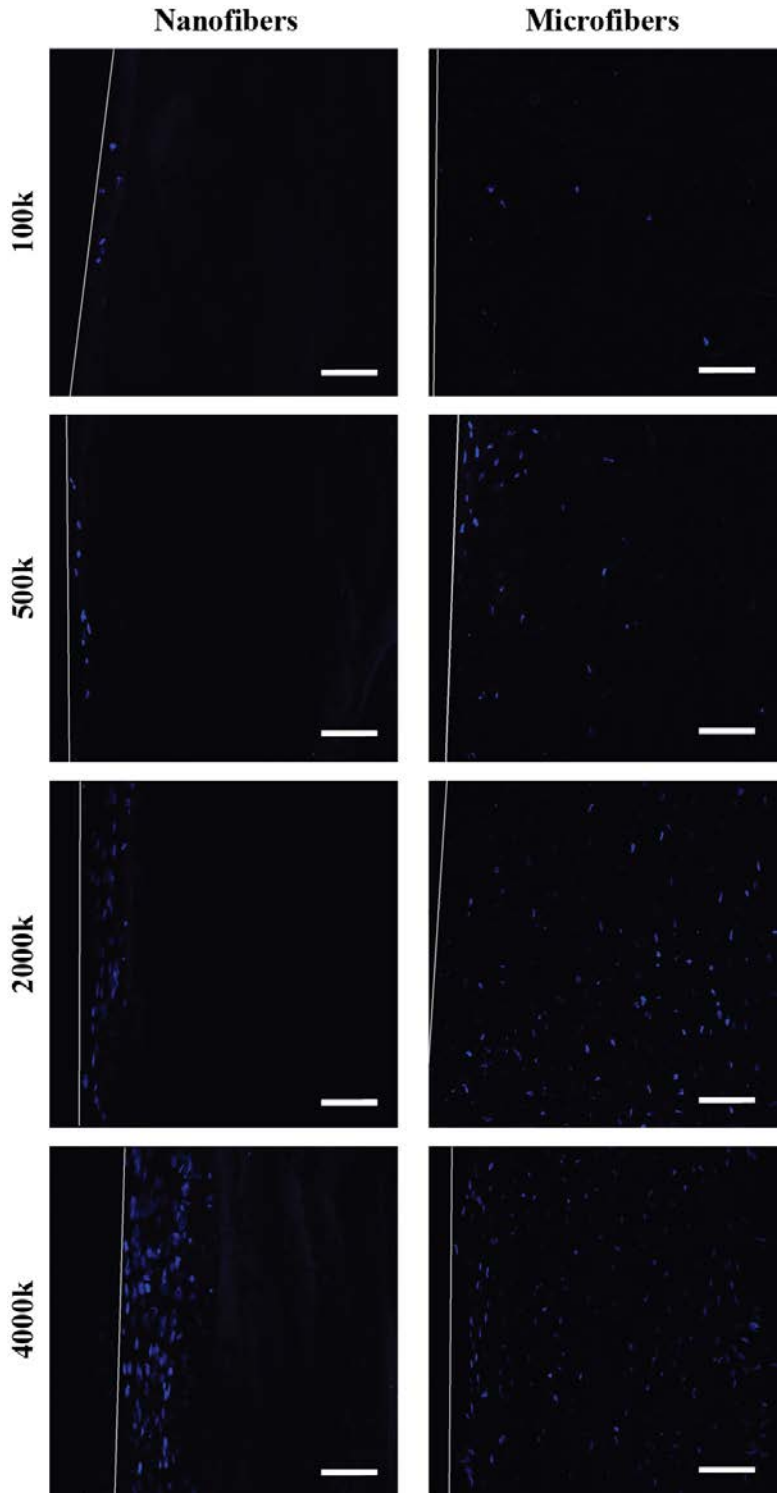

Figure 6. Cross-sections of scaffolds with fluorescently stained nuclei to evaluate cell penetration
Nuclei are stained with DAPI (blue). White lines indicate the edge of the scaffold. Images taken at 10x, scale bar = 200 μm.

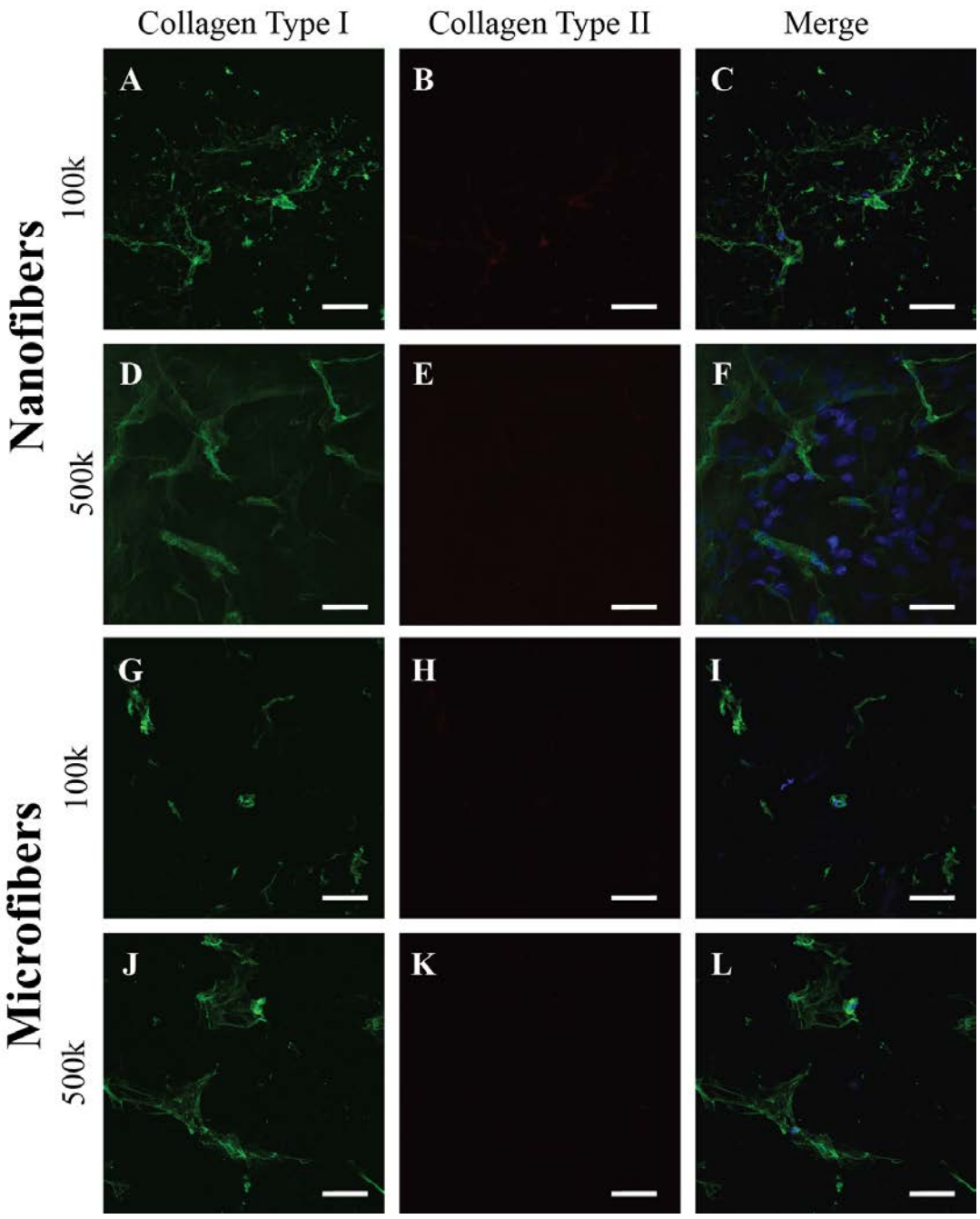

Figure 7. Confocal fluorescence microscopy images of scaffolds with low initial cell seeding density.
Nanofibers seeded with 100k (A-C) and 500k (D-F) cells/cm^3-scaffolds and microfibers seeded with 100k (G-I) and 500k (J-L) cells/cm^3-scaffolds. And stained for collagen type I (green) and collagen type II (red). Nuclei are stained with DAPI (blue) in the merged image. Images taken at 40x, scale bar = 50 µm.

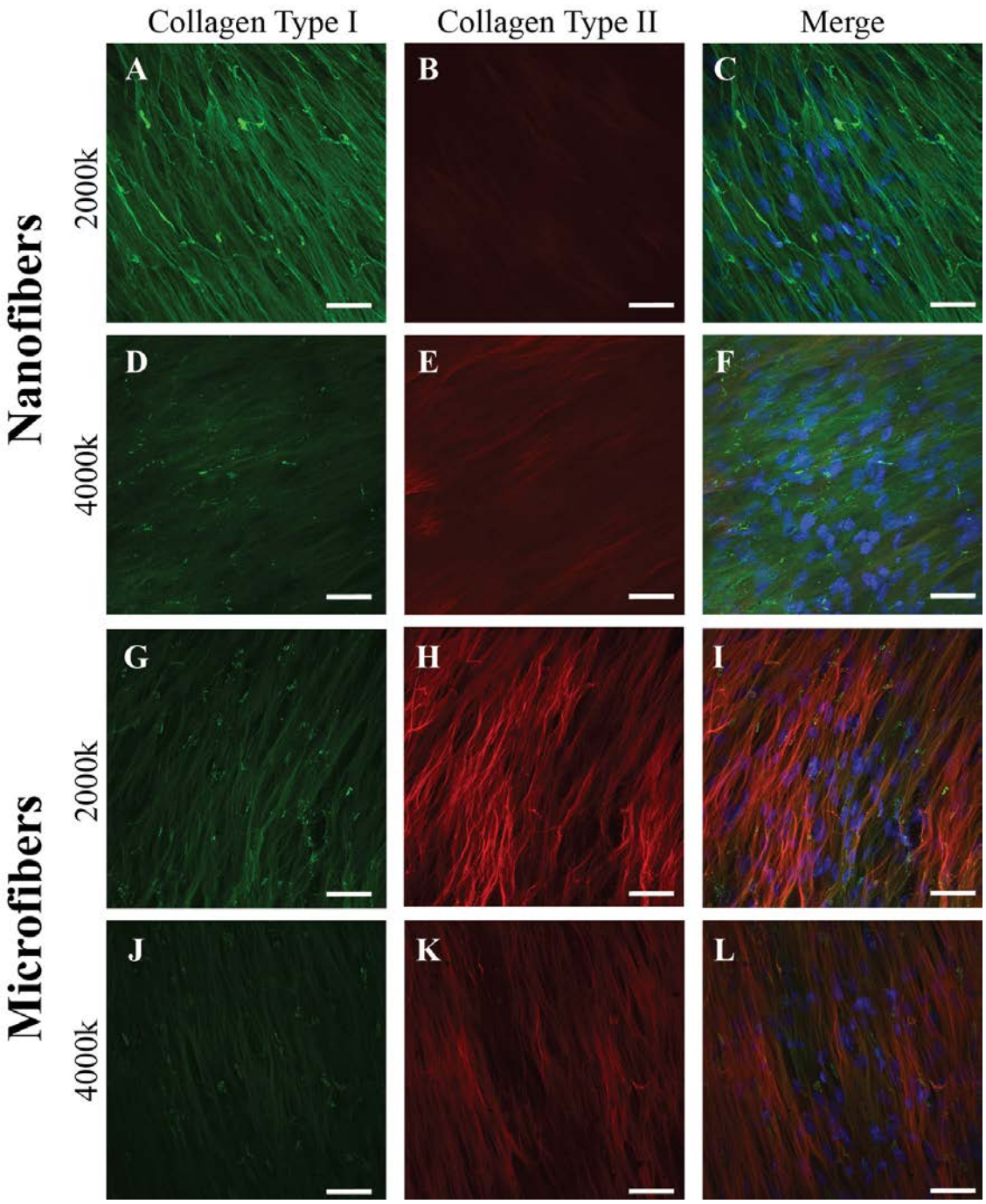

Figure 8. Confocal fluorescence microscopy images of scaffolds with high initial cell seeding density.
Nanofibers seeded with 2000k (A-C) and 4000k (D-F) cells/cm^3-scaffolds and microfibers seeded with 2000k (G-I) and 4000k (J-L) cells/cm^3-scaffolds. And stained for collagen type I (green) and collagen type II (red). Nuclei are stained with DAPI (blue). Nuclei are stained with DAPI (blue) in the merged image. Images taken at 40x, scale bar = 50 µm.

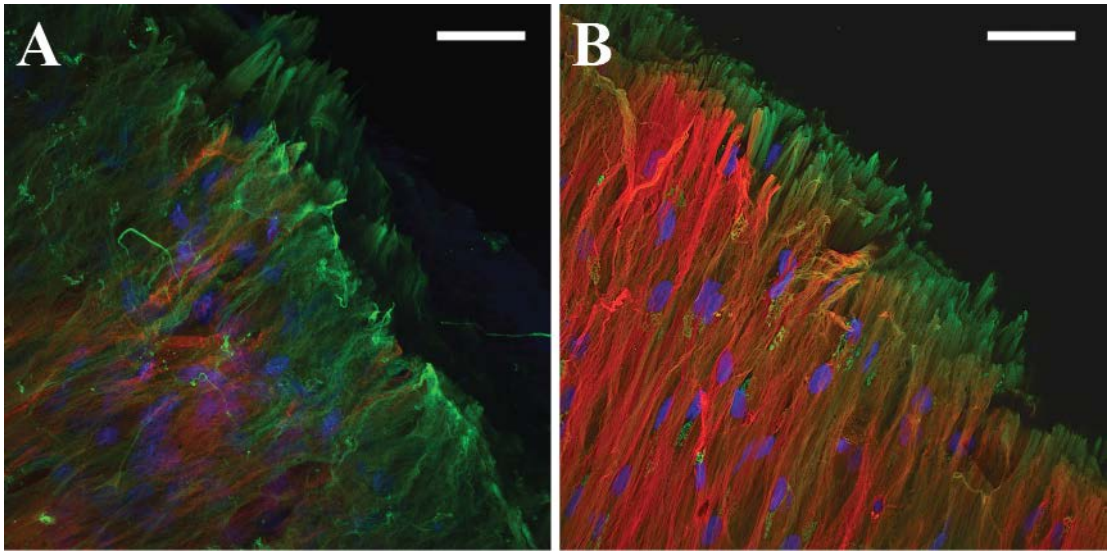

Figure 9. Collagen organization on edge of scaffolds seeded with a high initial cell density after 6 weeks
(A) Nanofibers with 4000k cells/cm^3-scaffold; (B) Microfibers with 4000k cells/cm^3-scaffold; Collagen type I (green), Collagen type II (red), DAPI (blue); Images taken at 40x, scale bar = 50 µm

2.3 DISCUSSION

Previous studies examining the effects of fiber diameter on chondrogenesis are difficult to compare due to variations not only in the fiber diameters and cell seeding densities used, but also other variables including the scaffold material, fiber alignment, cell type, medium composition, time points analyzed, and the methods used to determine the outcomes. Thus, although the results between studies may appear to be conflicting, with some suggesting that nanofibers induce better cartilage formation than microfibers while others conclude the opposite, these differences could in fact be attributable to other experimental variables that are not controlled for between studies. The results of this study suggest that scaffold diameter plays an important role in the chondrogenic differentiation of MSCs on PCL scaffolds *in vitro.* Furthermore, the effects of varying the fiber diameter are dependent on the initial cell seeding density.

Under the culture conditions utilized in this study, using microfiber scaffolds and higher cell seeding densities resulted in optimal chondrogenesis. This is likely in part due to differences in pore size between microfiber and nanofiber scaffolds. While the overall porosities of the scaffolds were similar, the average pore size of nanofiber scaffolds was approximately 75 times smaller than microfiber scaffolds. Since the average diameter of human MSCs in suspension is approximately 10-20μm,[103,104] it is unlikely cells would be able to penetrate into a scaffold with a pore size of only 1.2 μm^2 and thus would require significant modification of the scaffold organization to migrate to the center of the scaffold. In this experiment, only between 2% and 10% of the scaffold thickness was colonized by MSCs on nanofibers, while cells seeded onto the microfiber scaffolds containing larger pores were able to migrate throughout the entire depth of the scaffold and establish a relatively homogeneous cell distribution with high seeding densities.

In effect, reducing the pore size severely limits the surface area to which cells can attach, and may provide a partial explanation for the reduced tissue formation on nanofibers in comparison to microfiber scaffolds.

The first cellular step in mesenchymal chondrogenic differentiation is condensation of MSCs into high-density cell aggregates. Formation of these cell-cell contacts are mediated by adhesion molecules such as N-cadherin and N-CAM, and are essential for successful cartilage formation.[4] Following formation of these interactions, cells undergo commitment to the chondrogenic lineage and begin expression the transcription factor Sox9. When cells are seeded at a very low density, the potential for cell-cell interactions is limited, and therefore chondrogenic differentiation is likely to be reduced. In this study, seeding cells at a very low density (100k cells/cm^3-scaffold) resulted in low chondrogenic gene expression and protein production. There were no significant differences in chondrogenic gene expression or cell number between microfiber and nanofiber scaffolds, and the amounts of secreted collagen and GAG were not sufficient to be detected with the assays utilized. Immunofluorescence showed limited collagen type I deposition and staining for collagen type II was absent, with no apparent differences between microfiber and nanofiber scaffolds. These results therefore suggest that low seeding densities have limited utility for studying chondrogenesis on electrospun fibers, independent of the scaffold diameter.

During articular cartilage development, ECM composed of collagen type I in addition to other cell-adhesion molecules is initially deposited by MSCs prior to differentiation[4,105]. This profile of collagen type gene expression is thus different from that seen in the forming endochondral cartilage growth plate, where collagen type II expression is dominant. As differentiation commences following condensation, a shift towards a phenotype with high

collagen type II and proteoglycan deposition occurs. A similar pattern is seen in this experiment with microfiber constructs seeded at high initial cell densities. Gene expression of COL1 in addition to COL2 and ACAN is higher on microfibers at the 3-week time point, suggesting that cells may still be in a somewhat proliferative state, but are shifting towards differentiation and increased collagen type II and proteoglycan production. Confirmation of this is seen after 6 weeks in culture, where expression of COL1 on microfibers decreases in comparison to nanofibers. GAG and collagen protein deposition follow a similar pattern to gene expression, and immunofluorescence staining shows the presence of collagen type II on the surface of the construct in addition to collagen type I. In comparison, cells seeded on nanofibers also stain positively for both type I and collagen type II, but seem to have less collagen type II than microfibers. Thus, it appears that at high initial cell seeding densities, the microfibrous PCL scaffolds used in this study more efficiently promote an articular cartilage phenotype and related ECM protein deposition than nanofibrous scaffolds.

While seeding densities of 2,000k cells/cm^3-scaffold and higher appear to be superior for chondrogenesis, the lower seeding densities also provide some insight into cell behavior on scaffolds of different diameters. Adult human articular cartilage has an overall cell density of approximately $20x10^6$ cells/cm^3, while newborns may have cell densities that are 6-7 times higher.[106] The cell density near the surface of the scaffolds after 6 weeks of culture was between adult and newborn values on both nanofibers and microfibers for all groups except for the 100k seeding density group, suggesting that seeding densities of 500k cells/cm^3-scaffold or higher are likely to be needed for successful regeneration of cartilage tissue using MSCs.

After 6 weeks of culture, chondrogenic gene expression in the 500k group on microfibers increased to levels similar to the higher density groups and GAG and collagen production increased, indicating that chondrogenic differentiation is delayed at this seeding density, but can be induced over time. This delayed chondrogenic induction may be attributable to the number of cells reaching a threshold in cell density where enough cell-cell contacts are formed to induce chondrogenesis, and therefore stimulate increased expression of ACAN and COL2 as well as increased GAG and collagen deposition.

There were no significant differences in the number of cells attached to microfiber and nanofiber scaffolds one day after seeding. This suggests that the greater number of cells as well as higher chondrogenic gene expression and protein production on microfibers are due to differences in the scaffold architecture that influence cell behavior and are not simply a direct result of the seeding efficiency being higher for microfiber scaffolds. One explanation is that while both of the high-density seeding groups have a cell density sufficient to induce chondrogenesis, the presence of cells throughout the entire thickness of the microfibers results in a larger area for cells to migrate and deposit ECM. Since cells cannot migrate deeply into the nanofiber scaffold, tissue deposition is restricted to the surface. During the early periods of culture, cells on both types of scaffolds deposit ECM molecules at a similar rate due to an abundance of space surrounding each cell. However, with the reduced pore size, cells seeded on nanofibers have a limited area to which they can migrate, and may become surrounded by the ECM more quickly. This may lead to slowing of matrix protein secretion, thus resulting in decreased GAG and collagen per cell in comparison to microfiber constructs seen at the 6-week time point.

Another potential contributor to the enhanced chondrogenesis on microfibers may be that even though the overall void area is similar in microfibers and nanofibers, the architecture of the microfiber scaffolds promotes the clustering of cells between fibers while cells seeded on nanofibers are more likely to attach and spread out across fibers, limiting their interactions with other cells. The reduced cell-matrix communications and the forced clustering due to the fiber spacing may result in promotion of the cell-cell interactions that are required for induction of chondrogenesis. This phenomenon was also considered in a previous study examining cell behavior on PLLA scaffolds having different diameter and pore sizes, with MSC chondrogenesis enhanced on larger fibers with larger average pore size.[92] Studies conducted in our laboratory and by others have shown enhanced chondrogenic gene expression and a more round cellular morphology, characteristic of those cells found below the superficial zone of native cartilage, when chondrocytes are seeded onto nanofiber scaffolds than nanofiber scaffolds.[93,94] However this may be an effect of the phenotype of the cells, with chondrocytes benefiting from being exposed to a nanofibrous environment more similar to that seen in the native cartilage matrix, while MSC differentiation is enhanced under conditions similar to those found during development. Increasing the cell seeding density would increase the initial packing of cells between microfibers, thus promoting chondrogenesis in the higher seeding density groups in comparison to the lower seeding groups.

Cell morphology on scaffolds may also provide some insight into the differences in cell behavior on microfiber and nanofiber scaffolds. In native cartilage, the superficial zone is a thin layer containing flattened chondrocytes, while in the intermediate and deep zones chondrocytes are more round. A similar morphology is found on microfiber scaffolds seeded at high cell densities. In contrast, cells seeded on nanofiber scaffolds appear to mostly form a thicker layer of

flattened superficial zone-like cells near the surface of the scaffold. *In vivo*, the cells of the intermediate and deep zones are the main synthesizers of proteoglycans, which could explain the decreased GAG formation in these scaffolds, and there is also evidence that collagen expression is higher in these areas as well.[107]

The results of this study strongly suggest that seeding MSCs onto microfibers promotes chondrogenesis better than nanofibers, although it remains unclear whether the differences are simply due to increased pore size leading to enhanced cell penetration, or if other aspects of the scaffold architecture are influencing differentiation. Additionally, while studies often utilize lower seeding densities to reduce cell-cell interactions and increase cell-material interactions to understand the role of materials on cell behavior, this may not be useful in cartilage tissue engineering applications due to the importance of the cell-cell interactions in inducing chondrogenic differentiation. Future studies seeding MSCs at high densities onto microfiber and nanofiber scaffolds fabricated to have similar pore size may provide additional insight into optimal environmental conditions for developing a tissue engineered cartilage construct.

2.4 CONCLUSION

In conclusion, utilizing the three-pronged approach to tissue engineering strategies combining scaffolds, cells, and other bioactive stimulants creates a large number of potential variables that can influence experimental outcomes and makes comparing between studies difficult. In this experiment, we examined two variables at the same time—seeding density and fiber diameter—in order to more fully understand the role that each of these variables play in influencing interactions that occur between MSCs and electrospun fibers under *in vitro* chondrogenic

conditions. Our findings suggest that seeding MSCs at a high initial density onto a microfibrous scaffold that facilitates cell-cell interactions while allowing for cells to migrate throughout the entire thickness, stimulates chondrogenesis *in vitro* more effectively in comparison to using nanofiber scaffolds and/or low seeding densities.

If only low seeding densities had been utilized in this study, it may have been concluded that the fiber diameter was unimportant for chondrogenesis. Or, if only nanofibers had been utilized, the knowledge gained by understanding the potential importance of pore size and cell infiltration in conjunction with seeding density would have been lost. While it is not feasible to test all potential combinations of culture parameters at once, understanding the interplay between different parameters by examining multiple variables may be a beneficial strategy in attempting to a successful tissue engineered construct.

3.0 EFFECTS OF CELL SOURCE AND FIBER DIAMETER ON CHONDROGENIC AND OSTEOGENIC MESENCHYMAL STEM CELL DIFFERENTIATION

3.0 INTRODUCTION

In Section 2 above, we demonstrated that the fiber diameter plays an important role in chondrogenesis of BMSCs on PCL scaffolds. In addition to the scaffold, choosing the optimal cell type is essential. MSCs are an attractive cell source since they can be obtained either autologously or allogenically, differentiated into multiple cell types, and expanded *in vitro* while maintaining their multipotential character. Additionally, mimicking the *in vivo* developmental process may enhance tissue formation, and MSCs are the precursors to the terminally differentiated cells found in musculoskeletal tissues including bone and cartilage. MSCs have been isolated from several different locations including bone marrow, adipose tissue, synovium, muscle, and umbilical cord and peripheral blood[108]. BMSCs are the most commonly used type of MSC, with excellent differentiation potential and even immunomodulatory and immunosuppressive properties. However, isolation of bone marrow is a painful procedure that carries some risk, and the isolation efficiency is low, necessitating *in vitro* expansion to obtain sufficient cell numbers. Another source of MSCs that is gaining popularity are adipose-derived

stem cells (ADSCs). ADSCs are an appealing cell source for tissue engineering of musculoskeletal tissues due to ease of obtaining large quantities of cells which reduces the time needed for *in vitro* culture, along with minimal risk and discomfort caused by the procedure.

Previous studies have shown that both BMSCs and ADSCs have the ability to undergo chondrogenic, osteogenic and adipogenic differentiation[109]. Some past reports have suggested that ADSCs do not undergo as robust chondrogenesis as BMSCs[110–112]. However, other studies have shown that this limitation can be overcome by altering the media composition, specifically by including BMP-2 or BMP-6 in addition to TGF-β in the cell culture medium[113–116]. Similarly, BMSCs have been suggested to have greater osteogenic potential than ADSCs[109,117,118]. However, all of these studies were performed in monolayer and not in 3D culture. Only a few studies have examined the chondrogenic and osteogenic potential of ADSCs on electrospun scaffolds[71,119–122], and none have compared BMSCs and ADSCs, nor the effects of fiber diameter on ADSC differentiation.

In this study, we investigated the effects of fiber diameter and MSC source on both chondrogenesis and osteogenesis in order to determine if the cell source or fiber diameter affects the formation of tissue engineered cartilage or bone constructs.

3.1 MATERIALS & METHODS

3.1.1 Electrospinning

PCL (80 kDa, Sigma-Aldrich, St. Louis, MO) microfiber and nanofiber scaffolds were fabricated using a custom-made electrospinning device as previously described in Section 2.2.1. Fibers were collected on the electrically grounded mandrel until the sheets reached approximately 1 mm in thickness.

3.1.2 Scaffold characterization

Images of microfibers and nanofiber scaffolds were taken by SEM and the pore size and fiber diameter were analyzed using an automated algorithm as described in Section 2.2.2.

3.1.3 Cell culture

Bone marrow-derived MSCs (BMSCs) were isolated using a standard technique based on adhesion to tissue culture plastic as described previously in section 2.2.3.

Adipose-derived stem cells (ADSCs) were isolated with IRB approval (University of Pittsburgh, Pittsburgh, PA) from donor lipoaspirate using the automated Icellator Cell Isolation System (Tissue Genesis, Honolulu, HI). The isolated cells were seeded into tissue culture flasks and cultured in proliferation medium composed of DMEM with 10% FBS and 1% antibiotic-antimycotic.

For each cell type, cells from three age- and sex-matched donors (females age 28 to 55 years of age) were pooled at passage 1. During expansion, when cells reached approximately 80% confluency, they were detached from flasks with 0.5% trypsin/EDTA (Gibco), pelleted, resuspended and reseeded at $5x10^3$ cells/cm^2 in fresh proliferation medium.

3.1.4 Cell seeding

1 cm diameter scaffolds were cut and hydrated as described in section 2.2.3. Passage 5 cells were pipetted onto the scaffold surface at a density of $2x10^6$ cells/ml of scaffold in 50 μl of medium. Constructs were placed into individual wells of non-treated 24-well plates coated with Sigmacote (Sigma, St. Louis, MO) and incubated for 2 hours to allow for cell adhesion, followed by addition of 1 ml of proliferation medium to each well. The following day, the proliferation medium was replaced with 2 ml of either chondrogenic medium or osteogenic medium Appendix A to induce differentiation. Medium was changed every 3 days and constructs were harvested after 3 and 6 weeks of culture.

3.1.5 RNA isolation and qPCR

RNA isolation, reverse transcription, and qPCR assays were performed as described in section 2.2.4, with six constructs pooled into each tube to obtain ample quantities of RNA. Relative expression of chondrogenic and osteogenic genes was determined using validated primers (Appendix B) and the $\Delta\Delta C_T$ method, with cyclophilin A as the endogenous control.

3.1.6 Assays for Chondrogenesis

The DNA, GAG and collagen content of scaffolds that underwent chondrogenic differentiation were determined in the manner described in Section 2.2.6. Commercial PicoGreen and Blyscan assay kits were used to determine quantities of DNA and GAG, respectively, while the modified hydroxyproline assay was used to quantify overall collagen production.

3.1.7 Assays for Osteogenesis

Samples cultured in osteogenic differentiation medium were rinsed in PBS, blotted gently on filter paper, and placed into tubes containing 500 μl of 2% Triton-X lysis buffer and frozen at -80°C. Samples were then subjected to three freeze-thaw cycles of 30 minutes at 37°C followed by 30 minutes at -80°C and sonicated for 10 seconds.

DNA content was determined using the PicoGreen assay described above. Alkaline phosphatase activity was determined using the Sensolyte pNPP assay kit, following the manufacturers recommendations (Anaspec, Fremont, CA).

In order to determine the calcium content of scaffolds, an equal volume of 1 N acetic acid was added to the remaining solution in the sample tube and left overnight with gentle agitation in order to dissolve calcium into solution. 30 μl of samples and $CaCl_2$ standards (Sigma) with concentrations ranging from 0 to 100 μg/ml were added to 300 μl of Arsenazo III reagent (Pointe Scientific (Canton, MI) in a 96-well plate and read at 650 nm.[123]

3.1.8 Immunofluorescence

Whole constructs were utilized for immunofluorescence staining in order to examine tissue structure in three dimensions. Constructs were fixed with 4% paraformaldehyde for 20 minutes followed by immunofluorescence detection using antibodies to chondrogenic (aggrecan, collagen type I, collagen type II) or osteogenic (collagen type I, osteocalcin, osteonectin) markers (Appendix C). After performing the necessary antibody-specific antigen retrieval and/or cell permeabilization steps, non-specific binding of antibodies in samples was blocked with 5% goat serum for 30 minutes. Constructs were then incubated with primary antibodies overnight at 4°C, followed by detection with fluorescently tagged secondary antibodies. Three-dimensional stacks of images were obtained using confocal scanning laser microscopy and images were processed using NIS Elements.

3.1.9 Statistics

Quantitative outcome measures for biochemical assays are expressed as mean ± standard deviation. Statistical analysis was performed using a two-way analysis of variance, followed by Tukey's test for post-hoc comparisons. $p<0.05$ was considered statistically significant.

3.2 RESULTS

3.2.1 Scaffold characterization

The scaffolds utilized in this study had the same physical characteristics as those used in Chapter 2.3.1. Nanofiber scaffolds had a diameter of 445±173 nm, average pore size of 1.2 μm^2, and overall porosity of 88%. Microfiber scaffolds had a diameter of 4.37±0.78 μm, average pore size of 91 μm^2, and overall porosity of 90%.

3.2.2 Chondrogenic gene expression

qPCR was performed on nanofiber and microfiber scaffolds seeded with either BMSCs or ADSCs to determine gene expression for COL1, COL2, and ACAN to assess the chondrogenic differentiation of cells after 3 weeks (Figure 10) and 6 weeks (Figure 11). Overall, chondrogenic gene expression was higher for BMSCs than ADSCs, and on microfibers than on nanofibers. At the 3-week time point, COL2 expression was 3-fold higher and 8-fold higher on microfibers than nanofibers for BMSCs and ADSCs, respectively. ADSCs had a 6-fold higher expression of ACAN when seeded on microfibers in comparison to nanofibers, while fiber diameter altered ACAN expression in BMSCs modestly, with 1.8-fold higher expression on microfibers than nanofibers. COL1 expression at 3 weeks was highest when ADSCs were seeded on microfibers, with no differences between nanofibers and microfibers seeded with BMSCs. The ratio of COL2 to COL1 expression was highest for BMSCs seeded on nanofibers, while the ratio was much lower for ADSCs, particularly those seeded on nanofibers.

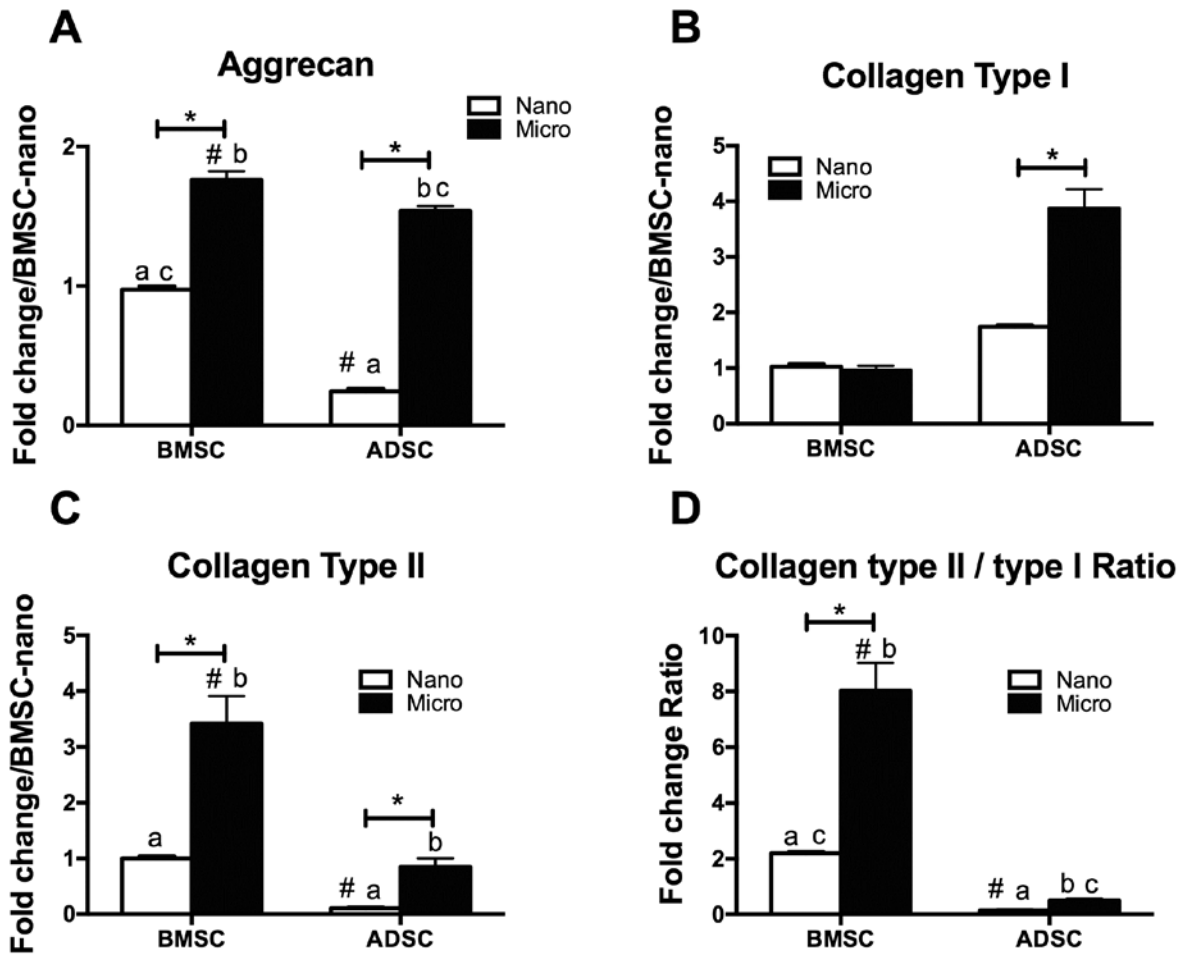

Figure 10. Chondrogenic gene expression after 3 weeks in culture

Fold change in gene expression at week 3 normalized to the BMSC nanofiber group. (A) Collagen type I, (B) Collagen type II, (C) Aggrecan; (D) Ratio of collagen type I to collagen type II expression. $^{*,\#,a,b,c}p<0.05$, n=3.

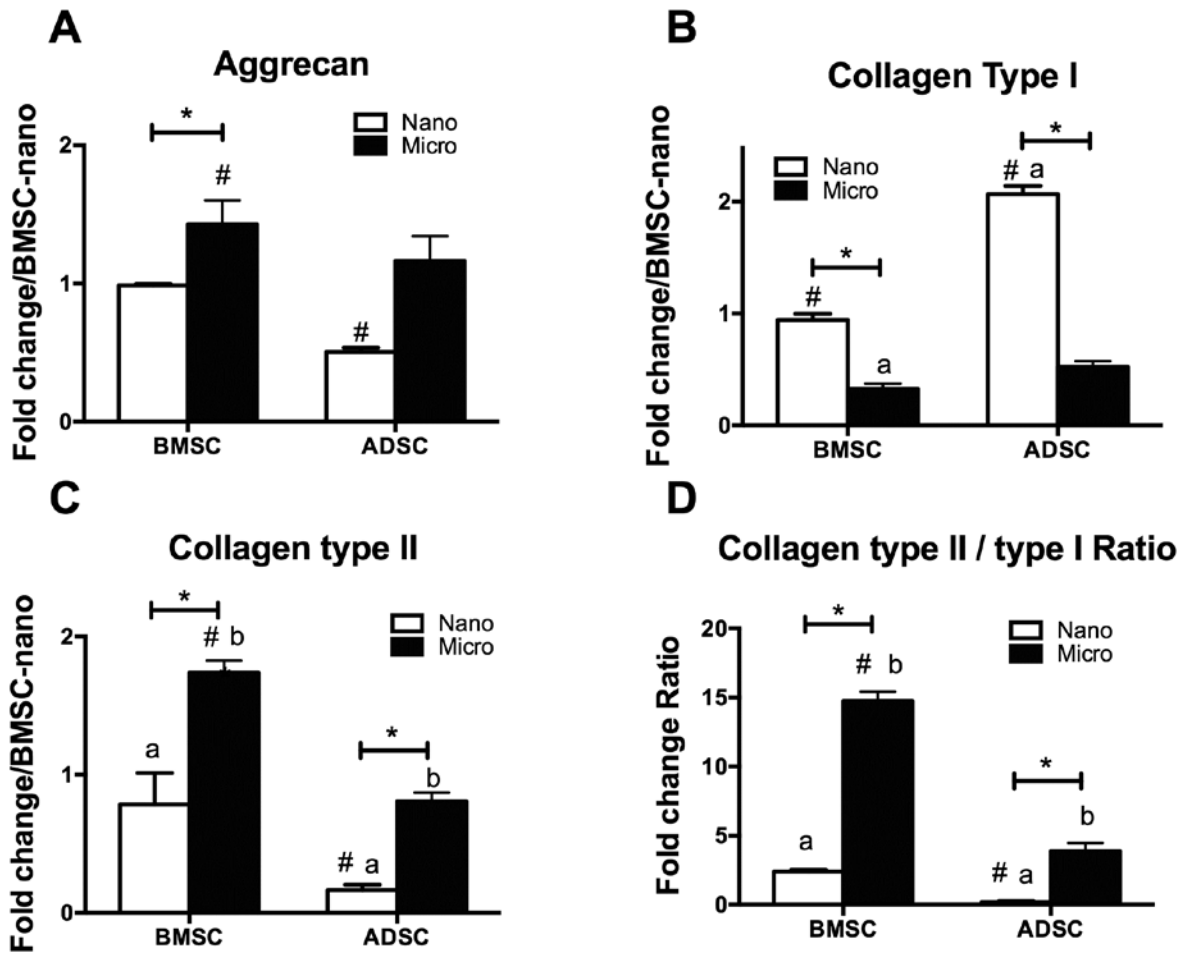

Figure 11. Chondrogenic gene expression after 6 weeks of culture

Fold change in gene expression at week 3 normalized to the BMSC nanofiber group. (A) Collagen type I, (B) Collagen type II, (C) Aggrecan; (D) Ratio of collagen type I to collagen type II expression. $^{*,\#,a,b}p<0.05$, n=3.

3.2.3 Osteogenic gene expression

Gene expression for COL1, osteonectin and osteocalcin was evaluated after 3 and 6 weeks of culture in osteogenic medium (Figure 12). ADSCs had an approximately 10-fold increase in COL1 expression after 3 weeks on both microfiber and nanofibers in comparison to BMSCs on nanofibers, while BMSCs on microfibers had a 4-fold increase in COL1 expression. After 6 weeks of osteogenic culture COL1 expression was less than 2-fold different between all groups. Osteonectin expression was approximately 2-fold higher on BMSCs seeded on nanofiber and ADSCs seeded on microfibers than BSMCs on microfibers and ADSCs on nanofibers after 3 weeks, but after 6 weeks of culture, osteonectin expression was 5-fold higher in BMSCs on microfibers, while ADSCs had approximately 7- and 10-fold higher osteonectin expression on nanofibers and microfibers respectively. Osteocalcin expression was about 9-fold higher in BMSCs seeded on nanofibers than in ADSCs seeded on microfibers or nanofibers, and twice that of BMSCs on nanofibers at 3 weeks. After 6 weeks, this relationship was also altered, with cells seeded on microfibers having higher gene expression than cells on nanofibers. ADSCs had over a 20-fold increase in osteocalcin gene expression when seeded onto microfibers rather than nanofibers. BMSCs had a more measured response, increasing gene expression approximately 3-fold when seeded on microfibers rather than nanofibers.

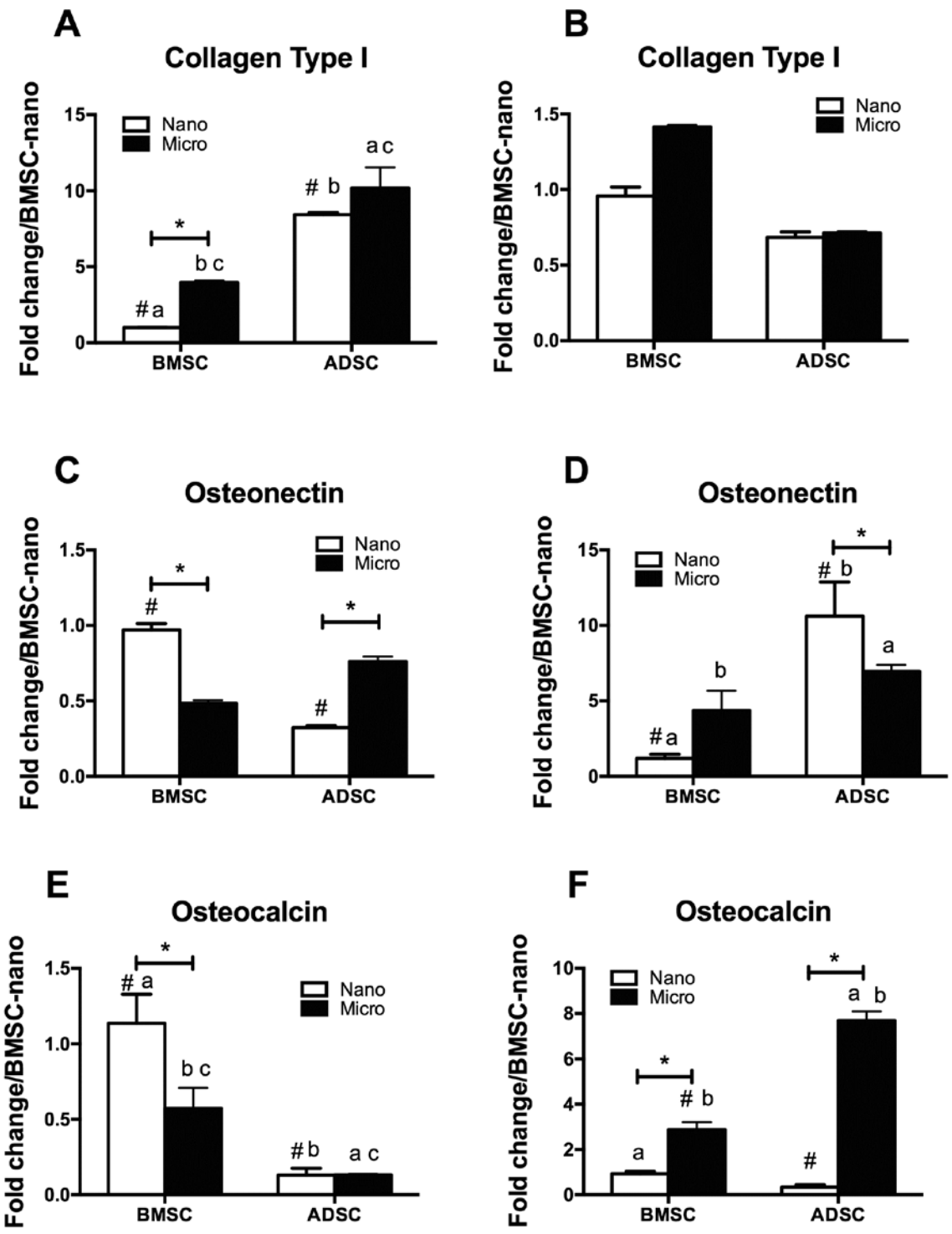

Figure 12. Osteogenic gene expression after 3 and 6 weeks of culture
Fold change in gene expression of collagen type I (A,B), osteonectin (C,D), and osteocalcin (E,F) normalized to the BMSC nanofiber group at week 3 (A, C, E) and week 6 (B, D, F). $^{*,\#,a,b,c}p<0.05$, n=3.

3.2.4 Biochemical characterization of chondrogenesis.

The cellularity, GAG and collagen content was compared between groups following chondrogenic differentiation. At 3 weeks, DNA quantification by PicoGreen showed a higher number of BMSCs than ADSCs on each type of scaffold (Figure 13). ADSCs seeded on nanofibers had significantly fewer cells than BMSCs on either nanofiber or microfiber scaffolds. At the 6-week time point, there were no significant differences in cell number between any of the groups.

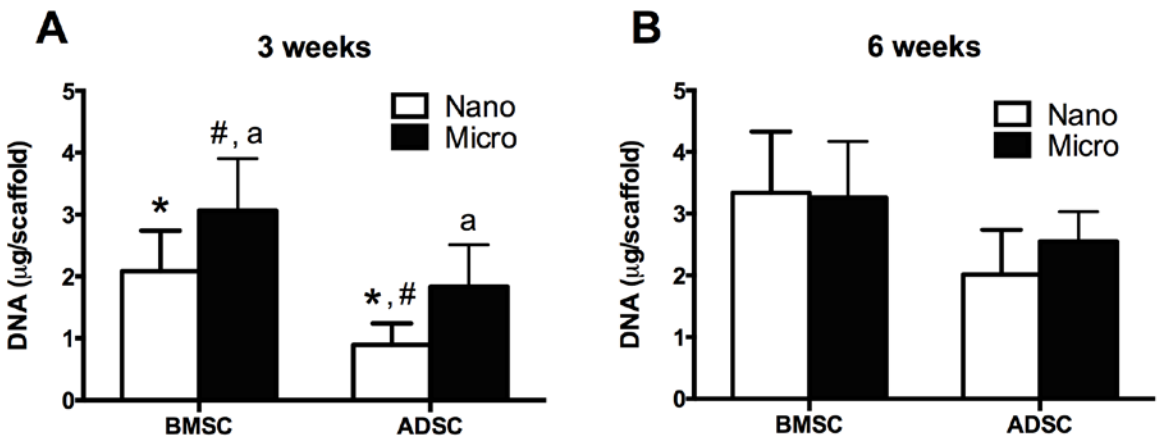

Figure 13. DNA quantification on microfiber and nanofiber scaffolds with BMSCs and ADSCs after 3 & 6 weeks of chondrogenic differentiation
Picogreen assay for DNA quantification at (A) 3 weeks, and (B) 6 weeks. Statistical significance between groups is indicated by matching symbols $^{*,\#,a,}p<0.05$, n=6.

After 3 weeks of culture, no significant differences between fiber types were found in GAG and collagen deposition, either total or on a per cell basis, for a given cell type (Figure 14). However, BMSCs on both microfibers and nanofibers secreted significantly higher amounts of GAG and GAG per DNA. BMSCs seeded on microfibers had higher total collagen content than ADSCs on either microfibers or nanofibers; however, when normalized to DNA, these differences disappeared.

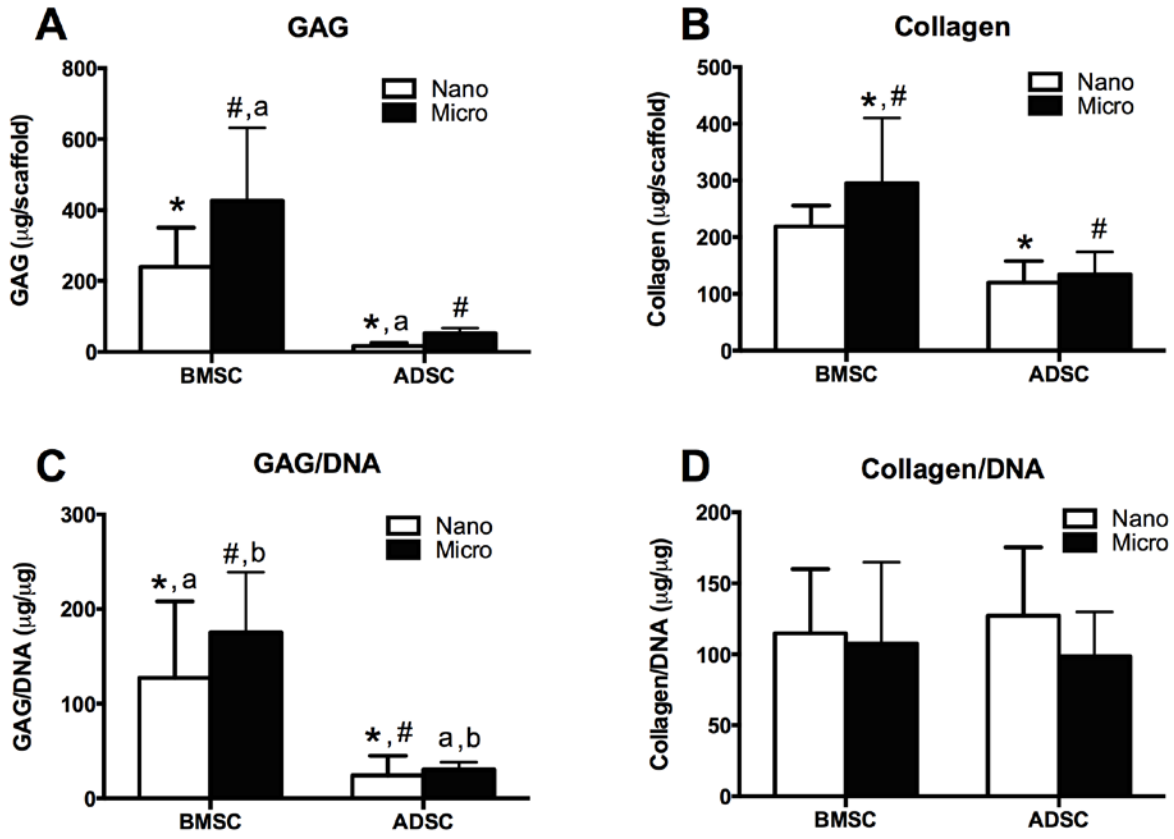

Figure 14. GAG and collagen quantification on microfiber and nanofiber scaffolds with BMSCs and ADSCs at 3 weeks

(A) GAG/scaffold; (B) Collagen/scaffold; (C) GAG/DNA; (D) Collagen/DNA Statistical significance between groups is indicated by matching symbols $^{*,\#,a,b}p<0.05$, n=6.

At week 6, the total amount of GAG and collagen deposited was higher in microfibers than nanofibers for both BMSCs and ADSCs (Figure 15). When GAG and collagen were normalized to the DNA content, microfibers still had higher amounts of deposition in comparison to nanofibers within each cell group as before, however there were not significant differences between deposition by BMSCs and ADSCs when seeded on the same fiber diameter.

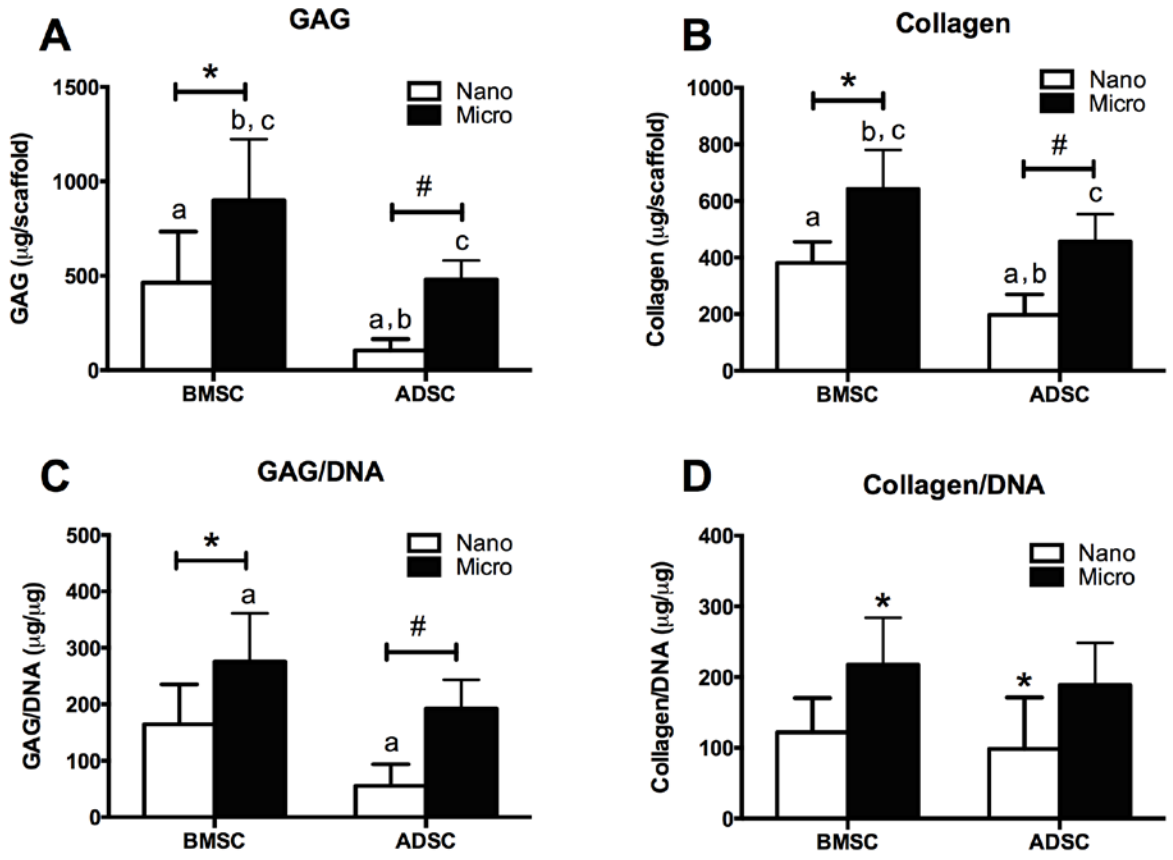

Figure 15. Chondrogenic biochemical characterization on microfiber and nanofiber scaffolds with BMSCs and ADSCs at 6 weeks

(A) GAG/scaffold; (B) Collagen/scaffold; (C) GAG/DNA; (D) Collagen/DNA Statistical significance between groups is indicated by matching symbols $^{*,\#,a,b,c}p<0.05$, n=6.

3.2.5 Biochemical characterization of osteogenesis.

At week 3, there were no differences in cell number between any of the groups cultured in osteogenic medium. Alkaline phosphatase activity and calcium content were significantly higher on microfibers seeded with ADSCs than BMSCs seeded on either microfibers or nanofibers. When measured at 6 weeks, a significantly higher number of cells were found in BMSC-seeded than ADSC-seeded scaffolds for both fiber diameters. The number of cells found on ADSCs cultured on nanofibers was significantly lower than all other groups. ALP activity and calcium content had a similar pattern among groups at 6 weeks, with significantly more ALP activity on microfibers seeded with ADSCs in comparison to the other groups.

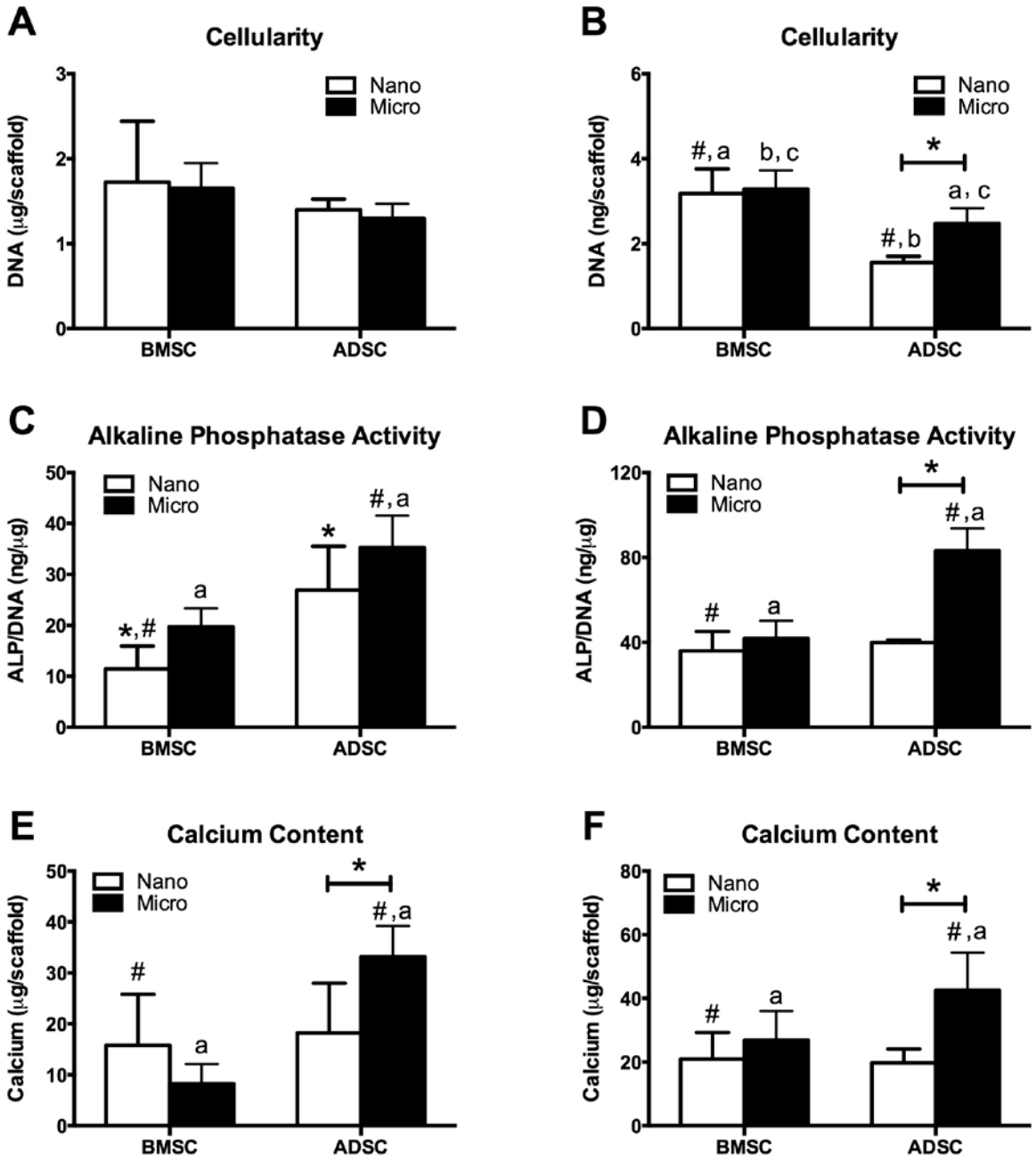

Figure 16. Osteogenic biochemical characterization on microfiber and nanofiber scaffolds with BMSCs and ADSCs at 3 and 6 weeks

(A,B) DNA, (C,D) Alkaline phosphatase activity, (E.F) Calcium content. At 3 weeks (A,C,E) and 6 weeks (B,D,F). Statistical significance between groups is indicated by matching symbols $^{*,\#,a,b}p<0.05$, n=6.

3.2.6 Confocal immunofluorescence analysis of chondrogenesis

Scaffolds cultured under chondrogenic conditions for 6 weeks all stained positively for collagens type I and type II, though the organization and quantity varied (Figure 17). Qualitative differences between the collagen labeled on the scaffold were not apparent when seeded with BMSCs, with a dense layer of both collagen types I and II on the surface of the scaffolds. However, ADSCs appeared to have a less smooth or organized pattern of collagen type I deposition and stained much less strongly for collagen type II than scaffolds seeded with BMSCs. Additionally, the density of cells seen per area was greater on the surface of nanofibers than microfibers.

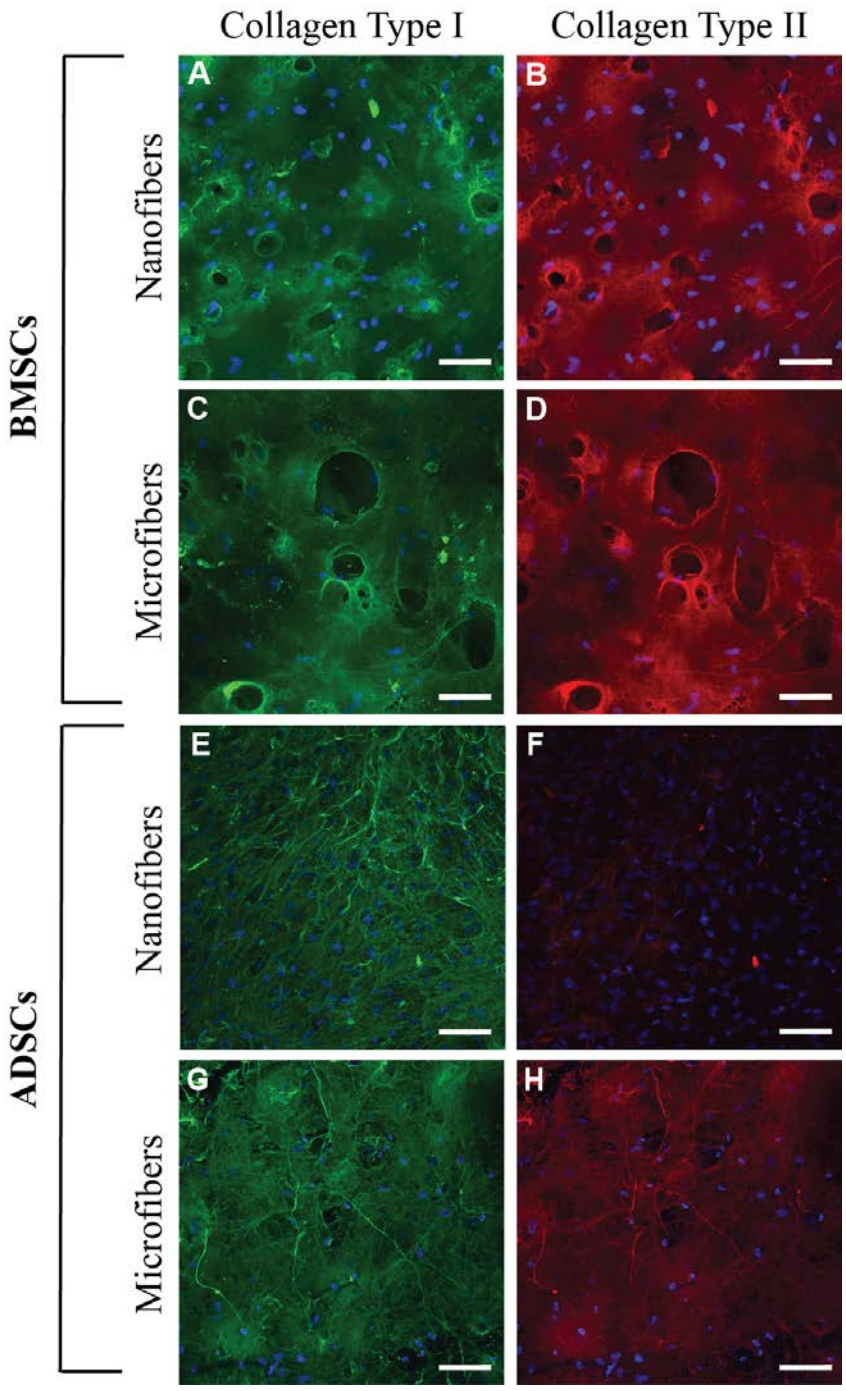

Figure 17. Confocal immunofluorescence staining for collagen type I and type II in chondrogenic cultures with BMSCs and ADSCs after 6 weeks
Collagen type I (green) staining of BMSCs on (A) nanofibers and (B) microfibers, and ADSCs on (E) nanofibers and (G) microfibers. Collagen type II (red) staining of BMSCs on (B) nanofibers and (D) microfibers, and ADSCs on (F) nanofibers and (H) microfibers. Nuclei stained with DAPI (blue). Images taken at 20x magnification, scale bar = 100 μm.

3.2.7 Confocal immunofluorescence analysis of osteogenesis

All groups showed positive staining for each of the osteogenic marker proteins collagen type I, osteonectin, and osteocalcin (Figure 18). ADSCs seemed to lay down a thicker collagen network than BMSCs on both microfibers and nanofibers resulting in a smooth appearance on the surface of the scaffold, while the contours of the fibers could be seen on scaffolds seeded with BMSCs. Staining for both osteonectin and osteocalcin appeared to be more dense on nanofibers than microfibers for a given volume at the surface of the scaffold, but the overall pattern appeared to be similar.

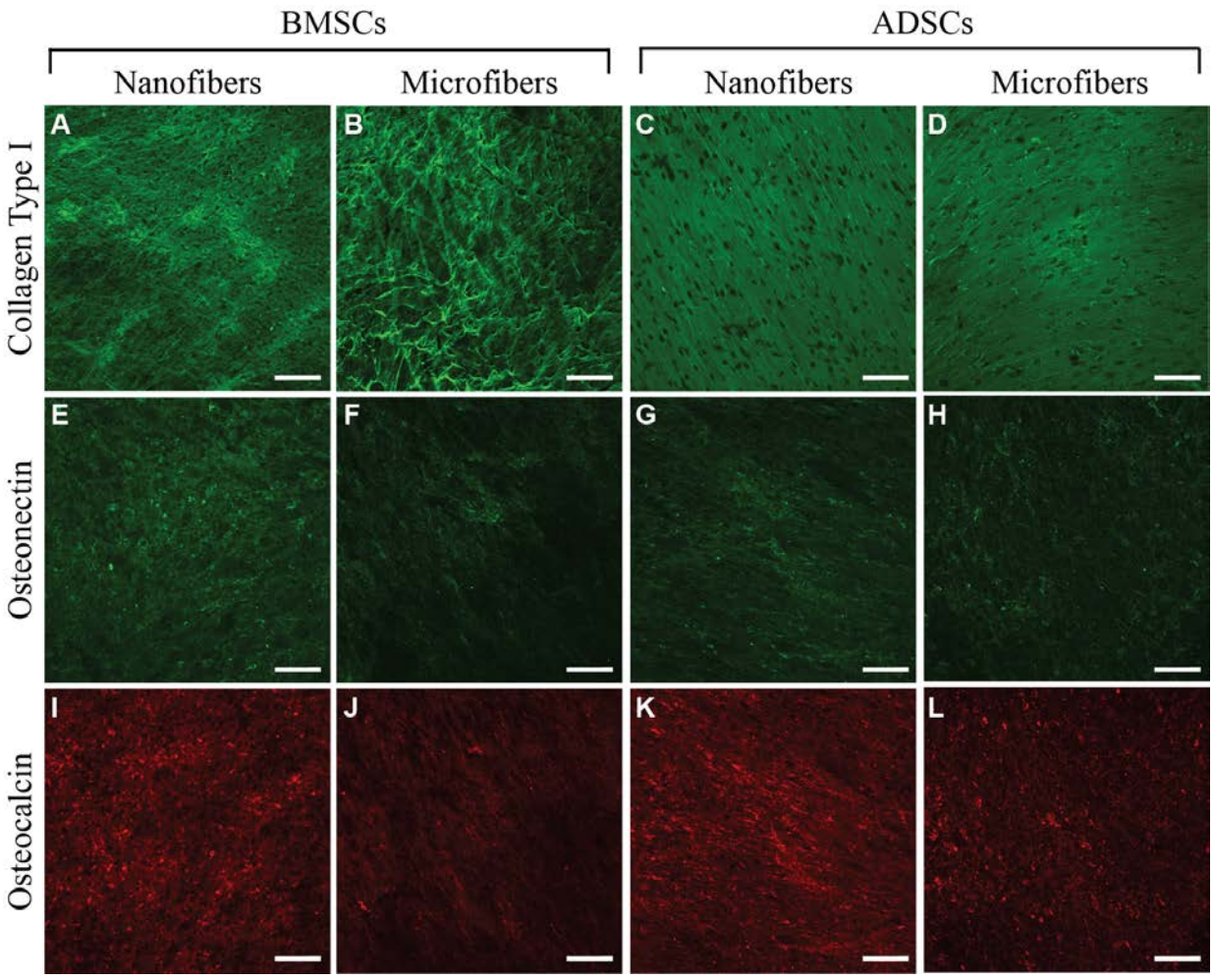

Figure 18. Confocal immunofluorescence staining for collagen type I, osteonectin, and osteocalcin in osteogenic cultures with BMSCs and ADSCs after 6 weeks

Collagen type I (A,B,C,D; green), osteonectin (E,F,G,H; green), and osteocalcin (I,J,K,L; red). Images taken at 20x magnification, scale bar = 100 μm.

3.3 DISCUSSION

The results of this study suggest that BMSCs and ADSCs have different potential for cartilage and bone regeneration when seeded on electrospun PCL scaffolds, and that the effects of fiber diameter are dependent on whether cells are cultured under chondrogenic or osteogenic conditions.

Chondrogenic differentiation of MSCs was enhanced when cells were seeded on microfibers in comparison to nanofibers, and with BMSCs in comparison to ADSCs. Increased chondrogenesis of ADSCs and BMSCs seeded onto microfibers is in agreement with the results from experiments described in Chapter 2. A high initial seeding density in conjunction with the larger pores of the microfibers likely promoted mesenchymal condensation and formation of the cell-cell contracts important for chondrogenesis.

Increased gene expression of COL2 and ACAN in cells seeded on microfibers and BMSCs after both 3 and 6 weeks of culture suggests that cells under these conditions are developing a more chondrogenic phenotype. At the 3-week time point, COL1 expression was higher with microfibers and BMSCs, while this pattern reversed at the 6-week time point. While COL1 expression is typically indicative of a fibrocartilagenous phenotype and therefore undesirable in articular cartilage tissue engineering, this increased level of expression early in culture may be indicative of undifferentiated MSCs more actively laying down a matrix to which they can attach prior to undergoing condensation and chondrogenic differentiation, and then remodel as the cells mature into chondrocytes.

The differences in gene expression under chondrogenic differentiation conditions were also reflected in GAG and collagen deposition over the 6-week period. While at 3 weeks there were no differences in the amount of GAG or collagen on fibers with different diameters seeded

with the same cell type, by 6 weeks, cells seeded on microfibers had deposited more of these proteins than cells on nanofibers. Additionally, constructs seeded with BMSCs contained more GAG and collagen than those seeded with ADSCs. Staining for collagen types I and II further demonstrated the enhancement of chondrogenesis by BMSCs. All cultures stained strongly for collagen type I, while collagen type II staining was somewhat less intense on ADSCs seeded on microfibers, and quite limited on nanofibers. Additionally, constructs seeded with ADSCs had surface collagen staining that appeared fibrous, while constructs seeded with BMSCs resulted in collagen staining that appeared to be more smooth and dense, with potential evidence of lacuna-like morphology similar to that seen in native cartilage. The inability to discern individual collagen fibers on BMSC constructs may be due to the collagen fibers becoming more finely divided while also becoming more densely packed, making it impossible to see individual fibers due to the resolution limits of confocal laser microscopy. Additionally, the appearance of the smooth collagen staining correlated strongly with the amount of GAG that was detected within the construct. An increasing amount of proteoglycan deposition may result in decreased size of the collagen fibers, as these matrix components interweave with each other. The presence of collagen type I staining suggests that the secreted matrix is not equivalent to that of the native cartilage, but it is possible that longer incubation times or implantation *in vivo* could lead to more significant matrix remodeling and a higher ratio of collagen type II in comparison to collagen type I.

Addition of BMP-6 to chondrogenic medium has been shown to enhance chondrogenic differentiation of ADSCs, likely by inducing expression of the TGF-β-receptor-I protein required for response to TGF-β3.[113,114] The combination of growth factors utilized in this study—10 ng/ml each of TGF-β3 and BMP-6—was previously shown to induce chondrogenesis similar to

BMSCs cultured in TGF-β3 alone in pellet cultures.[113] Similar results were found in our additional studies (see Appendix D). Compared to data presented in Chapter 2, where medium contained only TGF-β3 and not BMP-6, addition of BMP-6 increased DNA and GAG production by both BMSCs and ADSCs. Interestingly, the amount of collagen produced was actually lower with the addition of BMP-6, particularly on microfibers, but it is unclear whether the increase is due to an increase in collagen type I or type II since all samples stained strongly for both types of collagen and no quantitative analysis, such as ELISA, was performed. ADSCs seeded on microfibers cultured in TGF-β3 and BMP-6 appeared to be somewhat in-between the two BMSC groups, with areas that had fibrous-appearing staining, and others where the density appeared to be higher.

While BMP-6 has been shown to induce chondrogenesis of ADSCs *in vitro*, it is expressed by hypertrophic chondrocytes and can induce endochondral ossification *in vivo*.[124] Studies investigating the use of BMP-6 for chondrogenesis of ADSCs are somewhat inconclusive, with some studies suggesting that BMP-6 increases the expression of COL10, a marker of chondrocyte hypertrophy, while others show strict down-regulation.[113,114,116] Therefore, evaluating the expression of hypertrophic and osteogenic genes and proteins in addition to the chondrogenic studies already performed may be useful for determining whether cells are halting differentiation when they become mature chondrocytes, or if they are continuing on towards bone formation.

While clear dependence on both fiber diameter and MSC tissue source was found when culturing constructs under chondrogenic conditions, a slightly different pattern was found when cells were cultured under osteogenic conditions. At both 3 and 6 weeks of culture, ALP activity and calcium deposition were higher in microfiber constructs seeded with ADSCs, while no

differences were found with different fiber diameters when seeded with BMSCs. This suggests that while BMSC differentiation is not sensitive to fiber diameter, ADSC differentiation appears to be, with microfibers promoting osteogenesis more than nanofibers. Gene expression changes also provide some evidence of enhanced osteogenic differentiation in ADSCs, particularly on microfibers. COL1 expression is increased in ADSCs at 3 weeks of culture, while ON and OC are upregulated after 6 weeks. COL1 expression is considered an early marker of osteogenesis as collagen deposition eventually leads cells to slow their proliferation and begin to undergo differentiation.[125] Osteonectin (ON) is a commonly used marker for developing osteoblasts and is thought to play a role in initiation of mineralization[126], while osteocalcin (OC) is a marker of fully differentiated osteoblasts.[127] Thus, the increase of ON in ADSCs at 6 weeks is indicative of ongoing osteoblastic differentiation and beginning mineralization. ADSCs seeded on microfibers have a much higher level of OC expression than on nanofibers, while ON is slightly lower. This may indicate that more cells in the microfiber group have become fully differentiated osteoblasts or even early osteocytes, though high levels of ALP expression suggest that many cells may still be actively undergoing the differentiation process. Visualization of osteogenic proteins by immunofluorescence showed increased organization and density of collagen fiber deposition by ADSCs, while differences in osteonectin and osteocalcin were more difficult to detect, though it appeared that the density of staining may be greater on nanofibers in comparison to microfibers. This might be explained by different cell penetration depth into the scaffold, with cells migrating and depositing matrix throughout the scaffold when seeded on microfibers, while matrix formation only occurred near the surface for nanofibers since the small pores of the nanofibers inhibit cell migration beyond the scaffold surface.

Previous studies have examined the effects of fiber diameter on osteogenesis in immature osteoblasts as well as BMSCs, with results suggesting that either fiber diameter had no effect on or that larger fiber diameters enhance osteogenesis.[128–132] One study examined osteogenesis of BMSCs on polyethylene terephthalate fibers between 2 and 42 μm in diameter, concluding that microfibers between 9 and 12 μm in diameter most effectively promoted osteogenesis of BMSCs, by increasing ALP activity and osteocalcin synthesis.[128] Another study seeded osteoprogenitor cells onto PLLA scaffolds with either 140 nm or 2.1 μm fiber diameters, and saw no differences in ALP activity between groups, though larger fibers promoted increased cell proliferation.[129] These findings are supported by the results in our study that showed modest increases in gene expression of ON and OC by BMSCs seeded on microfibers, with no significant differences in ALP activity, calcium deposition, or staining for osteonectin and osteocalcin. Interestingly, ADSCs seemed to be more affected by the fiber diameter, with enhanced osteogenesis occurring on microfibers. This is in contrast to many studies that have indicated that ADSCs have reduced osteogenic potential in comparison to BMSCs. However, these previous studies were all performed in monolayer cultures, suggesting that 3D culture conditions may be a more effective method for evaluating differentiation potential of cells for tissue engineering applications.

It should be noted that the BMSCs and ADSCs used in this study were not isolated from the same patient. Donor variability is common, making it difficult to conclude that MSCs derived from one tissue will always be more effective than another. The cells in this study were chosen based on matching of the age and sex of the donors as well as qualitative differentiation potential in monolayer. Additionally, cells from multiple donors were pooled in order to obtain a more generalized perspective on how cell source might affect differentiation. When moving towards

clinical application, an individualized approach where direct comparisons between MSCs isolated from different tissues from a single patient are performed may be warranted; however, if expanded studies show consistency in outcomes, this may be unnecessary.

3.4 CONCLUSION

BMSCs constitute only 0.001 to 0.01% of the total cells isolated from bone marrow, with numbers also decreasing with increasing age. Thus, *in vitro* expansion is likely necessary prior to use of cells in tissue engineering applications since only very limited volumes of bone marrow can be safely and effectively obtained and large numbers of cells are likely required.[133] In comparison, much larger quantities of adipose tissue are more easily obtained with less associated pain and risk to the donor, reducing the time needed to obtain a sufficient quantity of cells and avoiding potential changes in cell phenotype caused by extended *in vitro* culture. Therefore, when choosing a cell source, it is important to consider not only the differences in differentiation potential but also risks incurred in order to provide treatment. Additionally, the differences in cell differentiation potential seen during *in vitro* culture may not translate *in vivo*, and further optimization of culture conditions could likely enhance both ADSC and BMSC chondrogenic and osteogenic differentiation.

While there have been a number of studies comparing the chondrogenic or osteogenic potential of BMSCs and ADSCs, to our knowledge, this is the first comparing the differentiation of these cell types on electrospun fibers as well as evaluate the effects of fiber diameter on ADSC behavior. Under the specific culture conditions utilized, the important findings of this study are summarized as follows: (1) PCL microfibers provide a better substrate than nanofibers

for chondrogenesis; (2) BMSCs have increased chondrogenic potential on PCL fibers in comparison to ADSCs using medium containing TGF-β3 and BMP6; (3) Fiber diameter does not influence osteogenesis of BMSCs; and, (4) ADSCs have improved osteogenic potential on microfibers in comparison to nanofibers.

4.0 SEQUENTIAL SEEDING STRATEGIES INFLUENCE OSTEOGENESIS IN CO-CULTURES OF MESENCHYMAL STEM CELLS AND ENDOTHELIAL CELLS

4.0 INTRODUCTION

Co-culture of MSCs with endothelial cells (ECs) has been shown to cause increased MSC secretion of VEGF leading to increased BMP2 production by endothelial cells, and enhanced MSC osteogenesis as a result.[79] Many studies have examined the potential benefits of co-culturing endothelial cells (ECs) with MSCs in 3D scaffolds for bone tissue engineering with promising results. Most of these studies were performed using hydrogel scaffolds, which have limited potential for bone tissue engineering due to a lack of sufficient mechanical properties. Only one previously published study with 3D co-culture of ECs and MSCs has used electrospun scaffolds.[134] In this study, MSCs and umbilical vein ECs were seeded onto electrospun PCL scaffolds with a 10 μm fiber diameter and cultured for 7-14 days in osteogenic medium. The co-cultured scaffolds had higher levels of alkaline phosphatase (ALP) activity and calcium production than constructs seeded with MSCs alone, although this effect was decreased when scaffolds were cultured in a flow perfusion bioreactor in comparison to static culture. These findings suggest that electrospun scaffolds should be further investigated for use in co-culture studies where both osteogenesis and angiogenesis is essential.

While most co-cultures on scaffolds are typically initiated by simultaneously seeding ECs and osteogenic cells at the chosen cell density and ratio, there are a few studies examining the effects of sequential seeding where one cell type is seeded onto the scaffold prior to the other. Seeding ECs onto collagen-GAG scaffolds three days prior to seeding MSCs resulted in enhanced formation of vessel-like structures *in vitro* and increased vascularization *in vivo*.[135] However, MSCs were not induced to undergo osteogenesis, leaving the effects that these co-culture conditions have on bone formation unclear. Another study utilized a sequential seeding protocol where endothelial progenitor cells were seeded onto PCL-hydroxyapatite scaffolds three days prior to seeding of osteoblasts.[136] Capillary density *in vivo* increased in the co-culture group in comparison to endothelial progenitor cells alone on scaffolds, along with increased osteogenesis and decreased necrosis of the tissue within the scaffold in comparison to cultures with osteoblasts only. Unfortunately, there was not a group where the two cell types were seeded at the same time, and thus the effects of sequential seeding in comparison to co-seeding could not be evaluated.

Other studies have taken the opposite approach, pre-seeding primary osteoblasts (pOBs) or MSCs prior to addition of ECs. Silk scaffolds seeded with pOBs one day prior to the addition of ECs formed more blood vessels and had higher osteogenic gene and protein expression in comparison to monocultured pOBs *in vitro*.[137] Another group investigated the effects of seeding MSCs onto porous PLGA scaffolds under osteogenic conditions for one week followed by addition of HUVECs.[138] Greater vessel formation was observed *in vivo* with MSC co-culture than when ECs were cultured alone.

While the benefits of co-culture seem clear regardless of the choice of the sequence of cell seeding, a controlled direct comparison evaluating vascularization and osteogenesis with sequential or concurrent seeding of osteogenic cells and ECs has not been conducted. In this study we performed co-culture experiments seeding MSCs and human dermal microvascular endothelial cells on microfiber PCL scaffolds seeded either at the same time or sequentially with three days between the seeding of each cell type to determine whether this strategy can lead to improvements in the development of a functional tissue engineered bone replacement.

4.1 METHODS

4.1.1 Electrospinning and scaffold characterization

Microfiber scaffolds were electrospun using the same parameters and characterized as previously described in Sections 2.2.1 and 3.2.1. SEM was performed and scaffold fiber diameter and pore size were determined using the automated algorithm described above.

4.1.2 Cell culture and seeding

MSCs were isolated from bone marrow and cultured as described in Sections 2.2.2 and 3.2.2. Passage 5 cells were utilized in this study. The human dermal microvascular cell line, HMEC-1 (US Center for Disease Control and Prevention, Atlanta, GA) was maintained in endothelial growth medium (EGM-2 BulletKit; Lonza, Walkersville, MD) and expanded to Passage 9.

The day prior to seeding, scaffolds were cut into 0.8mm disks, hydrated with 70% ethanol for 2 hours, rinsed with PBS, and soaked overnight in growth medium. Five different seeding conditions were utilized, with the individual groups detailed in Table 2. Cells were trypsinized, counted, and resuspended at a concentration of $6.7x10^6$ cells/ml. 15 µl ($2x10^6$ cells/cm^3-scaffold) of the cell suspension was then seeded onto the surface of the scaffold and cells were allowed to attach, with addition of 10 µl of medium after 1 hour to prevent drying, followed by addition of 2 ml of medium after 2 hours. Between Phase I and Phase II seeding, constructs were maintained in cell-specific growth medium (Appendix A) After culturing the constructs for 3 days, Phase II of seeding was performed in the same manner as Phase I.

Table 2. Groups for sequential seeding experiment

Group #	Phase I (cells/cm^3-scaffold)	Phase II (cells/cm^3-scaffold)	Culture Medium Prior to Differentiation
1	ECs ($2x10^6$)	MSCs ($2x10^6$)	EGM[a]
2	MSCs ($2x10^6$)	ECs ($2x10^6$)	MGM[b]
3	-	ECs & MSCs ($2x10^6$ each)	1:1 EGM:MGM
4	-	MSCs ($4x10^6$)	MGM
5	-	ECs ($4x10^6$)	EGM

[a]Endothelial growth medium [b]MSC growth medium

4.1.3 Osteogenic differentiation

24 hours after Phase II seeding, the culture medium was switched from growth to osteogenic medium to induce differentiation. Medium was changed every 2-3 days and constructs were analyzed after 7, 14, and 21 days of differentiation. Figure 19 summarizes the experimental timeline for this experiment.

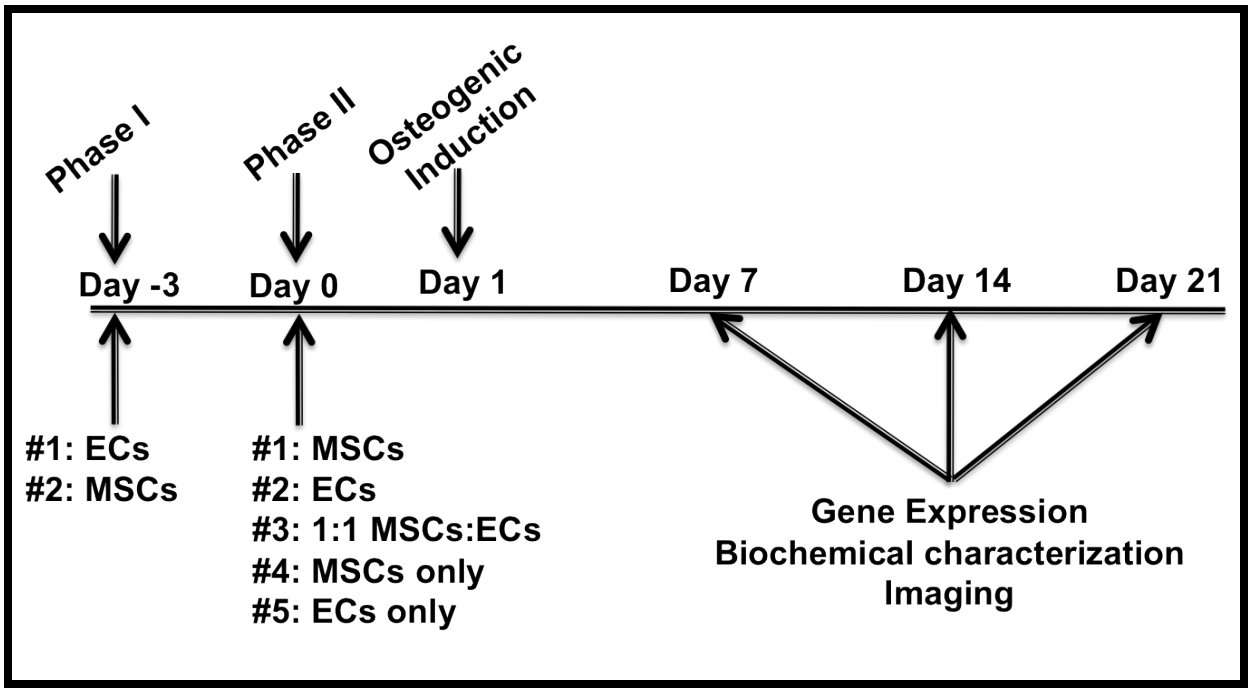

Figure 19. Experimental timeline for sequential seeding study

4.1.4 RNA Isolation and qPCR

RNA was isolated, reverse transcribed, and then amplified using qPCR, as described in Section 2.2.4, to determine relative gene expression. The genes examined were COL1, ON, OC, RUNX2, alkaline phosphatase, osteopontin, VEGF and angiopoeitin-1. Sequences of primers and conditions used for qPCR can be found in Appendix B.

Since reverse transcription was performed using the same amount of RNA for each sample, without normalization the relative gene expression by MSCs for Groups 1-3 that contain both MSCs and ECs would be skewed negatively since these groups have fewer MSCs than Group 4. Therefore, we normalized the data by weighting to the number of MSCs initially seeded onto the scaffolds (i.e. Group 4 expression was divided by 2).

4.1.5 Assays for osteogenesis

Osteogenic assays for quantification of total DNA, ALP activity, and calcium content were performed as described in section 3.2.7. For ALP activity and calcium content, the values were normalized to the number of MSCs originally seeded on the scaffolds in order to account for differences between co-culture groups and Group 4.

4.1.6 Enzyme-linked immunosorbance assay (ELISA)

The culture medium was collected at 7, 14, and 21 days, centrifuged at 2,000 rpm and 4°C for 10 minutes to remove cell debris, and frozen at -80°C until the assay was performed. The quantity of VEGF secreted by the cells into the media was analyzed using an ELISA kit (R&D systems) according to the manufacturers instructions.

4.1.7 Immunofluorescence

Constructs were fixed for 20 minutes in 4% PFA and stained using methods described in section 3.2.8. Samples were permeabilization in PBS containing 0.1% Triton-X 100 for 10 minutes, followed by blocking in 5% goat serum. Primary antibodies for collagen type I, osteocalcin, osteonectin and osteopontin were applied to constructs, and kept at 4°C overnight. Secondary antibodies were applied for 1 hour at room temperature to detect primary antibodies, followed by staining with DAPI to detect nuclei. Samples were examined using laser confocal scanning microscopy and images were processed and analyzed with NIS Elements software.

4.2 RESULTS

4.2.1 Scaffold characterization

Electropsun PCL microfiber scaffolds had a diameter of 4.63 ± 0.76 μm, an overall porosity of 90%, and an average pore size of 90 μm^2. A representative SEM image of the scaffold is shown in Figure 20.

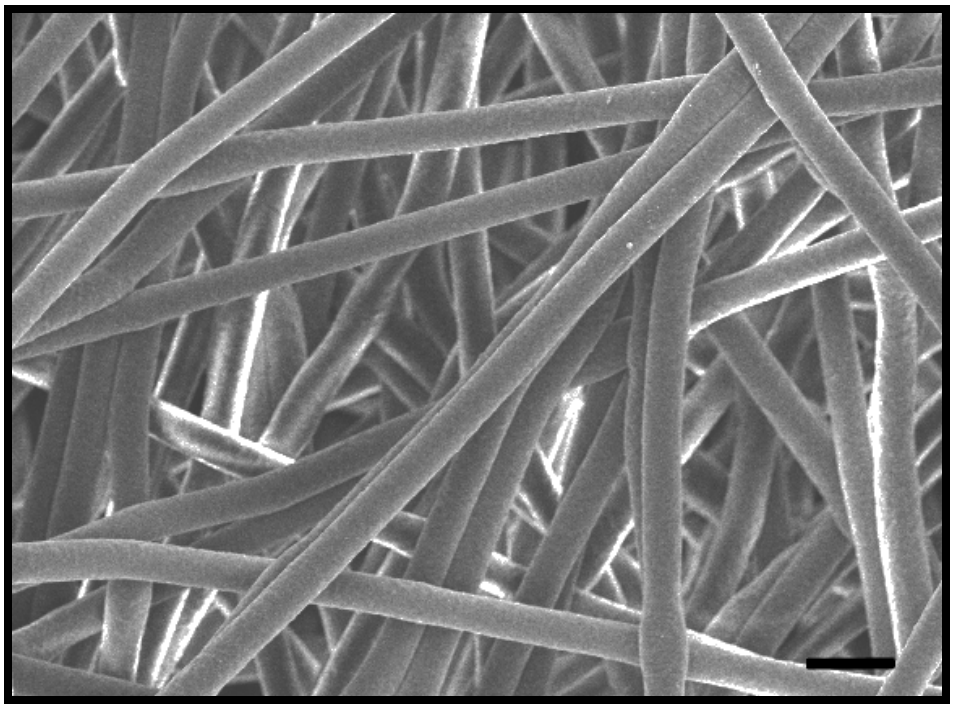

Figure 20. SEM image of microfibers
Image taken at 500x. Scale bar = 10 μm

4.2.2 Gene expression

Results of qPCR analysis for gene expression are shown in Figure 21. The results show lower expression in Group 4 for all genes examined except for osteocalcin and osteopontin. RUNX2 expression was relatively stable overall, but was slightly higher in Group 3 at day 7 and 14, decreasing to a level similar to Groups 1 and 2 at day 21. ALP expression was similar at day 7 for Groups 1 and 2 and remained relatively stable at days 14 and 21, while it was higher at day 7 in Group 3 and then decreased at the later time points. COL1 expression was similar for all co-cultured groups and decreased from day 7 to day 21. Osteopontin expression increased in all groups between day 14 and 21, and was highest in Groups 1 and 4. Osteonectin expression increased similarly for all co-culture groups over the culture period. Osteocalcin expression was stable in Group 3 across all time points, while expression decreased from day 7 to day 14 in both Groups 1 and 2. At day 21, osteocalcin expression increased to day 7 levels for Group 2, while not changing in Group 1. VEGF expression sharply increased from day 7 to day 21 in Group 2, while in Groups 1 and 3 the increase was more moderate. ANG1 expression was similar for Groups 1 through 3.

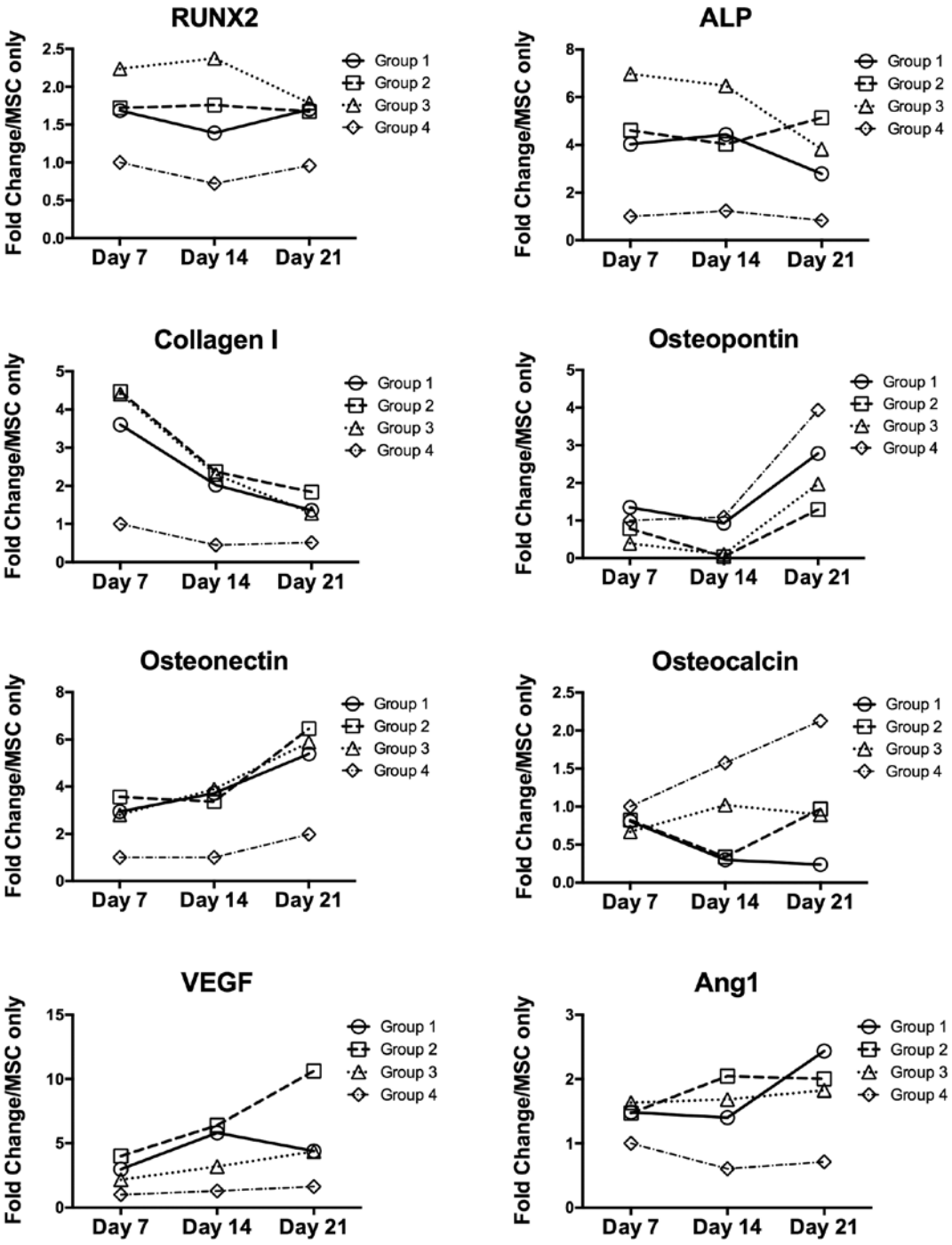

Figure 21. Gene expression profiles in osteogenic MSC-EC co-cultures
Gene expression for osteogenic differentiation at days 7, 14, and 21. Groups are normalized to the expression in the MSC-only group in addition to normalization for the initial MSCs seeded. Endothelial-only group expression is not shown since expression was quite low (C_T values > 35).

4.2.3 Biochemical content

Results for cellularity, ALP activity and calcium deposition are presented in Figure 22. No significant differences in the DNA content as measured by the Picogreen assay were found between groups at day 7 or 14, while at day 21 Group 4 had significantly more cells than the other groups. ALP activity was similar for all groups at day 7; however, it decreased significantly in Group 4 at day 14 and 21, while Groups 1-3 had no significant differences between them. The calcium content was also not significantly different between groups at day 7; however, at day 14 and day 21, the calcium content of the cultures in Group 2 was significantly higher than in the other groups. Group 5, which contained only ECs had negligible ALP activity and calcium deposition at all time points, and was thus excluded from the analysis.

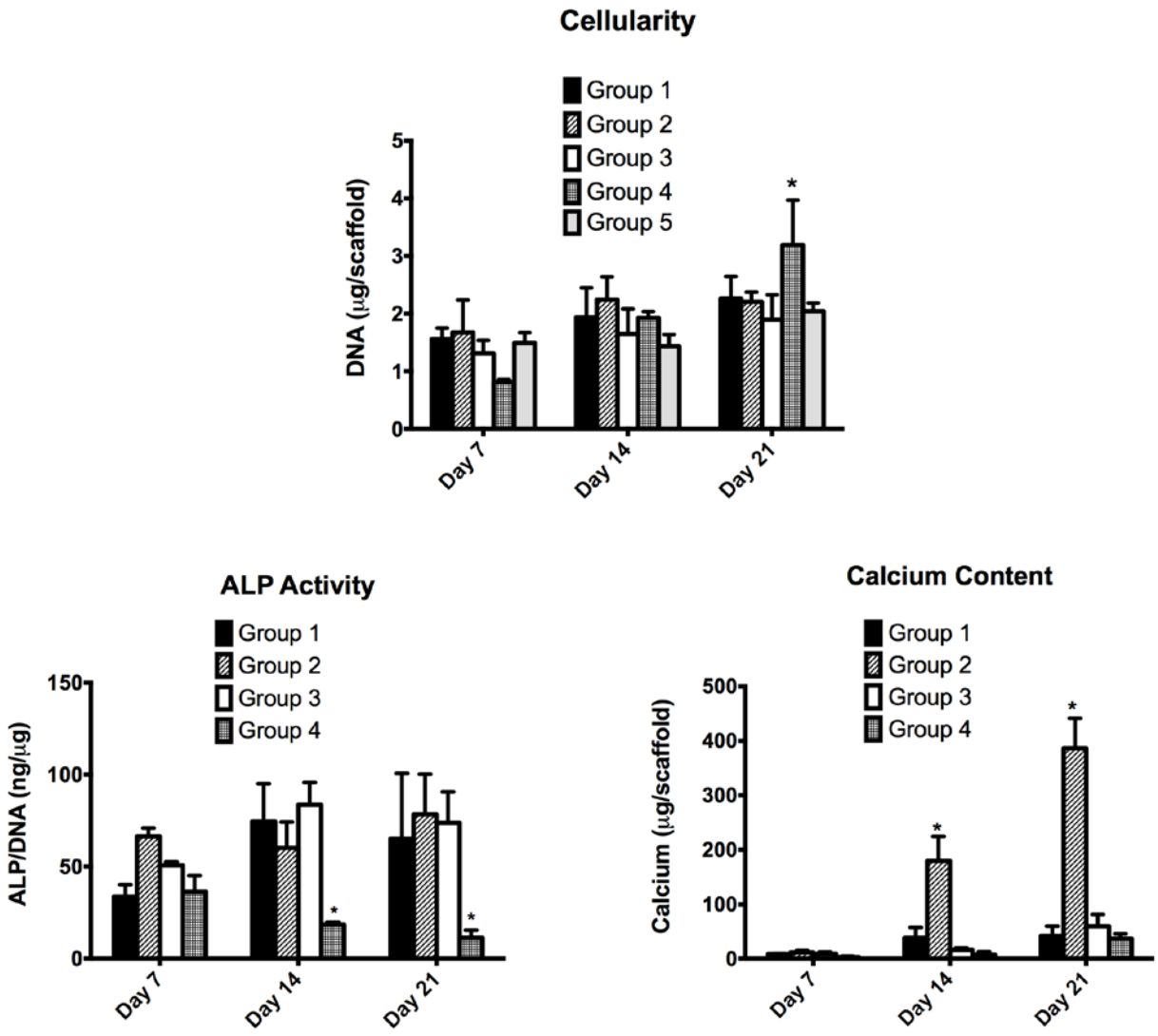

Figure 22. Biochemical characterization of scaffolds in MSC-EC osteogenic co-culture conditions

(A) DNA content, (B) ALP activity, and (C) total calcium content. Values for Group 4 were divided by 2 to normalize number of cells. *$p<0.05$, n=3

4.2.4 VEGF secretion

The quantity of VEGF released into the medium was measured using a standard ELISA kit. The amount of VEGF increased over time and was significantly higher for Groups 1-3 than Group 4. There were no significant differences at any of the time points between the co-culture groups (Figure 23).

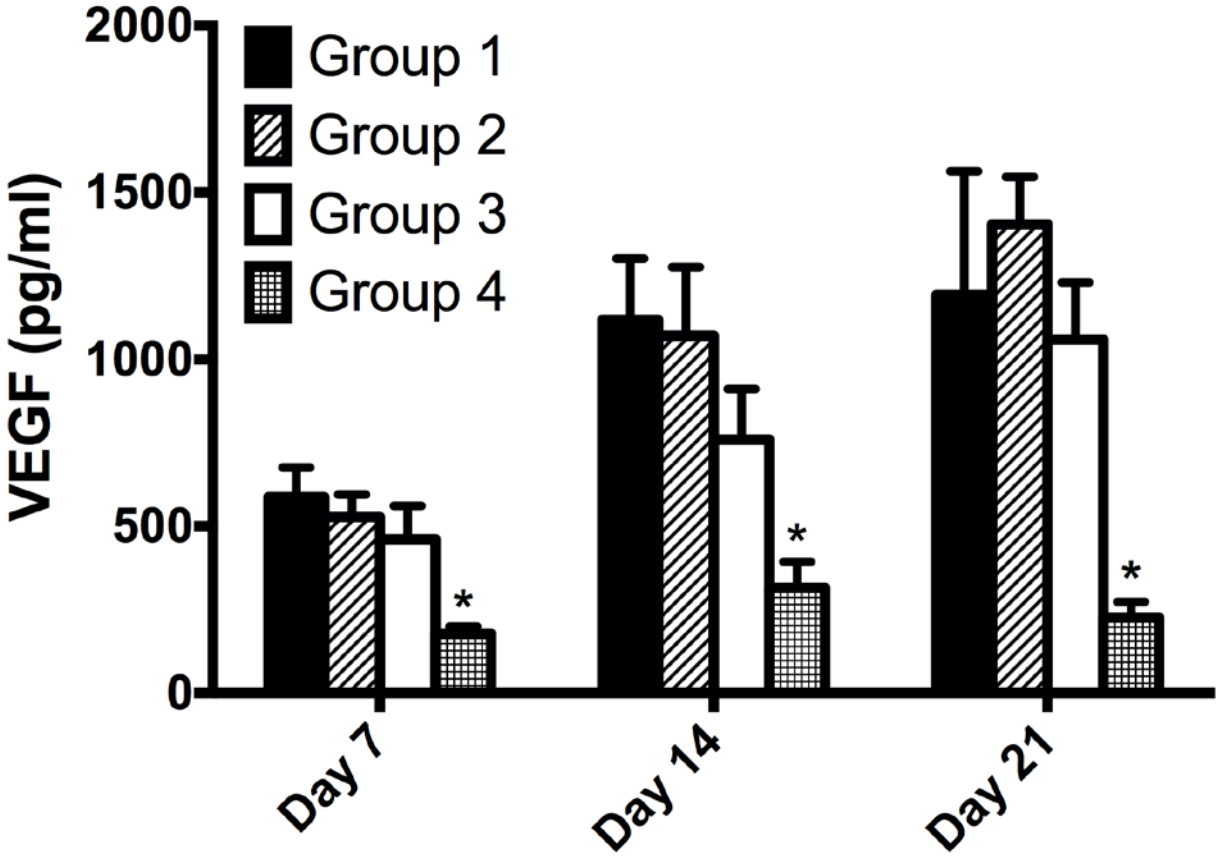

Figure 23. VEGF secretion in MSC-EC co-cultures

VEGF secretion by cells over a 72 hour period and measured at days 7, 14, and 21. *$p<0.05$ indicates significantly different than all other groups at the time point, n=3.

4.2.5 Osteogenic matrix deposition

Representative images for immunofluorescence staining of collagen type I, osteonectin, osteopontin and osteocalcin are shown in Figure 24. Collagen type I organization varied between groups. In Group 4, dense deposits of randomly oriented collagen fibers are seen, while in Groups 1 and 3, thin collagen fibers appeared to be mostly oriented along a single axis. In Group 2, larger fiber bundles are apparent and appeared to be arranged in a web-like network interspersed with fine collagen fibers below.

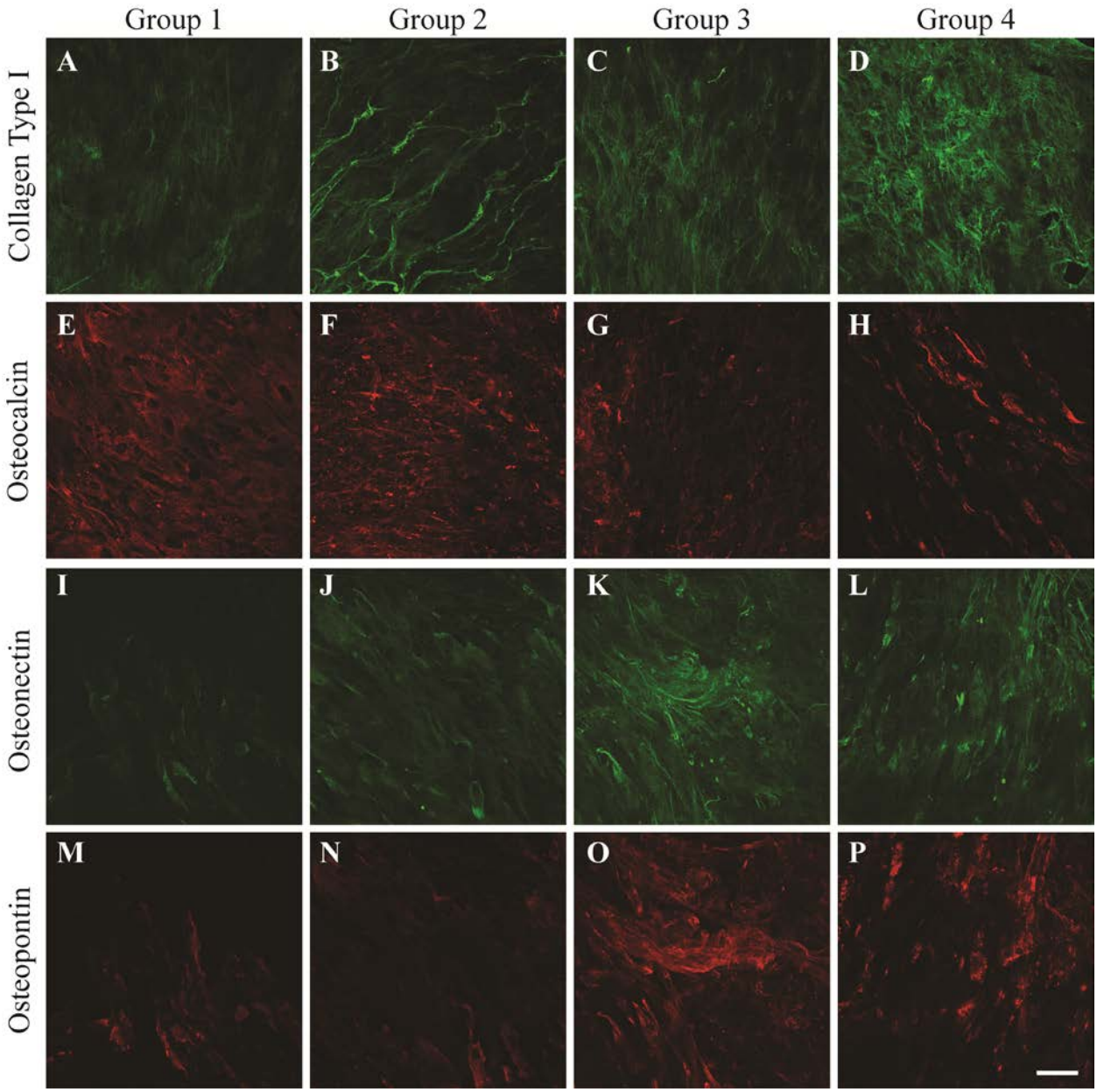

Figure 24. Confocal immunofluorescence imaging for osteogenic markers in MSC-EC co-cultures

Collagen type I (A,B,C,D; green), osteocalcin (E,F,G,H; red), osteonectin (I,J,K,L; green), and osteopontin (M,N,O,P; red). Images taken at 20x magnification, scale bar = 100 μm.

4.3 DISCUSSION

Several previous studies have seeded MSCs and ECs sequentially in order to improve osteogenesis and/or angiogenesis.[135–138] However, there have been no investigations into whether sequentially seeding cells is beneficial compared to simultaneous seeding or if seeding MSCs or ECs first results in better osteogenic differentiation of the co-culture. In this study, we have found that in co-culturing osteogenic cells with ECs, pre-seeding MSCs onto PCL scaffolds three days prior to endothelial cells significantly improves osteogenic differentiation in comparison to monoculture of MSCs or pre-seeding ECs prior to adding MSCs.

RUNX2 is considered the master regulatory gene for differentiation of MSCs into osteoblasts, inducing the induction of gene expression of ALP, collagen type I, osteopontin and bone sialoprotin-2.[139] Our results showed increased expression of RUNX2 as well as other markers of osteogenic differentiation in co-culture compared to MSC monoculture conditions, suggesting the presence of ECs at any time promoted enhanced osteogenic differentiation. In particular, ALP expression and activity were both increased with co-culture; however, no significant differences were found in ALP activity between any of the co-culture groups. ALP expression is typically turned on at the early stages of osteoblast differentiation, marking the shift from proliferation to differentiation and then plateaus or decreases at the onset of mineralization.[125] The cell number in the monoculture group continued to increase through the 21 day period, compared to more modest increases in the co-culture groups, suggesting that the presence of ECs may induce earlier differentiation of MSCs and may explain the unchanged ALP expression and activity levels at later time points.

Collagen type I is the main macromolecular component of bone, making up 90% of the protein matrix. In this study, COL1 expression decreased over the culture period, which may be an indication that cells underwent a shift from a proliferative state to one of differentiation. Previous studies have shown that collagen matrix deposition actually induces differentiation, and that increased collagen deposition occurs in co-culture between endothelial cells and osteoprogenitors.[125,140] Additionally, the reduced secretion of collagen type I may be associated with remodeling of the matrix during differentiation to form a more organized ECM structure. In this study, we saw differences in collagen organization with MSC-EC co-culture by means of immunostaining for collagen type I. While collagen fibers appeared to have random orientations in the MSC group in monoculture, co-culture with ECs resulted in a more aligned matrix with distinct fiber orientation. Moreover, in the group with MSCs seeded prior to ECs, collagen fibers on the surfaces appeared to be organized into cord-like structures. This feature suggest that ECs could be organizing into a pre-vascular-like network that may contribute to improved vessel formation in an *in vivo* environment.

Non-collagenous proteins play an important role in osteogenic differentiation and bone formation. Osteonectin is used as a marker of osteogenic differentiation and is found after the initiation of mineralization, where it may play a role in controlling the growth and size of hydroxyapatite crystals. In our study, we see a gradual increase in osteonectin gene expression over the culture period that is not different between the co-cultured groups, and somewhat higher amounts of staining in Groups 1 and 2, although staining is seen in Groups 3 and 4 as well. It is likely that while osteonectin can be utilized as a marker for the onset of osteogenesis, that the levels at which it is expressed or produced are weak indicators of functional outcomes, particularly since it may not play an important role during early bone formation and has also

been shown to be expressed in endothelial cells during angiogenesis.[141] The role of osteopontin during bone formation is somewhat unclear; however it strongly binds to calcium and is known to function during the initiation of mineralization, and it has been hypothesized that it may play a role in regulating crystal formation.[142] Osteopontin has been found to be expressed during the proliferative stages of osteogenesis, then down regulated during early differentiation, and then increased again at the beginning of mineralization. Results in this study follow a similar pattern, where there is a decrease in osteopontin expression between days 7 and 14, followed by a significant increase at day 21. Osteocalcin is considered a late marker of osteogenic differentiation and similar to osteonectin is not active at the site of crystal initiation, but is thought to play a later role in regulating crystal growth.[142] Unlike other markers examined, osteocalcin expression was higher in the monoculture group and did not increase in co-culture groups over time, suggesting that the presence of ECs inhibited its expression. However, previous studies have shown that changes in osteocalcin gene expression may not necessarily correlate with differentiation potential.[143–145]

In this study, gene expression of traditional markers of bone differentiation such as RUNX2, ALP osteopontin, osteonectin and osteocalcin were not useful for distinguishing differences in cell behavior between groups since there was little difference between each of the three co-culture conditions. However, significantly greater calcium deposition within the Group 2 constructs, onto which MSCs were seeded 3 days prior to ECs, suggests that there is an interactive process between MSCs and ECs that is stimulating enhanced mineralization in this group compared to the other co-cultures. MSC-EC interactions have been shown to occur both through growth factor and cytokine release, as well as by direct contact between cells via cell-cell junctions.[140,146–148] Soluble factors, including fibroblast growth factors (FGFs), bone

morphogenetic protein (BMPs), insulin-like growth factors (IGFs), platelet derived growth factor (PDGF) and VEGF, have all been shown to play a role in both mesenchymal osteogenic differentiation and bone formation during either development or healing.

VEGF is an important mediator between osteogenesis and angiogenesis, acting both in a paracrine and autocrine manner.[149] VEGF produced by hypertrophic chondrocytes in the developing bone is a chemotactic factor that attracts ECs from the surrounding vasculature, promoting the expression of matrix-degrading enzymes to allow for capillary invasion into the calcified cartilage matrix. This action leads to recruitment of osteoclasts from the vasculature as well as induces osteoprogenitor differentiation, resulting in remodeling of the matrix into mineralized bone. Blocking VEGF action *in vivo* using a soluble chimeric receptor protein prevents vascular invasion and bone formation, both during development as well as during bone repair.[150,151] VEGF is also important for intramembranous bone formation, which is similar to the mesenchymal osteogenic differentiation process by MSCs observed *in vitro.* In this process, mesenchymal cells differentiate directly into bone without a cartilage intermediate, enhancing both neovascularization as well as inducing ECs to secrete growth factors and cytokines that promote osteogenic differentiation.[153] Inhibition of VEGF using the same soluble blocking protein as described above in a mouse cortical tibia defect resulted in delayed turnover of the hematoma and slowed maturation of the bone from a woven to a lamellar bone. Previous studies have shown that VEGF is typically expressed at low levels until the onset of mineralization, where it increases significantly.[154] In this study, VEGF gene expression was upregulated at day 21 in Group 2 compared to both of the other two co-culture groups and Group 1 with only MSCs. VEGF secretion into the medium as measured by ELISA was not significantly different between the co-culture groups, although the values were significantly higher than the

monoculture group and continued to increase over the 21 day period. These results suggest that direct co-cultures with ECs increases VEGF secretion by MSCs, leading to increased osteogenesis. However, the 5 to 7 times higher amount of calcium in Group 2 compared to the others in conjunction with no differences in VEGF suggests that there are likely other mechanisms contributing to the increased calcium accumulation when MSCs are seeded onto PCL scaffolds 3 days prior to ECs. It is possible that VEGF is not released into the medium, but instead is sequestered within the matrix. Further investigations into the location of VEGF or other angiogenic growth factors within the construct would be valuable.

One potential explanation for the increased mineralization seen in Group 2 could be that seeding MSCs first established the formation of cell-cell contacts, collagen matrix deposition, and secretion of growth factors prior to the addition of ECs. This is similar to intramembranous ossification, where MSCs undergo condensation and then begin differentiation to osteoblasts prior to the invasion of endothelial cells. While we initially considered that seeding ECs first would allow them to establish a pre-vascular network prior to the addition of MSCs and therefore enhance future vessel formation throughout the tissue, the vast difference in mineralization suggests that might not be the optimal strategy. The mechanisms underlying the enhanced differentiation of MSCs when seeded prior to ECs may be explained by the positive feedback loop that has previously been shown to occur between MSCs and ECs when they are seeded in direct culture. MSCs have been shown to express and secret growth factors such as VEGF and EGFL6 that enhance recruitment of ECs and promote angiogenesis.[151,155,156] Once recruited, ECs then secrete growth factors that enhance osteogenesis, such as BMPs and endothelin-1, thereby leading to improved bone as well as vessel formation.[156–158] By seeding MSCs prior to ECs in the manner described in this study, MSCs may have produced angiogenic

factors that enhanced attachment of ECs and their subsequent secretion of osteogenic factors. Future investigation into the the kinetic profile of expression and production of these growth factors may lead to better understanding of the mechanisms that resulted in the enhanced osteogenesis seen when MSCs were seeded before ECs.

Additional investigation into the differences in the organization of the collagen fiber network and how it may affect mineralization could provide further insight into the mechanism of enhanced mineralization in Group 2. The disorganized arrangement of collagen fibers in woven bone results in reduced crystal size and lack of orientation of deposited mineral. Collagen fibers were more organized in Group 2, resembling the organization in lamellar bone, and least organized in Group 4, where they appeared to be more like woven bone. Groups 1 and 3 had collagen matrices that were somewhat aligned, but did not appear as robust as Group 2.

4.4 CONCLUSION

Development of a functional tissue engineered bone construct for implantation will require that it be vascularized, either before or soon after implantation in order to avoid necrosis. Co-culture of ECs with MSCs or osteoprogenitors is an attractive approach since these two cell types are naturally coupled *in vivo* and may enhance each other's activities and function. In this study, we have examined the effects of pre-seeding either MSCs or ECs in comparison to seeding both cell types at the same time, or maintaining cells in monoculture. It was clear that co-culture greatly enhanced osteogenesis regardless of seeding approach. Additionally, seeding MSCs for 3 days prior to seeding ECs generated a much higher amount of calcium per construct than any other group. Interestingly, gene expression for osteogenic markers, ALP activity, VEGF production

and proliferation were not significantly different from the other co-culture groups, suggesting that the reason for the apparent enhancement of osteogenic differentiation is at least in part due to yet to be defined mechanisms. One hypothesis is that seeding MSCs prior to ECs closely resembles the developmental process of intramembranous ossification, with establishment of cell-cell communications between MSCs, a basic collagen network, and secretion of growth factors which recruit ECs and initiate a positive feedback loop that enhances osteogenic diffrentiation. More refined examination of the collagen matrix architecture as well as inspection of the interactions occurring between cells and growth factor production may be useful in order to understand the benefits of pre-seeding of MSCs.

5.0 SUMMARY AND FUTURE DIRECTIONS

Current methods for treating bone and cartilage defects are severely limited in their effectiveness. Successful development of functional tissue engineered replacements has the potential to greatly reduce the morbidity and long-term economic burden associated with treating patients suffering from skeletal diseases. Combining stem cells with scaffolds that mimic the native tissue structure and applying stimuli, both mechanical and/or biochemical, researchers aim to create new tissues *de novo* that can be successfully integrated with the patient's body and restore original structure and function. In this work, we have focused on obtaining further understanding of the complex interactions that occur between cells and materials to improve future tissue engineering designs for bone and cartilage.

In the first aim of this thesis, we evaluated the chondrogenic differentiation of MSCs seeded at different initial cell densities onto microfiber (~4 μm) and nanofiber (~400 nm) scaffolds. We found that in order to stimulate chondrogenesis a minimum seeding density of 500,000 cells/cm^3-scaffold should be used, as lower seeding densities resulted in significantly reduced chondrogenic gene expression and minimal ECM production. Utilizing seeding densities up to 4,000,000 cells/cm^3-scaffold resulted in increased deposition of GAG and collagen. Additionally, microfibers were more effective than nanofibers at inducing chondrogenesis. We suspect that the mechanism driving enhanced chondrogenesis using microfibers and high cell seeding densities is multifactorial, and is likely related to the small pore size in nanofiber

scaffolds. Microfibers have an average pore size of 91 μm^2 while nanofibers have a pore size of 2.1 μm^2. This property limits cells to the superficial areas of the nanofiber scaffolds, therefore reducing the total surface area available for tissue formation. Additionally, the high fiber density per area on the surface of the scaffolds likely causes cells to interact with scaffolds instead of inducing the cell-cell interactions that are required to initiate chondrogenic differentiation. Conversely, the larger pores of microfibers allow cells to penetrate throughout the thickness of the scaffold as well as support cell-cell interactions as the cells can form clusters in the spaces between fibers. In native cartilage, the largest collagen fibers are similar in diameter to the nanofibers we used in our experiment, and most are much smaller. Therefore, at first glance, our results may appear to go against the widely applied view that closely mimicking the native tissue ECM is the optimal tissue engineering approach. However, in native cartilage, cells encase themselves within a nanofibrous matrix that is endogenously produced rather than being placed on top and having to migrate through a pre-formed matrix. Therefore, a more accurate approach to compare the effectiveness of nanofibers *versus* microfibers for cartilage tissue engineering would be to develop a nanofiber scaffold with similar pore size as the microfiber scaffold. This would eliminate the confounding variable of cells being trapped on the surface of the nanofiber scaffold, and would allow for a more equivalent comparison regarding cell-cell and cell-matrix interactions. Additionally, cell distribution into the scaffold would likely be more homogeneous by seeding and/or culturing cells under dynamic conditions such as in a perfusion bioreactor or spinner flask. This would maximize the area for tissue formation within the scaffold as well as equalize it to provide the most accurate comparison. While there were some limitations in the study design presented here due to the small pore size of nanofiber scaffolds, the importance of high cell seeding densities as well as ensuring that scaffolds promote cell-cell adhesions are

important factors that should be taken into account in experimental designs aimed at optimizing parameters for specific tissue engineering application. For instance, utilizing a low cell density (<500,000 cells/cm^3) to examine chondrogenesis on any fiber type may provide inaccurate information since it is unlikely that chondrogenesis will be sufficiently induced to provide an apt comparison between conditions, and particularly low values could end up being skewed during normalization.

In the second aim of this thesis, we examined the effect of fiber diameter and MSC tissue origin on both chondrogenesis and osteogenesis. Adipose-derived stem cells (ADSCs) are an attractive source of MSCs since they can be isolated in larger quantities with less invasive procedures than bone marrow-derived MSCs (BMSCs). Similar to the previous study, chondrogenesis was enhanced on microfibers in comparison to nanofibers, regardless of cell source. In this experiment, BMP-6 was added in addition to TGF-β3, since this combination has been shown to be required to optimize the chondrogenic differentiation of ADSCs.[114] This treatment enhanced GAG and reduced collagen deposition in comparison to chondrogenic media with TGF-β3 only. It is noteworthy that despite the addition of BMP-6, the chondrogenic potential of ADSCs was lower than BMSCs. Osteogenic differentiation was not as sensitive to changes in fiber diameter, with only ADSCs seeded on microfibers showing significantly higher ALP activity, calcium deposition and more organized collagen matrix deposition. These findings demonstrate that it is important to optimize culture conditions for each tissue source and for each cell type. In this study, we have used several cell populations that were matched by age and sex and pooled for the experiments presented here. Future experiments utilizing cells isolated from the same patients should be performed in order to determine if the patterns remain consistent across an extended population. Additionally, as in the first study it may be useful to seed and

culture cells under dynamic conditions to improve cell distribution throughout the scaffolds. Overall, the results of the first two studies suggest that scaffold fiber diameter plays a role in cell differentiation, particularly for chondrogenesis, and that while ADSCs are a promising cell source for tissue engineering of bone and cartilage, further optimization of both media components as well as scaffold architecture would be helpful.

In addition to the evaluation of the scaffold architecture's role in differentiation, the final study reported here was to determine if sequential seeding of MSCs and ECs was able to enhance osteogenic differentiation, perhaps via the establishment of a rudimentary vascular network that can anastamose with the host vasculature. Ideally, such an approach would minimize or prevent necrosis of the engineered tissue upon implantation *in vivo*. All co-culture conditions resulted in increased osteogenic gene expression and ALP activity in comparison to monoculture, suggesting that regardless of the seeding method, addition of ECs had a positive impact on the osteogenic differentiation of MSCs. Interestingly, seeding MSCs three days prior to ECs increased mineralization in the scaffold in comparison to seeding ECs before MSCs or seeding both cell types at the same time. This may have been in part due to an increase in MSC secretion of VEGF, which can enhance osteogenic differentiation via autocrine or paracrine effects. Another mechanism that may have led to increased osteogenesis by pre-seeding MSCs may be the establishment of requisite cell-cell interactions and deposition of a rudimentary collagenous matrix that help prime MSCs for differentiation prior to addition of ECs, similar to the sequential cellular processes that occur during endochondral bone formation. Future investigations to identify potential signaling molecules from MSCs and/or ECs that may act to induce increased mineralization as well as to explore the interactions between cells may be useful to decipher the mechanisms that can lead to development of a functional tissue engineered construct.

In conclusion, each component of a tissue engineering strategy—cells, scaffolds, and bioactive factors—plays an essential role in the *de novo* creation of a new tissue, and each of these components may influence the effects of another, often making it difficult to compare between different studies. In the experiments above, we showed that several different culture parameters including cell seeding density, cell source, scaffold fiber diameter, timing of cell seeding, and media composition influence cell behavior, and do so in a manner that is dependent on the other experimental parameters. As a result, we have developed new insight into the mechanisms guiding *in vitro* tissue formation, which should be applied in future studies in order to methodically and rationally design constructs for tissue engineering of bone and cartilage.

APPENDIX A

MEDIA COMPOSITIONS

Table 3. Medium compositions

Isolation Medium	Proliferation Medium	Chondrogenic Medium (Chapter 2)	Chondrogenic Medium (Chapter 3)	Osteogenic Medium (Chapters 2,3,4)
α-MEM[a]	DMEM[b]	DMEM	DMEM	DMEM
10% FBS[c]	10% FBS	1% ITS+[d]	1% ITS+	10% FBS
1% Anti-Anti[e]	1% Anti-Anti	1% Anti-Anti	1% Anti-Anti	1% Anti-Anti
10 ng/ml FGF-2[f]		50 μg/ml ascorbic acid	50 μg/ml ascorbic acid	50 μg/ml ascorbic acid
		100 nM dexamethasone	100 nM dexamethasone	10 nM dexamethasone
		50 μg/ml proline	50 μg/ml proline	5 mM β-glycerophosphate
		10 ng/ml TGF-β3	10 ng/ml TGF-β3	
			10 ng/ml BMP-6	

[a]alpha-minimal essential media (Invitrogen)
[b]Dulbecco's modified essential media (Invitrogen)
[c]Fetal bovine serum (Invitrogen)
[d]Insulin-transferrin-selenium plus (Invitrogen)
[e]Anti-biotic and anti-mycotic (Invitrogen)
[f]Fibroblast growth factor-2 (R&D)

APPENDIX B

PRIMER LIST

Table 4. qPCR primer sequences and conditions

Gene	Forward Primer	Reverse Primer	Annealing Temp (°C)	Chapters Utilized
Aggrecan (ACAN)	5'-AGG GGC GAG TGG AAT GAT GTT-3'	5'-GGT GGC TGT GCC CTT TTT-3'	56	2, 3
Alkaline phosphatase (ALP)	5'-GTG CCA GAG AAA GAG AAA GAC C-3'	5'-GTG GAG ACA CCC ATC CCA TC-3'	60	3, 4
Angiopoietin 1 (ANG1/ANGPT1)	5'-ACC GAG CCT ATT CAC AGT AT-3'	5'-ACA GTT GTC ATT ATC AGC ATC TT-3'	58	3, 4
Collagen, type I, alpha 1 (COL1)	5'-CGA AGA CAT CCC ACC AAT CAC-3'	5'-CAT CGC ACA ACA CCT TGC C-3'	60	2, 3, 4
Collagen, type II, alpha 1 (COL2)	5'-GGC AAT AGC AGG TTC ACG TAC A-3'	5'-CGA TAA CAG TCT TGC CCC ACT T-3'	52	2, 3
Cyclophilin A (PPIA)	5'-TTC TGC TGT CTT TGG GAC CT-3'	5'-CAC CGT GTT CTT CGA CAT TG-3'	60	2, 3, 4
Osteocalcin (OC/BGLAP)	5'-ATG AGA GCC CTC ACA CTC CTC-3'	5'-GCC GTA GAA GCG CCG ATA GGC-3'	60	3, 4
Osteonectin (ON/SPARC)	5'-TTG GAG AGT TTG AGA ACC TGT G-3'	5'-TGC AAG GCC CAG TGT AGT CC-3'	60	3, 4
Osteopontin (OP/SPP1)	5'-TGA TGA ATC TGA TGA ACT GGT C-3'	5'-GGT GAT GTC CTC GTC TGT AG-3'	60	3, 4
Runt-related transcription factor 2 (RUNX2)	5'-CAG ATG GGA CTG TGG TTA CTG-3'	5'-GGT GAA ACT CTT GCC TCG TC-3'	56	3, 4

APPENDIX C

ANTIBODY LIST

Table 5. Primary antibodies used in Chapter 2

1° Antibody	Digestion	Dilution	2° Antibody
Collagen type I (Abcam, ab292)	Pepsin[a]	1:200	Goat α Rabbit Alexa Fluor 488
Collagen type II (Millipore, MAB8887)	Pepsin	1:100	Goat α Mouse IgG_1 Alexa Fluor 594

[a]0.01% Pepsin in HCl, pH 3.0

Table 6. Primary antibodies used in Chapter 3

1° Antibody	Digestion	Dilution	2° Antibody
Collagen type I (Abcam, ab292)	Pepsin[a]	1:200	Goat α Rabbit Alexa Fluor 488
Collagen type II (Millipore, MAB8887)	Pepsin	1:100	Goat α Mouse IgG_1 Alexa Fluor 594
Osteonectin (DSHB, AON-1)	-	1:20	Goat α Mouse IgG_1 Alexa Fluor 594
Osteocalcin (Abcam, ab13420)	-	1:100	Goat α Mouse IgG_3 Alexa Fluor 594

Table 7. Primary antibodies used in Chapter 4

1º Antibody	Digestion	Dilution	2º Antibody
Collagen type I (Abcam, ab292)	Pepsin[a]	1:200	Goat α Rabbit Alexa Fluor 488
Osteonectin (DSHB, AON-1)	-	1:20	Goat α Mouse IgG_1 Alexa Fluor 594
Osteocalcin (Abcam, ab13420)	-	1:100	Goat α Mouse IgG_3 Alexa Fluor 488
Osteopontin (MPIIIB10(1))	-	1:20	Goat α Mouse IgG_1 Alexa Fluor 594

Table 8. Secondary antibodies

2º Antibody	Species	Dilution
Alexa Fluor 488 (Invitrogen, A-11008)	Goat α Rabbit	1:500
Alexa Fluor 594 (Invitrogen, A-21125)	Goat α Mouse IgG_1	1:1000

APPENDIX D

COMPARISON BETWEEN MSC CHONDROGENESIS WITH AND WITHOUT BMP-6

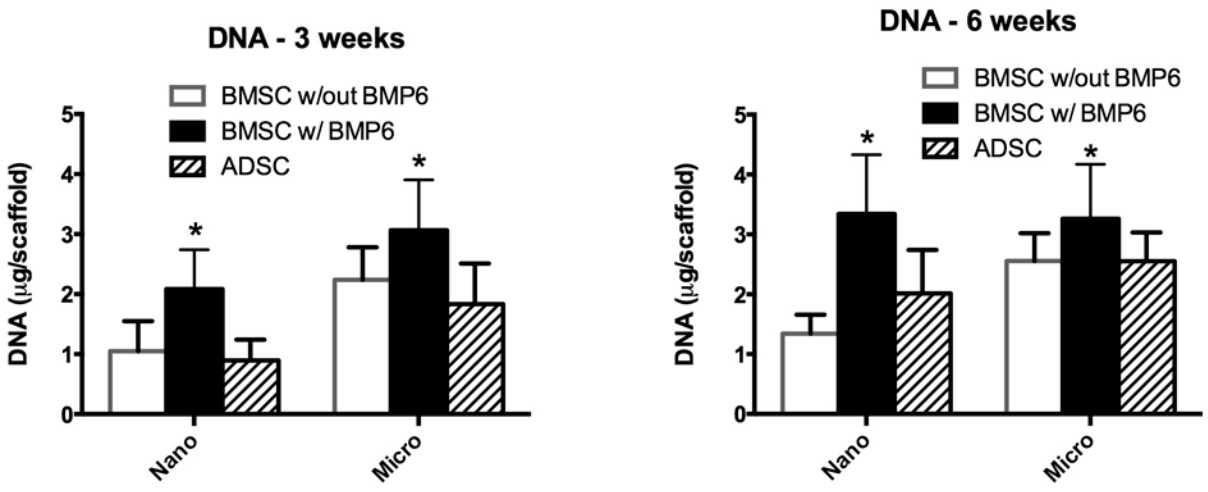

Figure 25. DNA content of cultures in chondrogenic medium with and without BMP-6

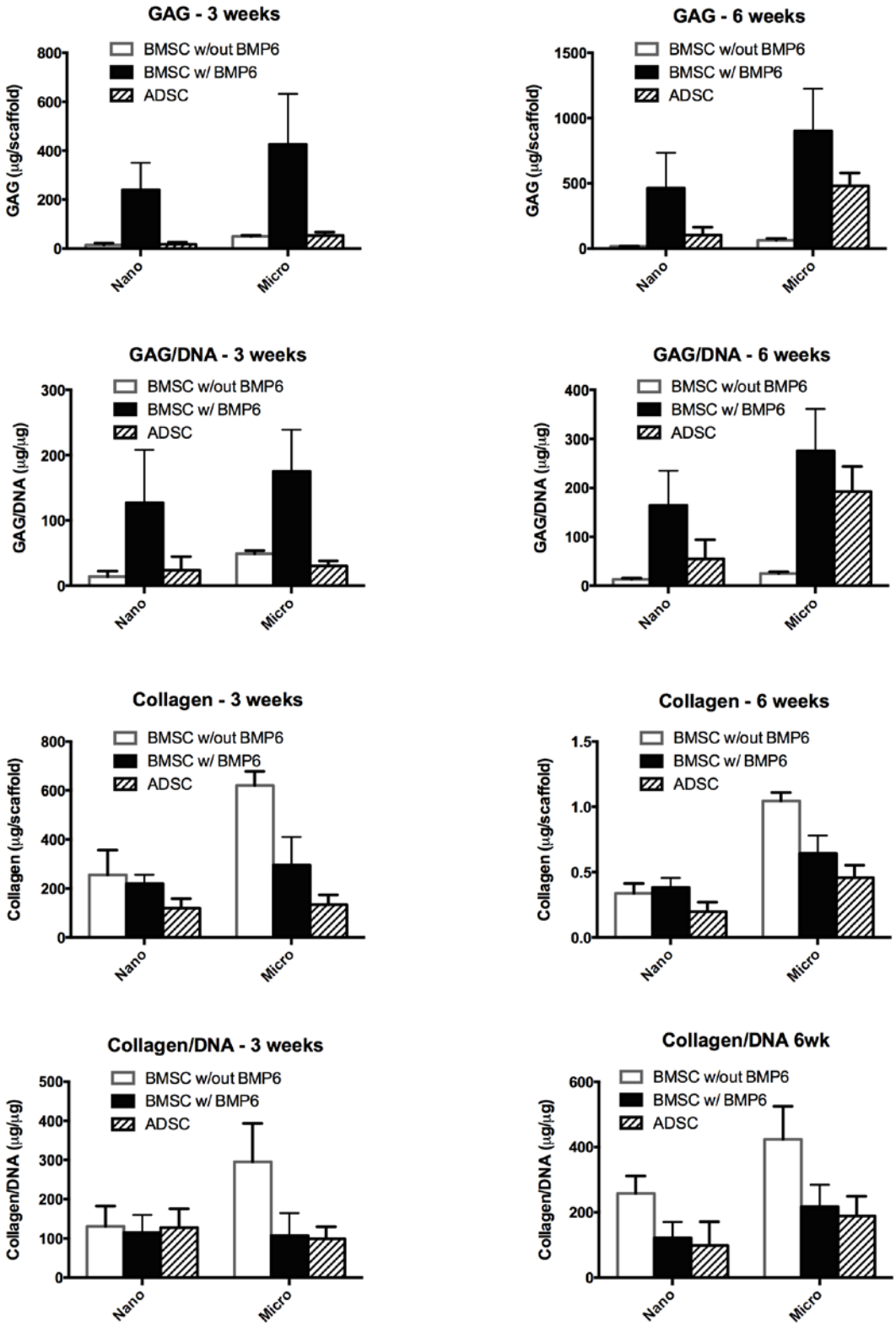

Figure 26. GAG and collagen content of cultures in chondrogenic media with and without BMP-6

BIBILOGRAPHY

1. Gilbert, S. F. Developmental Biology -- NCBI Bookshelf. *Dev. Biol.* (2000). at <http://www.ncbi.nlm.nih.gov/bookshelf/br.fcgi?book=dbio>

2. Oberlender, S. a & Tuan, R. S. Expression and functional involvement of N-cadherin in embryonic limb chondrogenesis. *Development* **120,** 177–87 (1994).

3. Widelitz, R. B., Jiang, T. X., Murray, B. a & Chuong, C. M. Adhesion molecules in skeletogenesis: II. Neural cell adhesion molecules mediate precartilaginous mesenchymal condensations and enhance chondrogenesis. *J. Cell. Physiol.* **156,** 399–411 (1993).

4. DeLise, a M., Fischer, L. & Tuan, R. S. Cellular interactions and signaling in cartilage development. *Osteoarthritis Cartilage* **8,** 309–34 (2000).

5. Tuan, R. S. Cellular and molecular regulation of embryonic skeletal development and morphogenesis. *Cells Mater.* **8,** 3–18 (1998).

6. Olsen, B. R., Reginato, A. M. & Wang, W. Bone development. *Annu. Rev. Cell Dev. Biol.* **16,** 191–220 (2000).

7. Clarke, B. Normal bone anatomy and physiology. *Clin. J. Am. Soc. Nephrol.* **3 Suppl 3,** S131–9 (2008).

8. Manolagas, S. C. Birth and death of bone cells: basic regulatory mechanisms and implications for the pathogenesis and treatment of osteoporosis. *Endocr. Rev.* **21,** 115–37 (2000).

9. Bonewald, L. F. The amazing osteocyte. *J. Bone Miner. Res.* **26,** 229–38 (2011).

10. U.S. Census Bureau. Statistical Abstract of the United States: 2009 (128th Edition). (2009).

11. Sen, M. K. & Miclau, T. Autologous iliac crest bone graft: should it still be the gold standard for treating nonunions? *Injury* **38 Suppl 1,** S75–80 (2007).

12. Pape, H. C., Evans, A. & Kobbe, P. Autologous bone graft: properties and techniques. *J. Orthop. Trauma* **24 Suppl 1,** S36–40 (2010).

13. Blokhuis, T. J. & Lindner, T. Allograft and bone morphogenetic proteins: an overview. *Injury* **39 Suppl 2,** S33–6 (2008).

14. Pitsillides, a a & Ashhurst, D. E. A critical evaluation of specific aspects of joint development. *Dev. Dyn.* **237,** 2284–94 (2008).

15. Staines, K. a, Pollard, a S., McGonnell, I. M., Farquharson, C. & Pitsillides, a a. Cartilage to bone transitions in health and disease. *J. Endocrinol.* **219,** R1–R12 (2013).

16. Ito, M. M. & Kida, M. Y. Morphological and biochemical re-evaluation of the process of cavitation in the rat knee joint: cellular and cell strata alterations in the interzone. *J. Anat.* **197 Pt 4,** 659–79 (2000).

17. Buckwalter, J. A. & Mankin, H. J. Articular cartilage: tissue design and chondrocyte-matrix interactions. *Instr. Course Lect.* **47,** 477–86 (1998).

18. Hunziker, E. B. Articular cartilage repair: are the intrinsic biological constraints undermining this process insuperable? *Osteoarthritis Cartilage* **7,** 15–28 (1999).

19. Mankin, H. The Response of Articular cartilage to Mechanical Injury. *J. bone Jt. surgery. Am.* … 460–466 (1982).

20. Kotlarz, H., Gunnarsson, C. L., Fang, H. & Rizzo, J. a. Insurer and out-of-pocket costs of osteoarthritis in the US: evidence from national survey data. *Arthritis Rheum.* **60,** 3546–53 (2009).

21. Lawrence, R. C. *et al.* Estimates of the prevalence of arthritis and other rheumatic conditions in the United States. Part II. *Arthritis Rheum.* **58,** 26–35 (2008).

22. Hootman, J. M. & Helmick, C. G. Projections of US prevalence of arthritis and associated activity limitations. *Arthritis Rheum.* **54,** 226–9 (2006).

23. Dean, D. D., Martel-Pelletier, J., Pelletier, J. P., Howell, D. S. & Woessner, J. F. Evidence for metalloproteinase and metalloproteinase inhibitor imbalance in human osteoarthritic cartilage. *J. Clin. Invest.* **84,** 678–85 (1989).

24. Mankin, H. J., Johnson, M. E. & Lippiello, L. Biochemical and metabolic abnormalities in articular cartilage from osteoarthritic human hips. III. Distribution and metabolism of amino sugar-containing macromolecules. *J. Bone Joint Surg. Am.* **63,** 131–9 (1981).

25. United States Bone and Joint Initiative: *The Burden of Musculoskeletal Diseases in the United States*. (American Academy of Orthopaedic Surgeons, 2011).

26. Bade, M. J., Kohrt, W. M. & Stevens-Lapsley, J. E. Outcomes before and after total knee arthroplasty compared to healthy adults. *J. Orthop. Sports Phys. Ther.* **40,** 559–67 (2010).

27. Langer, R. & Vacanti, J. P. Tissue engineering. *Science (80-.).* **260,** 920–926 (1993).

28. Thomson, J. a. Embryonic Stem Cell Lines Derived from Human Blastocysts. *Science (80-.).* **282,** 1145–1147 (1998).

29. Ben-David, U. & Benvenisty, N. The tumorigenicity of human embryonic and induced pluripotent stem cells. *Nat. Rev. Cancer* **11,** 268–77 (2011).

30. Kuhn, N. Z. & Tuan, R. S. Regulation of stemness and stem cell niche of mesenchymal stem cells: implications in tumorigenesis and metastasis. *J. Cell. Physiol.* **222,** 268–77 (2010).

31. Tse, W. T., Pendleton, J. D., Beyer, W. M., Egalka, M. C. & Guinan, E. C. Suppression of allogeneic T-cell proliferation by human marrow stromal cells: implications in transplantation. *Transplantation* **75,** 389–97 (2003).

32. Le Blanc, K., Tammik, C., Rosendahl, K., Zetterberg, E. & Ringdén, O. HLA expression and immunologic properties of differentiated and undifferentiated mesenchymal stem cells. *Exp. Hematol.* **31,** 890–6 (2003).

33. Leto Barone, A. a, Khalifian, S., Lee, W. P. A. & Brandacher, G. Immunomodulatory effects of adipose-derived stem cells: fact or fiction? *Biomed Res. Int.* **2013,** 383685 (2013).

34. Kaji, K. *et al.* Virus-free induction of pluripotency and subsequent excision of reprogramming factors. *Nature* **458,** 771–5 (2009).

35. Jia, F. *et al.* A nonviral minicircle vector for deriving human iPS cells. *Nat. Methods* **7,** 197–9 (2010).

36. Zhou, H. *et al.* Generation of induced pluripotent stem cells using recombinant proteins. *Cell Stem Cell* **4,** 381–4 (2009).

37. Kim, D. *et al.* Generation of human induced pluripotent stem cells by direct delivery of reprogramming proteins. *Cell Stem Cell* **4,** 472–6 (2009).

38. Yu, J. *et al.* Human induced pluripotent stem cells free of vector and transgene sequences. *Science* **324,** 797–801 (2009).

39. Mali, P. & Cheng, L. Human Cell Engineering: Cellular Reprogramming and Genome Editing. *Stem Cells* (2011). doi:10.1002/stem.735

40. Zhao, T., Zhang, Z.-N., Rong, Z. & Xu, Y. Immunogenicity of induced pluripotent stem cells. *Nature* **474,** 212–5 (2011).

41. Williams, D. F. On the nature of biomaterials. *Biomaterials* **30,** 5897–909 (2009).

42. Williams, D. Revisiting the definition of biocompatibility. *Med. Device Technol.* **14,** 10–3 (2003).

43. Stabenfeldt, S. E., Brown, A. C. & Barker, T. H. in *Biomater. as Stem Cell Niche* 1–18 (Springer, 2010). doi:10.1007/8415

44. Woo, K. M., Chen, V. J. & Ma, P. X. Nano-fibrous scaffolding architecture selectively enhances protein adsorption contributing to cell attachment. *J. Biomed. Mater. Res. A* **67,** 531–7 (2003).

45. Lee, C. H., Singla, a & Lee, Y. Biomedical applications of collagen. *Int. J. Pharm.* **221,** 1–22 (2001).

46. Lan, M. a, Gersbach, C. a, Michael, K. E., Keselowsky, B. G. & García, A. J. Myoblast proliferation and differentiation on fibronectin-coated self assembled monolayers presenting different surface chemistries. *Biomaterials* **26,** 4523–31 (2005).

47. Keselowsky, B. G., Collard, D. M. & García, A. J. Integrin binding specificity regulates biomaterial surface chemistry effects on cell differentiation. *Proc. Natl. Acad. Sci. U. S. A.* **102,** 5953–7 (2005).

48. Bashur, C. a, Shaffer, R. D., Dahlgren, L. a, Guelcher, S. a & Goldstein, A. S. Effect of fiber diameter and alignment of electrospun polyurethane meshes on mesenchymal progenitor cells. *Tissue Eng. Part A* **15,** 2435–45 (2009).

49. Buttafoco, L. *et al.* Electrospinning of collagen and elastin for tissue engineering applications. *Biomaterials* **27,** 724–34 (2006).

50. Matthews, J. a, Wnek, G. E., Simpson, D. G. & Bowlin, G. L. Electrospinning of collagen nanofibers. *Biomacromolecules* **3,** 232–8 (2002).

51. Chan, C. K. *et al.* Early adhesive behavior of bone-marrow-derived mesenchymal stem cells on collagen electrospun fibers. *Biomed. Mater.* **4,** 035006 (2009).

52. Li, M. *et al.* Electrospun protein fibers as matrices for tissue engineering. *Biomaterials* **26,** 5999–6008 (2005).

53. Jiang, H., Fang, D., Hsiao, B. S., Chu, B. & Chen, W. Optimization and characterization of dextran membranes prepared by electrospinning. *Biomacromolecules* **5,** 326–33 (2004).

54. Chu, X.-H., Shi, X.-L., Feng, Z.-Q., Gu, Z.-Z. & Ding, Y.-T. Chitosan nanofiber scaffold enhances hepatocyte adhesion and function. *Biotechnol. Lett.* **31,** 347–52 (2009).

55. Geng, X., Kwon, O.-H. & Jang, J. Electrospinning of chitosan dissolved in concentrated acetic acid solution. *Biomaterials* **26,** 5427–32 (2005).

56. Ryu, G. *et al.* Plasma surface modification of poly (-lactic-co-glycolic acid) (65/35) film for tissue engineering. *Surf. Coatings Technol.* **193,** 60–64 (2005).

57. Baker, S. C. *et al.* Characterisation of electrospun polystyrene scaffolds for three-dimensional in vitro biological studies. *Biomaterials* **27,** 3136–46 (2006).

58. He, W., Ma, Z., Yong, T., Teo, W. E. & Ramakrishna, S. Fabrication of collagen-coated biodegradable polymer nanofiber mesh and its potential for endothelial cells growth. *Biomaterials* **26,** 7606–15 (2005).

59. Ma, Z., He, W., Yong, T. & Ramakrishna, S. Grafting of Gelatin on Electrospun Poly(caprolactone) Nanofibers to Improve Endothelial Cell Spreading and Proliferation and to Control Cell Orientation. *Tissue Eng.* **11,** 1149–1158 (2005).

60. Croll, T. I., O'Connor, A. J., Stevens, G. W. & Cooper-White, J. J. Controllable surface modification of poly(lactic-co-glycolic acid) (PLGA) by hydrolysis or aminolysis I: physical, chemical, and theoretical aspects. *Biomacromolecules* **5,** 463–73 (2004).

61. He, W. *et al.* Biodegradable polymer nanofiber mesh to maintain functions of endothelial cells. *Tissue Eng.* **12,** 2457–66 (2006).

62. Pham, Q. P., Sharma, U. & Mikos, A. G. Electrospun poly(epsilon-caprolactone) microfiber and multilayer nanofiber/microfiber scaffolds: characterization of scaffolds and measurement of cellular infiltration. *Biomacromolecules* **7,** 2796–805 (2006).

63. Stankus, J. J., Freytes, D. O., Badylak, S. F. & Wagner, W. R. Hybrid nanofibrous scaffolds from electrospinning of a synthetic biodegradable elastomer and urinary bladder matrix. *J. Biomater. Sci. Polym. Ed.* **19,** 635 (2008).

64. Kidoaki, S., Kwon, I. K. & Matsuda, T. Mesoscopic spatial designs of nano-and microfiber meshes for tissue-engineering matrix and scaffold based on newly devised multilayering and mixing electrospinning techniques. *Biomaterials* **26,** 37–46 (2005).

65. Baker, B. M., Nerurkar, N. L., Burdick, J. A., Elliott, D. M. & Mauck, L. Fabrication and modeling of dynamic multi-polymer nanofibrous scaffolds. *J. Biomech.* **131,** 1–22 (2010).

66. Nisbet, D. R., Forsythe, J. S., Shen, W., Finkelstein, D. I. & Horne, M. K. Review paper: a review of the cellular response on electrospun nanofibers for tissue engineering. *J. Biomater. Appl.* **24,** 7–29 (2009).

67. Kumbar, S. G., James, R., Nukavarapu, S. P. & Laurencin, C. T. Electrospun nanofiber scaffolds: engineering soft tissues. *Biomed. Mater.* **3,** 034002 (2008).

68. Kock, L., van Donkelaar, C. C. & Ito, K. Tissue engineering of functional articular cartilage: the current status. *Cell Tissue Res.* **347,** 613–27 (2012).

69. Vater, C., Kasten, P. & Stiehler, M. Culture media for the differentiation of mesenchymal stromal cells. *Acta Biomater.* **7,** 463–77 (2011).

70. Ruckh, T. T., Kumar, K., Kipper, M. J. & Popat, K. C. Osteogenic differentiation of bone marrow stromal cells on poly(epsilon-caprolactone) nanofiber scaffolds. *Acta Biomater.* **6,** 2949–59 (2010).

71. Haslauer, C. M., Moghe, A. K., Osborne, J. a, Gupta, B. S. & Loboa, E. G. Collagen-PCL sheath-core bicomponent electrospun scaffolds increase osteogenic differentiation and calcium accretion of human adipose-derived stem cells. *J. Biomater. Sci. Polym. Ed.* **22,** 1695–712 (2011).

72. Zhang, Y. *et al.* Enhanced biomineralization in osteoblasts on a novel electrospun biocomposite nanofibrous substrate of hydroxyapatite/collagen/chitosan. *Tissue Eng. Part A* **16,** 1949–60 (2010).

73. Yoshimoto, H., Shin, Y. M., Terai, H. & Vacanti, J. P. A biodegradable nanofiber scaffold by electrospinning and its potential for bone tissue engineering. *Biomaterials* **24,** 2077–2082 (2003).

74. Shin, M., Yoshimoto, H. & Vacanti, J. P. In vivo bone tissue engineering using mesenchymal stem cells on a novel electrospun nanofibrous scaffold. *Tissue Eng.* **10,** 33–41 (2004).

75. Carmeliet, P. & Jain, R. K. Angiogenesis in cancer and other diseases. *Nature* **407,** 249–57 (2000).

76. Mikos, a G. *et al.* Prevascularization of porous biodegradable polymers. *Biotechnol. Bioeng.* **42,** 716–23 (1993).

77. Kneser, U. *et al.* Engineering of vascularized transplantable bone tissues: induction of axial vascularization in an osteoconductive matrix using an arteriovenous loop. *Tissue Eng.* **12,** 1721–31 (2006).

78. Rouwkema, J., Rivron, N. C. & van Blitterswijk, C. a. Vascularization in tissue engineering. *Trends Biotechnol.* **26,** 434–41 (2008).

79. Laranjeira, M. S., Fernandes, M. H. & Monteiro, F. J. Reciprocal induction of human dermal microvascular endothelial cells and human mesenchymal stem cells: time-dependent profile in a co-culture system. *Cell Prolif.* **45,** 320–34 (2012).

80. Li, W.-J. *et al.* A three-dimensional nanofibrous scaffold for cartilage tissue engineering using human mesenchymal stem cells. *Biomaterials* **26,** 599–609 (2005).

81. Li, W.-J., Danielson, K. G., Alexander, P. G. & Tuan, R. S. Biological response of chondrocytes cultured in three-dimensional nanofibrous poly(epsilon-caprolactone) scaffolds. *J. Biomed. Mater. Res. A* **67,** 1105–14 (2003).

82. Li, W. *et al.* Evaluation of articular cartilage repair using biodegradable nanofibrous scaffolds in a swine model: a pilot study. *J. Tissue Eng. Regen. Med.* **3,** 1–10 (2009).

83. Wise, J. K., Yarin, A. L., Megaridis, C. M. & Cho, M. Chondrogenic differentiation of human mesenchymal stem cells on oriented nanofibrous scaffolds: engineering the superficial zone of articular cartilage. *Tissue Eng. Part A* **15,** 913–21 (2009).

84. McCullen, S. D., Autefage, H., Callanan, A., Gentleman, E. & Stevens, M. M. Anisotropic fibrous scaffolds for articular cartilage regeneration. *Tissue Eng. Part A* **18,** 2073–83 (2012).

85. Christopherson, G. T., Song, H. & Mao, H.-Q. The influence of fiber diameter of electrospun substrates on neural stem cell differentiation and proliferation. *Biomaterials* **30,** 556–64 (2009).

86. Wang, H. B., Mullins, M. E., Cregg, J. M., McCarthy, C. W. & Gilbert, R. J. Varying the diameter of aligned electrospun fibers alters neurite outgrowth and Schwann cell migration. *Acta Biomater.* **6,** 2970–8 (2010).

87. Yao, L., O'Brien, N., Windebank, A. & Pandit, A. Orienting neurite growth in electrospun fibrous neural conduits. *J. Biomed. Mater. Res. B. Appl. Biomater.* **90,** 483–91 (2009).

88. He, L. *et al.* Synergistic effects of electrospun PLLA fiber dimension and pattern on neonatal mouse cerebellum C17.2 stem cells. *Acta Biomater.* **6,** 2960–9 (2010).

89. Bashur, C. a, Dahlgren, L. a & Goldstein, A. S. Effect of fiber diameter and orientation on fibroblast morphology and proliferation on electrospun poly(D,L-lactic-co-glycolic acid) meshes. *Biomaterials* **27,** 5681–8 (2006).

90. Kumbar, S. G., Nukavarapu, S. P., James, R., Nair, L. S. & Laurencin, C. T. Electrospun poly(lactic acid-co-glycolic acid) scaffolds for skin tissue engineering. *Biomaterials* **29,** 4100–7 (2008).

91. Tian, F. *et al.* Quantitative analysis of cell adhesion on aligned micro-and nanofibers. *J. Biomed. Mater. Res. Part A* **84,** 291–299 (2008).

92. Shanmugasundaram, S., Chaudhry, H. & Arinzeh, T. L. Microscale versus nanoscale scaffold architecture for mesenchymal stem cell chondrogenesis. *Tissue Eng. Part A* **17,** 831–40 (2011).

93. Li, W.-J., Jiang, Y. J. & Tuan, R. S. Chondrocyte phenotype in engineered fibrous matrix is regulated by fiber size. *Tissue Eng.* **12,** 1775–85 (2006).

94. Noriega, S. E., Hasanova, G. I., Schneider, M. J., Larsen, G. F. & Subramanian, A. Effect of fiber diameter on the spreading, proliferation and differentiation of chondrocytes on electrospun chitosan matrices. *Cells. Tissues. Organs* **195,** 207–21 (2012).

95. Talukdar, S., Nguyen, Q. T., Chen, A. C., Sah, R. L. & Kundu, S. C. Effect of initial cell seeding density on 3D-engineered silk fibroin scaffolds for articular cartilage tissue engineering. *Biomaterials* **32,** 8927–37 (2011).

96. Huang, A. H., Stein, A., Tuan, R. S. & Mauck, R. L. Transient exposure to transforming growth factor beta 3 improves the mechanical properties of mesenchymal stem cell-laden cartilage constructs in a density-dependent manner. *Tissue Eng. Part A* **15,** 3461–72 (2009).

97. Buxton, A., Bahney, C., Yoo, J. & Johnstone, B. Temporal Exposure to Chondrogenic Factors Modulates Human Mesenchymal Stem Cell chondrogenesis in hydrogels. *Tissue Eng. Part A* **17,** 371–380 (2010).

98. Kavalkovich, K. W., Boynton, R. E., Murphy, J. M. & Barry, F. Chondrogenic differentiation of human mesenchymal stem cells within an alginate layer culture system. *In Vitro Cell. Dev. Biol. Anim.* **38,** 457–66 (2002).

99. Kobayashi, S., Meir, A. & Urban, J. Effect of cell density on the rate of glycosaminoglycan accumulation by disc and cartilage cells in vitro. *J. Orthop. Res.* **26,** 493–503 (2008).

100. D'Amore, A., Stella, J. a, Wagner, W. R. & Sacks, M. S. Characterization of the complete fiber network topology of planar fibrous tissues and scaffolds. *Biomaterials* **31,** 5345–54 (2010).

101. Ye, J. *et al.* Primer-BLAST: a tool to design target-specific primers for polymerase chain reaction. *BMC Bioinformatics* **13,** 134 (2012).

102. Wang, L., Sheshareddy, K., Weiss, M. L. & Detamore, M. S. Effect of initial seeding density on human umbilical cord mesenchymal stromal cells for fibrocartilage tissue engineering. *Tissue Eng. Part A* **15,** 1009–17 (2009).

103. Lee, W. C. *et al.* High-throughput cell cycle synchronization using inertial forces in spiral microchannels. *Lab Chip* **11,** 1359–67 (2011).

104. Tan, F., Naciri, M., Dowling, D. & Al-Rubeai, M. In vitro and in vivo bioactivity of CoBlast hydroxyapatite coating and the effect of impaction on its osteoconductivity. *Biotechnol. Adv.* **30,** 352–62 (2011).

105. Dessau, W., von der Mark, H., von der Mark, K. & Fischer, S. Changes in the patterns of collagens and fibronectin during limb-bud chondrogenesis. *J. Embryol. Exp. Morphol.* **57,** 51–60 (1980).

106. Stockwell, R. A. The cell density of human articular and costal cartilage. *J. Anat.* **101,** 753–63 (1967).

107. Darling, E. M., Hu, J. C. Y. & Athanasiou, K. a. Zonal and topographical differences in articular cartilage gene expression. *J. Orthop. Res.* **22,** 1182–7 (2004).

108. Beane, O. S. & Darling, E. M. Isolation, characterization, and differentiation of stem cells for cartilage regeneration. *Ann. Biomed. Eng.* **40,** 2079–97 (2012).

109. Peng, L. *et al.* Comparative analysis of mesenchymal stem cells from bone marrow, cartilage, and adipose tissue. *Stem Cells Dev.* **17,** 761–73 (2008).

110. Winter, A. *et al.* Cartilage-like gene expression in differentiated human stem cell spheroids: a comparison of bone marrow-derived and adipose tissue-derived stromal cells. *Arthritis Rheum.* **48,** 418–29 (2003).

111. Sakaguchi, Y., Sekiya, I., Yagishita, K. & Muneta, T. Comparison of human stem cells derived from various mesenchymal tissues: superiority of synovium as a cell source. *Arthritis Rheum.* **52,** 2521–9 (2005).

112. Im, G.-I., Shin, Y.-W. & Lee, K.-B. Do adipose tissue-derived mesenchymal stem cells have the same osteogenic and chondrogenic potential as bone marrow-derived cells? *Osteoarthritis Cartilage* **13,** 845–53 (2005).

113. Hennig, T., Lorenz, H. & Thiel, A. Reduced chondrogenic potential of adipose tissue derived stromal cells correlates with an altered TGFb Receptor receptor and BMP profile and is overcome by BMP-6. *J. Cell. Physiol.* **211,** 682–691 (2007).

114. Estes, B. T., Wu, A. W. & Guilak, F. Potent induction of chondrocytic differentiation of human adipose-derived adult stem cells by bone morphogenetic protein 6. *Arthritis Rheum.* **54,** 1222–32 (2006).

115. Kim, H. & Im, G. Combination of Transforming Growth Factor-Beta2 and Bone Morphogenetic Protein 7 Enhances Chondrogenesis from Adipose Tissue-Derived Mesenchymal Stem Cells. *Tissue Eng. Part A* **15,** 1543–1551 (2008).

116. Hildner, F. *et al.* FGF-2 abolishes the chondrogenic effect of combined BMP-6 and TGF-beta in human adipose derived stem cells. *J. Biomed. Mater. Res. A* **94,** 978–87 (2010).

117. Shafiee, A. *et al.* A comparison between osteogenic differentiation of human unrestricted somatic stem cells and mesenchymal stem cells from bone marrow and adipose tissue. *Biotechnol. Lett.* **33,** 1257–64 (2011).

118. Park, S.-H. *et al.* Chip-Based Comparison of the Osteogenesis of Human Bone Marrow- and Adipose Tissue-Derived Mesenchymal Stem Cells under Mechanical Stimulation. *PLoS One* **7,** e46689 (2012).

119. Ravichandran, R., Venugopal, J. R., Sundarrajan, S., Mukherjee, S. & Ramakrishna, S. Precipitation of nanohydroxyapatite on PLLA/PBLG/Collagen nanofibrous structures for the differentiation of adipose derived stem cells to osteogenic lineage. *Biomaterials* **33,** 846–55 (2012).

120. Erisken, C., Kalyon, D. M., Wang, H., Ornek-Ballanco, C. & Xu, J. Osteochondral tissue formation through adipose-derived stromal cell differentiation on biomimetic polycaprolactone nanofibrous scaffolds with graded insulin and Beta-glycerophosphate concentrations. *Tissue Eng. Part A* **17,** 1239–52 (2011).

121. Van Aalst, J. a *et al.* Cellular incorporation into electrospun nanofibers: retained viability, proliferation, and function in fibroblasts. *Ann. Plast. Surg.* **60,** 577–83 (2008).

122. McCullen, S. D. *et al.* In situ collagen polymerization of layered cell-seeded electrospun scaffolds for bone tissue engineering applications. *Tissue Eng. Part C. Methods* **16,** 1095–105 (2010).

123. Leary, N. O., Pembroke, A. & Duggan, P. F. Single stable reagent (Arsenazo III) for optically robust measurement of calcium in serum and plasma. *Clin. Chem.* **38,** 904–8 (1992).

124. Gitelman, S. E. *et al.* Recombinant Vgr-1/BMP-6-expressing tumors induce fibrosis and endochondral bone formation in vivo. *J. Cell Biol.* **126,** 1595–609 (1994).

125. Lian, J. B. & Stein, G. S. Development of the osteoblast phenotype: molecular mechanisms mediating osteoblast growth and differentiation. *Iowa Orthop. J.* **15,** 118–40 (1995).

126. Jundt, G., Bergh�user, K.-H., Termine, J. D. & Schulz, A. Osteonectin - a differentiation marker of bone cells. *Cell Tissue Res.* **248,** 409–415 (1987).

127. Neve, A., Corrado, A. & Cantatore, F. P. Osteoblast physiology in normal and pathological conditions. *Cell Tissue Res.* **343,** 289–302 (2011).

128. Takahashi, Y. & Tabata, Y. Effect of the fiber diameter and porosity of non-woven PET fabrics on the osteogenic differentiation of mesenchymal stem cells. *J. Biomater. Sci. Polym. Ed.* **15,** 41–57 (2004).

129. Badami, A. S., Kreke, M. R., Thompson, M. S., Riffle, J. S. & Goldstein, A. S. Effect of fiber diameter on spreading, proliferation, and differentiation of osteoblastic cells on electrospun poly(lactic acid) substrates. *Biomaterials* **27,** 596–606 (2006).

130. Sisson, K., Zhang, C., Farach-Carson, M. C., Chase, D. B. & Rabolt, J. F. Fiber diameters control osteoblastic cell migration and differentiation in electrospun gelatin. *J. Biomed. Mater. Res. A* **94,** 1312–20 (2010).

131. Soliman, S. *et al.* Controlling the porosity of fibrous scaffolds by modulating the fiber diameter and packing density. *J. Biomed. Mater. Res. A* **96,** 566–74 (2011).

132. Hsu, Y.-M., Chen, C.-N., Chiu, J.-J., Chang, S.-H. & Wang, Y.-J. The effects of fiber size on MG63 cells cultured with collagen based matrices. *J. Biomed. Mater. Res. B. Appl. Biomater.* **91,** 737–45 (2009).

133. Pittenger, M. F. *et al.* Multilineage potential of adult human mesenchymal stem cells. *Science* **284,** 143–7 (1999).

134. Dahlin, R. L., Gershovich, J. G., Kasper, F. K. & Mikos, A. G. Flow Perfusion Co-culture of Human Mesenchymal Stem Cells and Endothelial Cells on Biodegradable Polymer Scaffolds. *Ann. Biomed. Eng.* (2013). doi:10.1007/s10439-013-0862-y

135. McFadden, T. M. *et al.* The delayed addition of human mesenchymal stem cells to pre-formed endothelial cell networks results in functional vascularization of a collagen-glycosaminoglycan scaffold in vivo. *Acta Biomater.* (2013). doi:10.1016/j.actbio.2013.08.014

136. Yu, H. *et al.* Promotion of osteogenesis in tissue-engineered bone by pre-seeding endothelial progenitor cells-derived endothelial cells. *J. Orthop. Res.* **26,** 1147–52 (2008).

137. Fuchs, S. *et al.* Dynamic processes involved in the pre-vascularization of silk fibroin constructs for bone regeneration using outgrowth endothelial cells. *Biomaterials* **30,** 1329–38 (2009).

138. Tsigkou, O. *et al.* Engineered vascularized bone grafts. *Proc. Natl. Acad. Sci. U. S. A.* **107,** 3311–6 (2010).

139. Ducy, P., Zhang, R., Geoffroy, V., Ridall, a L. & Karsenty, G. Osf2/Cbfa1: a transcriptional activator of osteoblast differentiation. *Cell* **89,** 747–54 (1997).

140. Villars, F. *et al.* Effect of HUVEC on human osteoprogenitor cell differentiation needs heterotypic gap junction communication. *Am. J. Physiol. Cell Physiol.* **282,** C775–85 (2002).

141. Iruela-Arispe, M. L., Hasselaar, P. & Sage, H. Differential expression of extracellular proteins is correlated with angiogenesis in vitro. *Lab. Invest.* **64,** 174–86 (1991).

142. Roach, H. I. Why does bone matrix contain non-collagenous proteins? The possible roles of osteocalcin, osteonectin, osteopontin and bone sialoprotein in bone mineralisation and resorption. *Cell Biol. Int.* **18,** 617–28 (1994).

143. Meury, T., Verrier, S. & Alini, M. Human endothelial cells inhibit BMSC differentiation into mature osteoblasts in vitro by interfering with osterix expression. *J. Cell. Biochem.* **98,** 992–1006 (2006).

144. Frank, O. *et al.* Real-time quantitative RT-PCR analysis of human bone marrow stromal cells during osteogenic differentiation in vitro. *J. Cell. Biochem.* **85,** 737–46 (2002).

145. Villars, F., Bordenave, L., Bareille, R. & Amédée, J. Effect of human endothelial cells on human bone marrow stromal cell phenotype: role of VEGF? *J. Cell. Biochem.* **79,** 672–85 (2000).

146. Otsu, K. *et al.* Concentration-dependent inhibition of angiogenesis by mesenchymal stem cells. *Blood* **113,** 4197–205 (2009).

147. Santos, M. I., Unger, R. E., Sousa, R. a, Reis, R. L. & Kirkpatrick, C. J. Crosstalk between osteoblasts and endothelial cells co-cultured on a polycaprolactone-starch scaffold and the in vitro development of vascularization. *Biomaterials* **30,** 4407–15 (2009).

148. Guerrero, J. *et al.* Cell interactions between human progenitor-derived endothelial cells and human mesenchymal stem cells in a three-dimensional macroporous polysaccharide-based scaffold promote osteogenesis. *Acta Biomater.* **9,** 8200–13 (2013).

149. Mayer, H. *et al.* Vascular endothelial growth factor (VEGF-A) expression in human mesenchymal stem cells: autocrine and paracrine role on osteoblastic and endothelial differentiation. *J. Cell. Biochem.* **95,** 827–39 (2005).

150. Gerber, H. P. *et al.* VEGF couples hypertrophic cartilage remodeling, ossification and angiogenesis during endochondral bone formation. *Nat. Med.* **5,** 623–8 (1999).

151. Street, J. *et al.* Vascular endothelial growth factor stimulates bone repair by promoting angiogenesis and bone turnover. *Proc. Natl. Acad. Sci. U. S. A.* **99,** 9656–61 (2002).

152. Scotti, C. *et al.* Recapitulation of endochondral bone formation using human adult mesenchymal stem cells as a paradigm for developmental engineering. *Proc. Natl. Acad. Sci. U. S. A.* **107,** 7251–6 (2010).

153. Yang, Y.-Q. *et al.* The role of vascular endothelial growth factor in ossification. *Int. J. Oral Sci.* **4,** 64–8 (2012).

154. Deckers, M. M. *et al.* Expression of vascular endothelial growth factors and their receptors during osteoblast differentiation. *Endocrinology* **141,** 1667–74 (2000).

155. Chim, S. M. *et al.* EGFL6 promotes endothelial cell migration and angiogenesis through the activation of extracellular signal-regulated kinase. *J. Biol. Chem.* **286,** 22035–46 (2011).

156. Peng, H. *et al.* Synergistic enhancement of bone formation and healing by stem cell–expressed VEGF and bone morphogenetic protein-4. *J. Clin. Invest.* **110,** 751–759 (2002).

157. Von Schroeder, H. P., Veillette, C. J., Payandeh, J., Qureshi, A. & Heersche, J. N. M. Endothelin-1 promotes osteoprogenitor proliferation and differentiation in fetal rat calvarial cell cultures. *Bone* **33,** 673–84 (2003).

158. Yamaguchi, A. *et al.* Effects of BMP-2, BMP-4, and BMP-6 on osteoblastic differentiation of bone marrow-derived stromal cell lines, ST2 and MC3T3-G2/PA6. *Biochem. Biophys. Res. Commun.* **220,** 366–71 (1996).